# INSTRUMENTATION AND PHOTOGRAPHIC TECHNIQUES FOR DETERMINING DISPLACEMENT, VELOCITY CHANGE, AND DECELERATION OF VEHICLES WITH BREAK-AWAY SIGN STRUCTURES

by

Robert M. Olson
Assistant Research Engineer

Research Report Number 68-3

Neilon J. Rowan, P. E.
Project Supervisor

Sign Support Structures
Research Project Number 2-5-63-68

Sponsored by

The Texas Highway Department
In Cooperation with the
U. S. Department of Commerce, Bureau of Public Roads

September, 1966

TEXAS TRANSPORTATION INSTITUTE
Texas A&M University
College Station, Texas

# FOREWORD

Studies by the Texas Transportation Institute aimed at the development of safer roadside sign supports have been conducted since 1963. These studies sponsored by the Texas Highway Department in cooperation with the U. S. Bureau of Public Roads led to the concept of a break-away sign support. By early 1965 the phenomenological behavior of the break-away concept had become well defined from careful observation of high-speed film records. These records provided qualitative information from full scale crash tests of collisions of automobiles with sign supports. Attempts were made to secure quantitative information concerning displacement, velocity changes and acceleration from the high-speed film data. However, reduction of displacement-time data proved arduous and inconclusive. For this reason a series of six tests was planned in which an accelerometer was mounted on the crash vehicle to provide a record of the apparent change in acceleration at a point on the frame of the vehicle. The data thus acquired proved to support the data obtained from the high-speed film record.

This progress report contains a description of the tests and of the instrumentation. Additionally its text explains a method for analysis of accelerometer data and correlation with high-speed film data. The report also includes information acquired from strain gages and chronology of a collision incident.

ACKNOWLEDGEMENTS

More than thirty people were employed in various capacities in this investigation, and recognition to each for his individual contribution is acknowledged here.

Particular recognition is made of the efforts of D. L. Hawkins, Supervising Design Engineer, Texas Highway Department, without whose perseverance and engineering judgment there would have been no break-away base sign support to study, and to T. J. Hirsch and C. H. Samson, Jr., without whose encouragement and critical review there would have been no completion of this work.

The opinions, findings and conclusions expressed in this publication are those of the author and not necessarily those of the Bureau of Public Roads.

TABLE OF CONTENTS

LIST OF TABLES

LIST OF FIGURES

## ABSTRACT

A series of six full-scale crash tests employing an automobile towed into a collision with one support of a two support highway roadside sign was conducted; these six instrumented tests were part of a research program embracing a total of forty-three crash tests. The series considered in this report was conducted for the purpose of refining electronic and photographic instrumentation techniques. Fixed base sign supports were struck in two of the six tests, and break-away base sign supports were struck in the remaining four tests.

High-speed motion picture films were made of each of the crash tests. These films provided a Displacement-Time record of each collision. A piezoelectric accelerometer was installed on the frame of each crash vehicle. The signal from this accelerometer was transmitted to a recording oscillograph, and a trace of the accelerometer behavior was recorded on light sensitive paper. This trace provided an Acceleration-Time record of each collision. Other electronic instrumentation was installed in order to provide Strain-Time information about the collision.

A method of successive summation of areas contained by the Accelerometer trace is presented which results in a Displacement-Time plot which has been compared with the corresponding data recorded from examination of the high-speed films.

Examination and comparison of information from each of the records obtained from the final two tests has led to a time dependent description, or chronology of

collision. This description of the collision incident and definition of critical events in the history of the collision provides an original description of the behavior of break-away sign supports subjected to collision by an automotive vehicle.

# CHAPTER I

## THE PROBLEM

Contemporary highway design provides for vehicle operation at high speed on multilane roadways. Exit ramps must be provided for egress from such facilities. Each vehicle operator travelling on a highway at a legal speed must make decisions concerning lane selection and exit ramp choice if he is to reach his destination. Guide signs are installed to aid an operator in this decision making process. Location, design, and construction of such signs on the Federal Interstate highway system are accomplished in accordance with policies established by the American Association of State Highway Officials. Engineers in the several state highway departments have discretionary authority in interpretation of the broad policies of the A.A.S.H.O. However, certain sign configurations are widely used.

The two post sign support seen in Figure 1 has been employed in increasing numbers. Many factors have been considered in the selection of this sign support design. It consists of a pair of vertical cantilever wide flange beams which are economical, strong, and stable when subjected to wind forces. It has aesthetic quality, supports a readable sign, and is located adjacent to the roadway. In short, the sign support is excellent in many respects, but can also be lethal. It is this last characteristic which has motivated the present


Reprinted by permission of THE HOUSTON POST

FIGURE 1

research.

The Texas Highway Department and the Texas Transportation Institute have been actively engaged in studies[1*] of the impact behavior of certain sign supports. The aim of these studies has been the development of a two post sign support which would present less of a hazard than the basic A.A.S.H.O. design. Consideration of this aim resulted in modifications of the basic two post sign support. The investigators introduced certain mechanical devices into each post. These devices permit the post to be released at its base upon impact and to be deflected in front of and above the crash vehicle. Details of these devices are shown in Figure 2. The break-away device is located at the base of the support post. It is fabricated by making a right-angle cut across the beam, welding plates to the adjacent post pieces, and reconnecting the pieces by bolting them together. The adjacent plates have notches which permit the bolts to become disengaged upon impact by a vehicle. This base detail is shown in isometric view in Figure 2.

The "plastic hinge" joint detail seen in Figure 2 is formed in the post at the lower edge of the sign face. This joint consists of a right-angle cut cross the forward flange and part of the web of the beam. The cut is terminated at the fillet of the rear flange and the forward flange is reconnected by a mechanical fuse. The fuse consists of either a cast-iron plate which is designed to fracture upon impact or a

*Superscript numbers refer to items in the List of References.

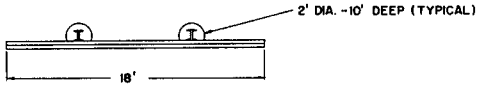


TOP VIEW

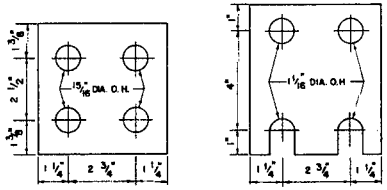


CAST IRON PLATE
3/8" THICK, A48, CLASS 30
TEST NO. 40

STEEL NOTCHED PLATE
3/8" THICK, A441
TEST NO. 41

MECHANICAL FUSE DETAILS

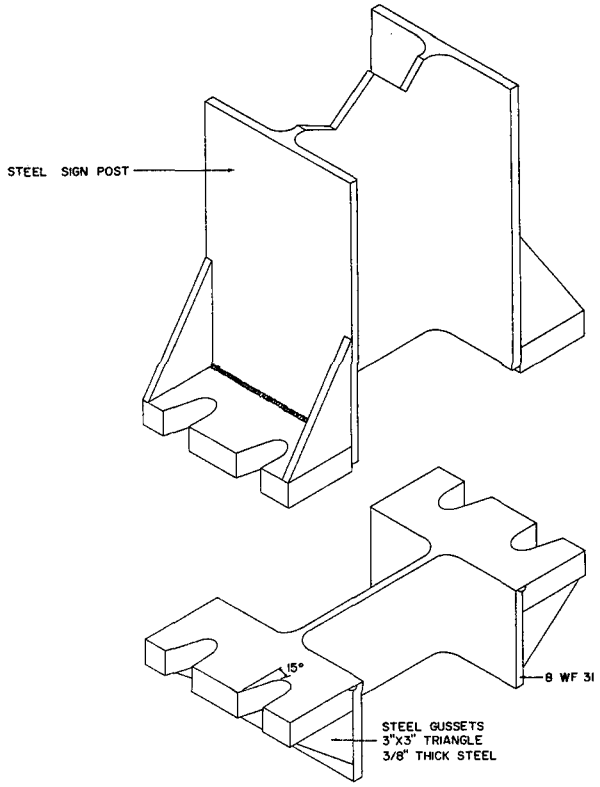


BASE DETAIL AT
JUNCTURE WITH POST

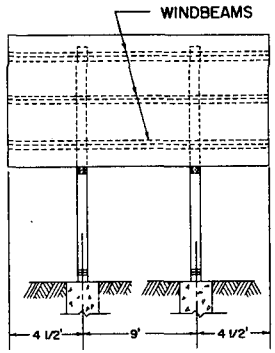


FRONT VIEW

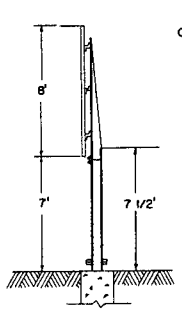


SIDE VIEW

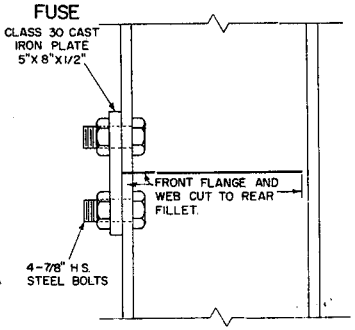


"PLASTIC HINGE" JOINT

POST CUT AS SHOWN AND REJOINED WITH CAST IRON PLATE. BACK FLANGE PROVIDES "PLASTIC HINGE".

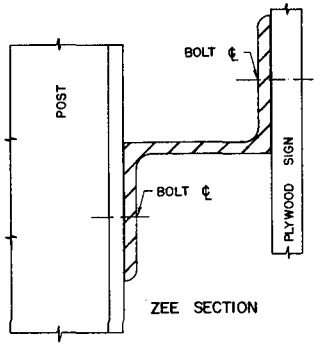


ZEE SECTION

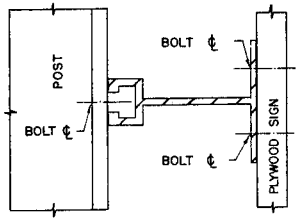


EXTRUDED SECTION

WINDBEAM DETAILS

FIGURE 2 - BREAK-AWAY DETAILS

steel notched plate which is designed to slip upon impact. The purpose of the fuse is to permit the break-away post section to be elevated over the crash vehicle. Details of the fuses are shown in Figure 2. The break-away base and "plastic hinge" joint are provided in each support post. The investigation reported here considers the case in which one break-away post is struck by the crash vehicle.

Sequence photographs of an early test are shown in Figure 3. These photographs illustrate the moment of impact (1), base release (2), fuse plate fracture (3), and "plastic hinge" action (4). The phenomenological behavior of the impact is thus defined.

The initial phase of the earlier studies resulted in the development of a full-scale crash test facility.[1] A high-speed motion picture camera was employed to record the behavior of the sign support and automobile during a controlled collision.[2]

The procedure employed in developing the break-away sign posts consisted of fabrication, testing, viewing films, making modifications and re-testing. This process resulted in design modifications which were adopted by the Texas Highway Department and were incorporated into their design and construction standards. The philosophy of this initial series of tests was to ascertain the phenomenological behavior of the sign supports, and to make modifications and improvements. The method has been characterized as phenomenological because the behavior of the post is evident, but not quantitatively interpreted or

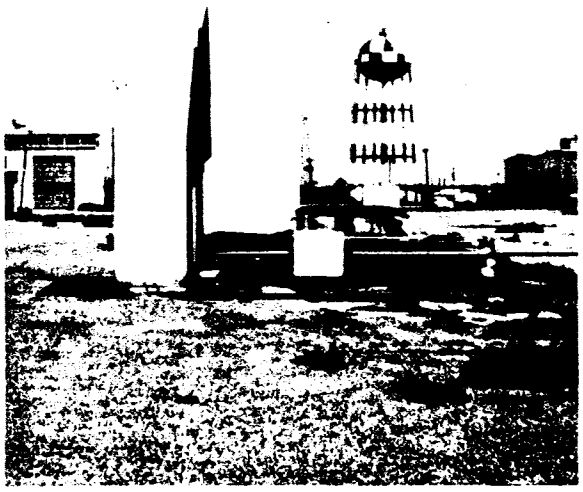

1

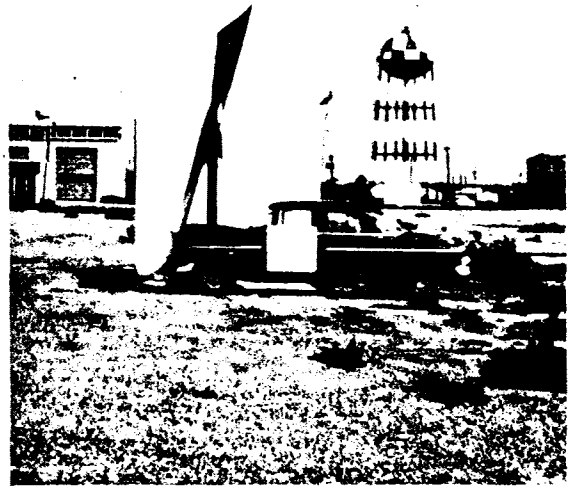

2

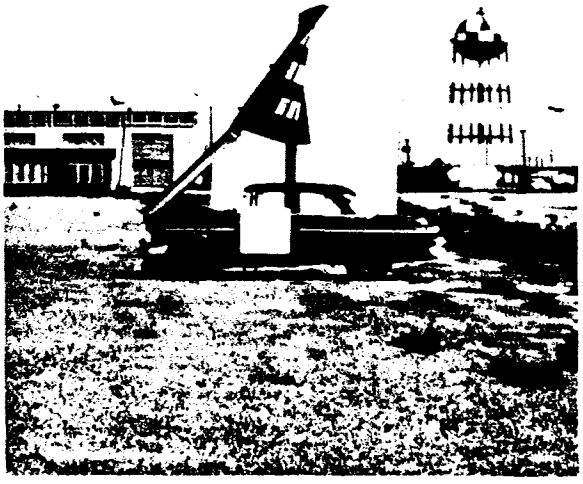

3

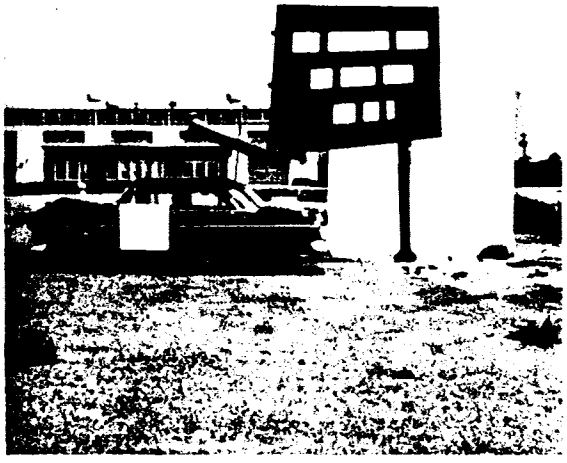

4

FIGURE 3 — SEQUENCE PHOTOGRAPHS

explained. However, through observation of films of actual crash tests an improved sign support was evolved.

The behavior of the improved sign support for a variety of post sizes, automobiles, trucks, and other vehicles might by studied by continuing this slow and expensive approach. In this investigation an alternate procedure has been adopted in which the high-speed films have been supplemented by electronic devices.

The general objective of the present research was to produce a time dependent description of vehicle and break-away support post behavior during a collision incident. In addition to the general objective the specific objectives were:

(1) to develop a technique for acquiring and reducing high-speed film data of the collision incident,

(2) to develop a technique for reducing and analyzing data from an accelerometer mounted on the frame of the crash vehicle,

(3) to correlate the information from the two data gathering systems,

(4) to secure information concerning strain and stress in elements of the "plastic hinge" joint during the collision incident, and

(5) to determine the force in the support post at bumper height during the collision incident.

An examination of the literature relating to crash research leads one to the conclusion that data gathering techniques have improved considerably during the past twenty years; however, it is apparent that data reduction and analysis have lagged behind the improved instrumentation capabilities. The literature reviewed in Chapter II contains many

references to methods of instrumentation and presents data records from crash tests, but none of the investigators has presented a correlation of data from the independent gathering systems. In the present study a correlation of data from independent systems has been accomplished, and original descriptions of collision incidents have been presented.

# CHAPTER II

## REVIEW OF LITERATURE

The present research involves the collisions of automotive vehicles with highway sign supports, and a study of available literature related to crash research has been made. For more than thirty years vehicle designers and engineers at General Motors have been conducting crash tests in order to evaluate the structural integrity of automobiles. These tests were made before the development of high-speed cameras or high-response accelerometers; the results were in terms of visual observation made at the time of the crash test.[3] In the years since World War II, testing techniques, equipment and instrumentation have been improved. A review of the development of crash research techniques at the General Motors Proving Grounds has proven valuable.

Other researchers have attempted full-scale tests of concrete bridge rails subjected to automobile impacts. The California Division of Highways has conducted a series of full-scale tests of concrete bridge barrier rails, a barrier rail and curb combination and barrier curbs without rails.[4] Photographic and mechanical systems of instrumentation were employed to record all actions and reactions during the high-speed collisions involved in this test program. A calibrated speedometer was installed in the crash vehicle. A camera was used to record longitudinal and lateral changes in acceleration during the history of the crash event;

instrumented anthropometric dummies were placed inside the crash vehicle. An interesting feature of this test was the employment of a radio to control the vehicle prior to collision.

A paper on the testing of various guard rails[5] was presented at the Annual General Meeting of the Engineering Institute of Canada at Quebec. An interesting feature of this research was the vehicle projection system which consisted of a wooden trough that provided a trajectory for the impacting vehicle. Vehicle speeds prior to impact were determined by using radar and high-speed cameras. Films were taken of the vehicle prior to impact, at impact, and following impact. The test speed was set at 55 mph and a variety of test vehicles was employed. A tabulation of results for eleven test vehicles is presented. Included in the table are speeds before and after impact determined by radar and from film analysis, and average changes in acceleration. These changes in acceleration were presumably calculated from an analysis of the film records of the test. Electronic instrumentation was apparently not employed in this study.

Sixty-four full-scale collision experiments were conducted during the years between 1949 and 1963 by the Institute of Transportation and Traffic Engineering, University of California, Los Angeles. High-speed cameras and electronic instrumentation were employed in these tests, which were conducted under a variety of conditions. One series involved

automobiles crashing into fixed barriers,[6] another was related to rear end collisions,[7] and another involved head-on collisions of two automobiles.[8] Also investigated were automobile side-impact collisions;[9] the final fourteen tests[10] were intersection collision experiments. This last series of collisions was conducted to obtain detailed information on the dynamic interaction between motorist and vehicle structure. The UCLA-ITTE experiments employed increasingly complex and expensive instrumentation.

A British publication[11] gives an account of results from impact tests on telegraph poles. These tests, carried out at the Road Research Laboratory of the Department of Scientific and Industrial Research, were made to determine which types of street lighting column and telegraph pole are likely to cause least injury to the occupants of a colliding vehicle. The impact velocities were approximately 23 to 28 mph. Potentiometric accelerometers attached to the chassis of the crash vehicles indicated their acceleration change during collisions, and high-speed cameras recorded the motion of the cars and the poles. The relative velocity between the head of an unrestrained occupant in a vehicle and the windshield of the car, and the time from the moment of impact of the vehicle with the pole to the moment of contact of the head with the windshield are tabulated. Included for comparison in the tabulation are results for telegraph poles fabricated from creosote

treated baltic redwood and thin sheet steel lighting columns.

Other researchers[12] at the Road Research Laboratory have conducted tests on lamp columns fabricated from thin sheet steel, tubular steel, and concrete. These British investigators used high-speed film analysis and accelerometer records as a check of relative accuracy of the instrumentation. A discussion of the difficulties encountered with accelerometer analysis indicated that the procedure adopted involved considerable adjustment of the accelerometer record to produce computed velocities. These computed velocities were then compared with velocities obtained from the films.[13] It is clear from the text that a process of integration is employed in the accelerometer analysis and it is assumed that the velocities obtained from the films are determined by computing the slope of the Displacement-Time data taken from the film record.

An important discussion of accelerometer analysis is contained in a paper[14] by Stapp. He was interested in human exposures to linear acceleration, and the tests were performed using a sled propelled by solid-fuel rockets. These famous tests were performed at Muroc Air Force Base, California, in 1949. Stapp[15] discusses factors limiting the accuracy of acceleration records. He also states that "...the oscillograph trace was arbitrarily smoothed to disregard vibrations".[16] Manual techniques of analyzing oscillographic records were employed, including the use of

planimeters for determination of areas under curves. These experiments were not collison tests but a considerable amount of useful information is contained in the report. The abstract of Stapp's paper is quoted here:

> "A linear decelerator was used to expose three healthy young males to decelerations from back to chest in the seated position. Two series of decelerations at approximately 5 g increments up to 30 g's were carried out with initial rates of change of deceleration at 500 and 1000 g's per second. Total duration of exposures range from .15 to .42 seconds. Subjective accounts of the experience of each individual are given and oscillographic records of the decelerations on the chest, on the helmet, and on the seat discussed. No more than mild discomfort or injury was experienced. Ultimate decelerations voluntarily tolerable to the subjects used was not reached, since the tests were halted to improve the mechanical reliability of the decelerator".

Stapp's values of 30 g's for deceleration and 1000 g's per second for initial change of deceleration as well as the total duration of exposure are widely quoted in the literature as human tolerance levels. Stapp concludes that

> "Linear decelerations of 30 g lasting for .11 second can be tolerated by human subjects in the backward facing position. The mild degrees of injury and discomfort noted indicate that higher values of deceleration can be survived by humans in this position if the body is uniformly supported".[17]

The values reported by Stapp are dependent upon curve smoothing and determination of slopes of plotted curves. He describes the technique involved in arriving at his tabulated results. However, since no sample calculations are included, and since full-scale curves are not available, it was not possible to check Stapp's results. This is not to question the

value of Stapp's work, but is mentioned here in order to emphasize the point that detailed techniques must be applied in order to reproduce comparable results from data analyses.

Other investigations on dynamic tests of median barriers,[18] on collisions with lighting poles,[19] on appraisals of guardrail installations by car impact and laboratory test,[20, 21, 22] and related topics have been studied.

# C H A P T E R  I I I

## SUMMARY OF CRASH TESTS

A total of forty-three full scale crash tests have been conducted by the Texas Transportation Institute.[1, 2] Six of these were instrumented tests conducted in the spring and summer of 1965. Three tests (32, 33, and 35) were conducted in the spring to provide information concerning behavior of the test components and the electronic system under collision conditions. The experience gained from these tests served as a basis for planning the second series of three tests (39, 40, and 41), which were conducted in the summer of 1965. Critical review of the initial series of three tests resulted in changes in test components, test procedures, and instrumentation techniques. These changes are considered in subsequent chapters. The numbering of tests is not continuous, because Tests 34, 36, 37, and 38 were not a part of this instrumented series.

Two types of support posts were studied in this investigation: rigidly bolted base support posts (Tests 32 and 39), and break-away base support posts (Tests 33, 35, 40, and 41). A complete description of test components is contained in Chapter IV, details of instrumentation are discussed in Chapter V, and a comparison of behavior of the two types of support post is presented in Chapter VI.

# CHAPTER IV

## DESCRIPTION OF TEST COMPONENTS

The signs and sign supports were fabricated in accordance with Texas Highway Department Specifications. The fixed base support posts were fabricated in accordance with the standard Texas Highway Department design for roadside signs. These signs are similar in appearance to the developmental break-away support post signs shown in Figure 2. However, the base plate of each sign post is welded to the vertical post, and this base plate is connected by anchor bolts embedded in concrete foundations. The break-away base, "plastic hinge" joint, and mechanical fuse details were not employed in the bolted base support posts. These details were developmental until a standard design for break-away sign support posts was adopted by the Texas Highway Department in January, 1965. This design employed a cast-iron mechanical fuse for connecting the forward flange of the "plastic hinge" joint. The design specified that the sign face would be bolted to horizontal windbeams which would be fastened to the vertical support posts.

The windbeams were fabricated from extruded aluminum beams. The cross-sectional configuration of the beams consisted of a flange, a web, and a channel (see detail in Figure 2). The flange permits direct bolting of the sign face to the windbeams, and the channel is designed

to restrain the head of the bolt of a friction clamp. This clamp is employed to connect the windbeam to the support posts. The use of clamps greatly enhances construction operations in the field. However, it was found in Tests 33 and 35 that the clamps and the extruded aluminum windbeams failed under impact loading, whereas the cast-iron mechanical fuse did not fracture. As a consequence the support post did not behave as anticipated. In these tests the support post became disengaged from the sign face, and was cast aside by the crash vehicle. This behavior was considered unsatisfactory since it was not in accordance with the desired phenomenological behavior seen in Figure 3. A modification of the extruded aluminum windbeam and clamp connection was proposed and adopted. Aluminum "Z-Beams" were substituted for the extruded aluminum beams in Tests 40 and 41, and the windbeams were bolted to the support posts. Thus the clamps were eliminated and the support post behavior proved satisfactory.

A cast-iron plate mechanical fuse was employed in Test 40. However, difficulties in casting, handling, bolting and maintaining cast-iron fuses led to the development of another type of fuse. This fuse consisted of a steel plate with notches at one pair of bolt holes (see Figure 2), which permit the bolts to slip free upon impact. The notched steel plate fuses eliminate the difficulties found with the cast-iron plates. Using steel plates permits bolting in accordance with the

"turn of nut method," this is an additional advantage, for the bolted connection is in accordance with current bolting practice.[23]

Development of break-away post components, such as windbeams, connecting clamps, mechanical fuses, and other details resulted in variations in the several test components. A summary of the sign components is contained in Table I. The table also lists information concerning the crash vehicles employed in the testing program. Selection of crash vehicles was predicated upon availability of used vehicles on the local market. It was required that each vehicle be equipped with all major structural components including fenders, doors, and windows. It was further specified that each vehicle be equipped with radiator, engine, transmission, drive shaft, differential, and similar parts. Each vehicle weight was obtained at a public weighing scale just prior to the crash test.

TABLE I - DESCRIPTION OF TEST COMPONENTS

| TEST NO. | SIGNS AND SUPPORTS | | | | CRASH VEHICLES | |
|---|---|---|---|---|---|---|
| | SIGN FACE | SUPPORT POSTS | WIND BEAMS | MECHANICAL FUSE | DESCRIPTION | WEIGHT |
| 32 | 5'x6'x5/8" plywood | 2-5WF16 painted steel, ASTM A36 | extruded aluminum, ASTM B209, alloy 6061-T6 | None | 1954 Chevrolet 4-door sedan | 3230 lb. |
| 33 | 8'x16'x5/8" plywood | 2-8WF20 painted steel, ASTM A441 | extruded aluminum, ASTM B209, alloy 6061-T6 | cast-iron plate, ASTM A48 Class 30 | 1952 Ford 4-door sedan | 3130 lb. |
| 35 | 8'x16'x5/8" plywood | 2-8WF20 painted steel, ASTM A441 | extruded aluminum, ASTM B209, alloy 6061-T6 | cast-iron plate, ASTM A48 Class 30 | 1953 Chevrolet 2-door sedan | 3215 lb. |
| 39 | 8'x16'x5/8" plywood | 2-8WF20 painted steel, ASTM A36 | 3-3Z2.33 aluminum, ASTM B209, alloy 6061-T6 | None | 1955 Ford 4-door sedan | 3240 lb. |
| 40 | 8'x16'x5/8" plywood | 2-8WF20 hot-dip galvanized steel, ASTM A441 | 3-3Z2.33 aluminum, ASTM B209, alloy 6061-T6 | cast-iron plate, ASTM A48 Class 30 | 1955 Ford 4-door sedan | 3240 lb. |
| 41 | 8'x16'x5/8" plywood | 2-8WF20 painted steel, ASTM A36 | 3-3Z2.33 aluminum, ASTM B209, alloy 6061-T6 | notched steel plate, ASTM A441 | 1955 Ford 4-door sedan | 3620 lb. |

Note: Signs and sign supports were constructed in accordance with Texas Highway Department plans for Interstate Standard Roadside Plywood Guide Signs (SMD-4, Revised 1962), Fixed Base Type Posts; and for Interstate Standard Roadside Plywood Guide Signs, Break-Away Type Posts (SMD-8, issued 1-65), with modifications.

# CHAPTER V

# INSTRUMENTATION

## High-Speed Cameras

In the crash research a high-speed camera was employed as the basic instrument for recording the history of a collision. Quantitative data can be obtained from this film record. The camera was operated at a nearly constant speed and distance references were established on the test components. Time and displacement data were thus permanently recorded on the film. Observation and critical review of films of earlier tests[1] served as a guide to techniques employed in Tests 32, 33, and 35. Table II contains a list of devices used in these tests. The centi-revolution clock provided a supplementary time record on the film.

Reports by other investigators, combined with experience gained from earlier tests,[1] resulted in changes and improvements in equipment and techniques. In Tests 39, 40, and 41, stadia markers were provided on the side of the crash vehicle. These furnished a distinguishable unit of length on the crash vehicle. A stadia reference board and range poles were installed adjacent to the collision area, these devices established dimension and references lines on the film record. Table III describes the devices employed in Tests 39, 40, and 41. A comparison of Tables II and III illustrates the changes and additions to

TABLE II - PHOTOGRAPHIC INSTRUMENTATION - TESTS 32, 33, AND 35

| ITEM | DEVICE | DESCRIPTION | LOCATION | TO PROVIDE |
|---|---|---|---|---|
| 1 | High-speed motion picture camera | Wollensak, Fastax WF-3T, 16 mm Kodachrome II, Daylight KR 449 film, 1000 frames per second | Approximately 100 feet from impact point, at right angles to line of travel of crash vehicle | Crash vehicle Time-Displacement Data |
| 2 | Moderately high-speed motion picture camera | Kodak Cine Special II, 16 mm Kodachrome II, Daylight KR 449 film 64 frames per second | Random positions | General views of crash test |
| 3 | Standard-speed motion picture camera | Bell & Howell 70 HR, 16 mm Kodachrome II, Daylight KR 449 film 24 frames per second | Random positions | General views of crash test |
| 4 | Stadia markers | 3/4" wide drafting tape at 1'-0" intervals | On side of crash vehicle | Length reference for analysis of high-speed motion pictures |
| 5 | Centi-revolution clock | 2 foot diameter clock face, divided into 100 intervals, clock hand attached to 1800 rpm synchronous electric motor | Approximately 20 feet from impact point (about 90 feet from high speed camera) | Time reference for analysis of high-speed motion picture film |

TABLE III - PHOTOGRAPHIC INSTRUMENTATION - TESTS 39, 40, AND 41

| ITEM | DEVICE | DESCRIPTION | LOCATION | TO PROVIDE |
|---|---|---|---|---|
| 1 | High-speed motion picture camera | Wollensak, Fastax WF-3T, 16 mm Kodachrome II Daylight KR 449 film 1000 frames per second | Camera A, See Figure 5 | Crash vehicle Time-Displacement data |
| 2 | High-speed motion picture camera | Wollensak, Fastax, WF-3, 16 mm black and white Tri-X Reversal TXR 430 film, 1000 frames/sec | Camera B, See Figure 5 | Crash vehicle Time-Displacement data (back-up for Camera A) |
| 3 | Moderately high-speed motion picture camera | Kodak Cine Special II, 16 mm Kodachrome II, Daylight KR 449 film, 64 frames/second | Random positions | General views of crash test |
| 4 | Standard-speed motion picture camera | Bell & Howell 70 HR, 16 mm Kodachrome II, Daylight KR 449 film, 24 frames per second | Random positions | General views of crash test |
| 5 | Stadia reference board | 2"x6"x12'-0" pine board with black & white spaces in alternate 12-inch increments | Adjacent to impact area | A fixed horizontal length reference |

TABLE III - PHOTOGRAPHIC INSTRUMENTATION - TESTS 39, 40, AND 41
(CONTINUED)

| ITEM | DEVICE | DESCRIPTION | LOCATION | TO PROVIDE |
|---|---|---|---|---|
| 6 | Stadia markers (reference targets) | 6" x 16 gage sheet metal painted with 3"x3" diamond-shaped black triangles on white background | On side of crash vehicle | Length reference for analysis of high-speed motion pictures |
| 7 | Range poles | 3/4"x8'-0" pipe poles with black & white spaces in alternate 12-inch increments | Adjacent to stadia reference boards | Fixed reference points |
| 8 | Centi-revolution clock | 2-foot diameter clock face, divided into 100 intervals, clock hand attached to 1800 rpm synchromous electric motor | Mounted on back board, see Figure 5 | Time reference for analysis of high-speed motion picutre film |
| 9 | Backboard | 16'-0" x 12'-0" plyboard mounted on wood truss frame | See Figure 5 | Background for photography and pertinent test information |

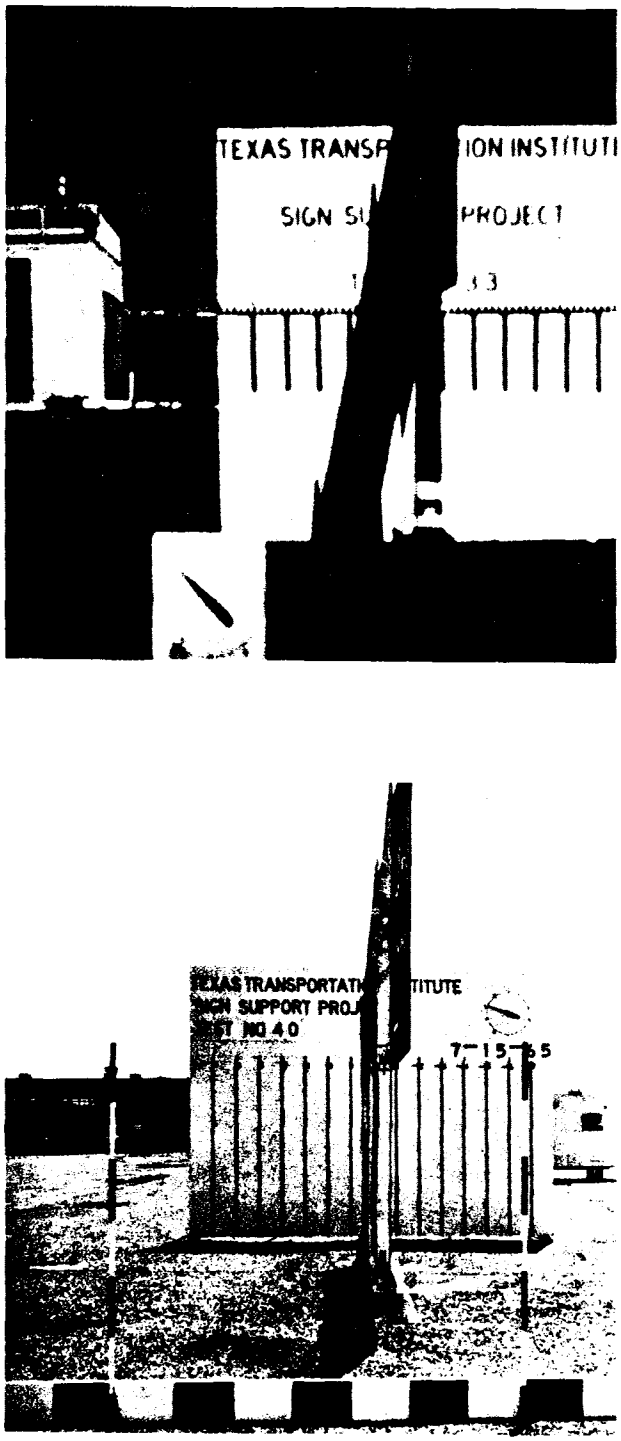


FIGURE 4 - CAMERA FIELDS OF VIEW

the basic photographic equipment. A visual comparison of the photographic field of view in Test 33 and Test 41 is found in Figure 4.

Experience gained from reviewing earlier test films resulted in more careful positioning of cameras. Transit and tape methods were employed to locate the cameras and other devices. The measurements and locations can be seen in Figure 5. Camera "B" was installed to provide a film record in the event that camera "A" might have failed to operate. The latter camera did perform satisfactorily in each test; and the film from this camera is the film record from which all data reduction was accomplished.

## Electronic Instrumentation

A variety of electronic instruments was employed in the tests. A complete listing and description of the devices installed for Tests 32, 33, and 35 is contained in Table IV; and Table V contains the listing for Tests 39, 40, and 41. Accelerometer displacement, and strain gage data were recorded on rolls of photographic paper by means of an oscillating galvanometer. Speed of the crash vehicle prior to impact was obtained by radar in Tests 40 and 41. A comparison of Tables IV and V will indicate that more instrumentation was employed in the later series than in the earlier series. Also, the strain gage instrumentation was changed in the later tests. These additions and substitutions

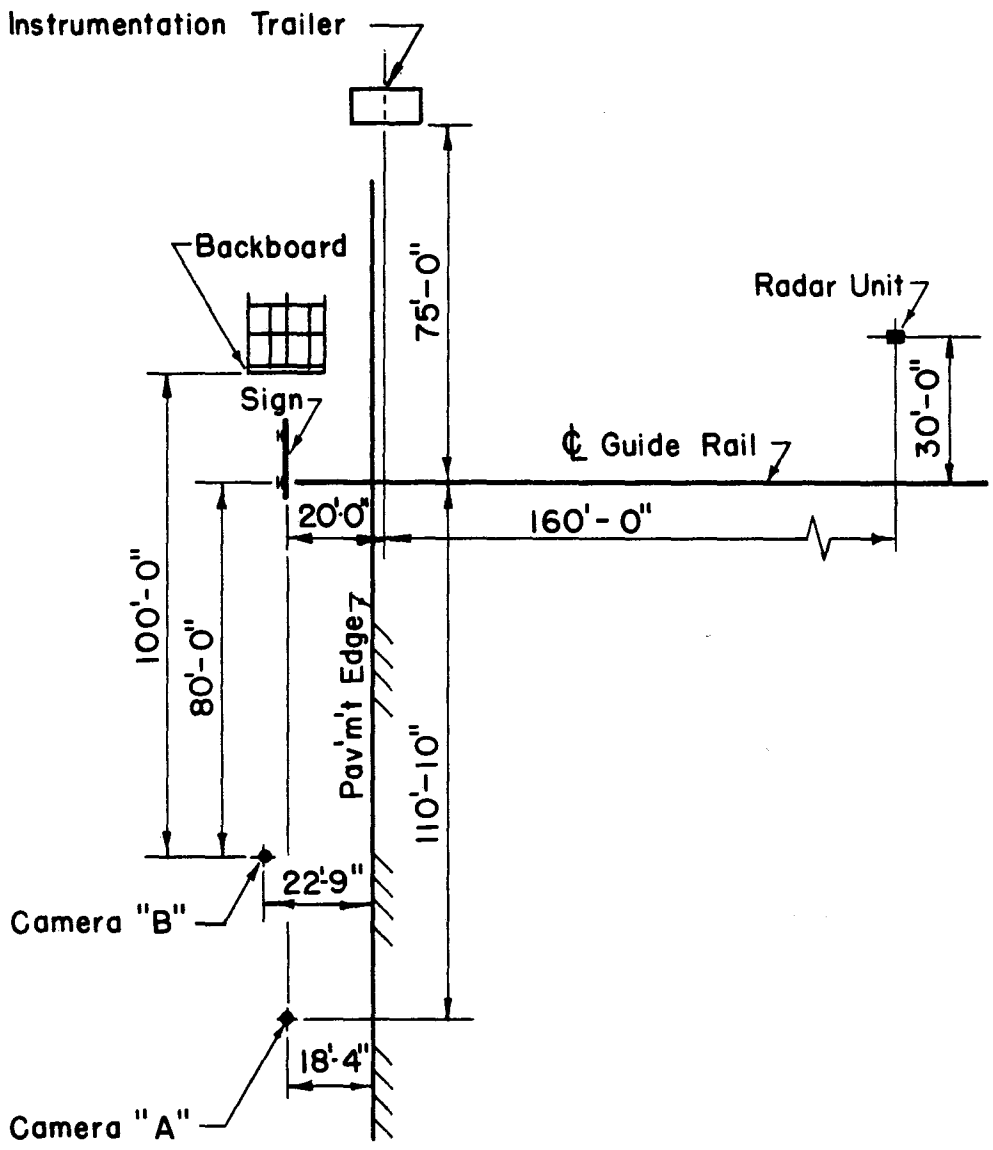


Camera A: WF 3T Fastax-KODACHROME II, Daylight, KR 449
Camera B: WF 3 Fastax—Tri-X Reversal Film, TXR 430

# FIGURE 5 — PLAN OF TEST AREA

TABLE IV - ELECTRONIC INSTRUMENTATION - TESTS 32, 33, AND 35

| ITEM | DEVICE | DESCRIPTION | LOCATION | TO PROVIDE |
|---|---|---|---|---|
| 1 | Piezoelectric Accelerometer | Endevco Model 2211C with Model 2614B Input Amplifier | Mounted on left main frame member, 9'-0" behind impact point on bumper | Deceleration data |
| 2 | Piezoelectric Accelerometer | Endevco Model 2211C with Model 2614B Input Amplifier | Mounted on 150 lb concrete block belted to driver's seat | Deceleration data |
| 3 | Recording Oscillograph | Honeywell Visicorder Oscillograph, Model 1508, paper speed: 80 inches per second | Situated in rear of station wagon 75 feet from target sign | Paper record of accelerometer and strain gage sensing under dynamic loading conditions |
| 4 | Shear force transducer (electric resistance strain gage bridge) (TESTS 33 & 35 ONLY) | 4 Budd Strain gages Metal film type C6-121 | Approximately 1'-0" above base of post on inside of front and rear flanges (TESTS 33 & 35 ONLY) | Measurement of slip joint shear force (time variable) |
| 5 | Electric resistance strain gage bridge (TEST 33 ONLY) | 2 Micro-Measurement strain gages, 90° Rosette (EA-13-125TF-120) | 7'-0" above base of post on rear flange (TEST 33 ONLY) | Measurement of strain in rear flange (time variable) |
| 6 | Electric resistance strain gage bridge (TEST 33 ONLY) | 2 Micro-Measurement strain gages, 90° Rosette (EA-13-125TF-120) | Approximately 8" above base of post on rear flange (TEST 33 ONLY) | Measurement of strain in rear flange (time variable) |
| 7 | Electric resistance strain gage bridge (TEST 35 ONLY) | 2 Micro-Measurement strain gages, 90° Rosette (EA-13-125TF-120) | Mounted on cast-iron fuse plate, 7'-0" above base of post (TEST 35 ONLY) | Measurement of strain in cast-iron plate (time variable) |

TABLE V - ELECTRONIC INSTRUMENTATION - TESTS 39, 40, AND 41

| ITEM | DEVICE | DESCRIPTION | LOCATION | TO PROVIDE |
|---|---|---|---|---|
| 1 | Piezoelectric Accelerometer | Endevco Model 2211C with Model 2614B input amplifier | Mounted on left main frame member, 9'-0" behind most forward point on bumper | Deceleration data (crash vehicle) |
| 2 | Piezoelectric Accelerometer | Endevco Model 2211C with Model 2614B input amplifier | Mounted on 150 lb concrete block belted to driver's seat | Deceleration data (crash vehicle) |
| 3 | Piezoelectric Accelerometer | Endevco Model 2215 with 2614B input amplifier | Mounted near base of post | Acceleration data (support post) |
| 4 | Recording Oscillograph | Honeywell Visicorder Oscillograph, Model 1508, paper speed: 80 inches per second | Situated in instrumentation trailer 75 feet from target sign | Paper record of accelerometer and strain gage sensing under dynamic loading conditions |
| 5 | Impact force transducer (electric resistance strain gage bridge) (TESTS 40 & 41 ONLY) | 4 Budd strain gages, metal film type C6-121 | Mounted on flanges of post (TESTS 40 & 41 ONLY) | Measurement of impact force (time variable) |
| 6 | Electric resistance strain gage bridge (TESTS 40 & 41 ONLY) | 2 Micro-Measurement strain gages, 90° Rosette, type EP-30 | Mounted on rear flange (TEST 40 & 41 ONLY) | Measurement of strain in rear flange (time variable) |

TABLE V - ELECTRONIC INSTRUMENTATION - TESTS 39, 40, AND 41
(CONTINUED)

| ITEM | DEVICE | DESCRIPTION | LOCATION | TO PROVIDE |
|---|---|---|---|---|
| 7 | Electric resistance strain gage bridge (TESTS 40 & 41 ONLY) | 2 Micro-Measurement strain gages, 90° Rosette, Type EP-03-125TF-120) | Mounted on mechanical fuse (TESTS 40 & 41 ONLY) | Measurement of strain in fuse plate (time variable) |
| 8 | Linear Displacement Transducer | 4" potentiometric displacement transducer | Slip-joint release mechanism at base of post, see Figure 6 | Precise determination of post displacement upon impact (time variable) |
| 9 | Linear Displacement Transducer | 19" potentiometric displacement transducer | Slip-joint release mechanism at base of post, see Figure 6 | Precise determination post displacement upon impact (time variable) |
| 10 | Radar Speed Meter | Electro-matic Radar speed meter, Model S2A | Near Impact area, see Figures 5 | Velocity of crash vehicle prior to impact |
| 11 | Recording Ammeter | Esterline Angus Graphic Ammeter, Model AW | Adjacent to Radar Speed Meter | Paper record of crash vehicle speed |

reflect the knowledge gleaned from literature review, as well as the experience gained from earlier tests in this study.

Reproductions of oscillogram records provided by the recording oscillograph are contained in Appendices A and B. The number of available channels on the recording oscillograph was limited: consequently the galvanometer traces overlap. Some of the traces exceeded the width of the recording paper; a condition which arose because the magnitude of certain parameters was unknown. The installation of certain of the devices was made in order to determine limitations of the devices and the recording equipment. These limitations will be discussed later in this work.

The piezoelectric accelerometer installed on the frame of each crash vehicle provided a valuable record of each impact event. This installation was made by welding a steel angle bracket on the frame. A hole was drilled in the bracket, and the accelerometer was thus readily installed or removed. An amplifier and power source were carefully packed in a wooden box which was bolted to the floor of the trunk of the crash vehicle. The signal generated by the accelerometer was transmitted to the recording oscillograph by means of a four-conductor, shielded cable (Belden 8404). This cable was 1000 feet long. It was pulled along by the crash vehicle during each test.

A piezoelectric accelerometer was attached to a 150-pound concrete block placed on the driver's seat. This block was strapped in place by

means of a commercial seat belt fastened to the floor of the vehicle. The signal was transmitted to the recording oscillograph by means of the cable described previously.

## Linear Displacement Transducers

Two devices to determine linear movement of the break-away base were installed in Tests 40 and 41. One of these devices consisted of a metal block attached by a nylon string to the upper part of the post by a nylon thread. This block was permitted to slide along grooves in a plastic arm cantilevered from the lower, or fixed portion of the post. The slide was in contact with an electrical conductor embedded in the plastic arm. The other device consisted of a metal rod which was in contact with an electrical conductor. The first device was constructed to permit a 19-inch travel, and the second device permitted a 4-inch travel. The 19-inch device failed to operate in each test. The 4-inch device produced useful information. The instruments were designed to produce a trace of resistance change as a function of time. This trace was pre-calibrated to indicate displacement of the upper portion of the post with respect to the fixed part of the post. The signal of the change in resistance was transmitted by a stranded wire to the recording oscillograph. Photographs of the displacement devices are found in Figure 6.

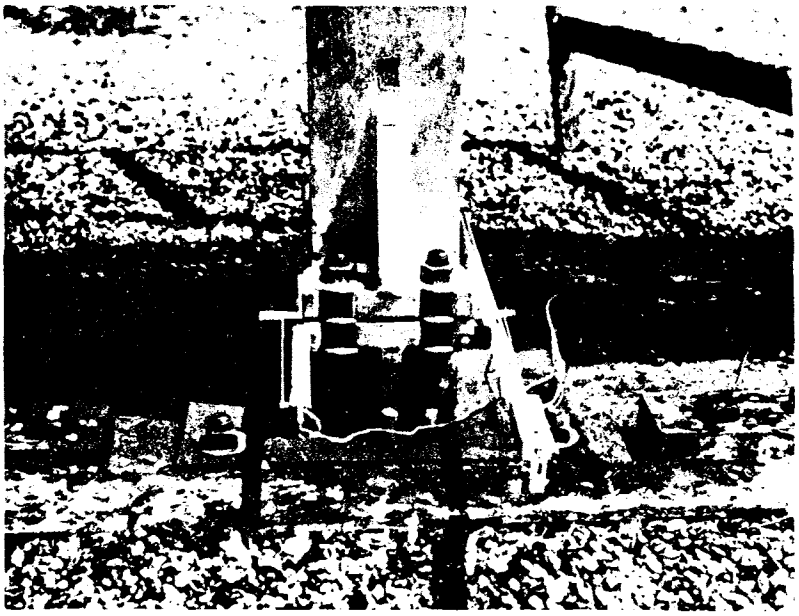

BEFORE IMPACT

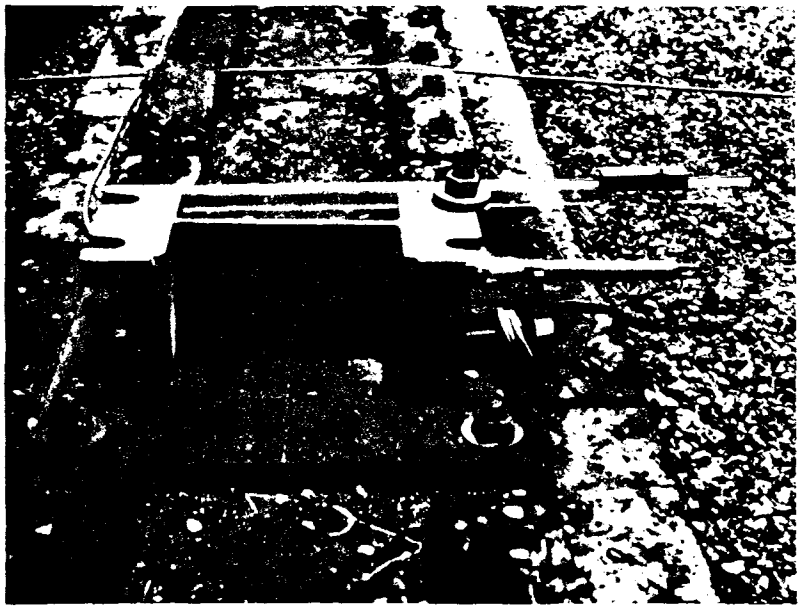

AFTER IMPACT

FIGURE 6 - DISPLACEMENT TRANSDUCERS

## Criteria of Instrumentation

Three requirements were established as criteria for selection of instrumentation. First, a device would provide data susceptible of analysis; second, supplementary instrumentation would be installed, whenever possible, to provide corroborative data; and third, certain installations would be made to ascertain the feasibility of such installations for future testing. At the outset little was known about the magnitude of forces involved. The capabilities of the instrumentation and recording equipment were uncertain. Finally data reduction methods and analysis of reduced data were imperfectly understood. Thus the criteria were established. It now appears that some of the instrumentation satisfied all three requirements, while the remainder of the devices proved to satisfy only the feasibility requirement.

The following chapter contains a discussion of data reduction; a description of a technique for analyzing Acceleration-Time data; and a correlation of film and accelerometer data. In Chapter VII a description of break-away support post behavior is presented. This description is predicated upon corroborative information obtained from the test records and the data analyses.

# CHAPTER VI

## DATA REDUCTION AND ANALYSIS

### High-Speed Motion Picture Analysis

The procedure for high-speed film data reduction consisted of recording crash vehicle displacement and time data for each collision incident, then plotting this crash vehicle displacement as a function of time. High-speed film data were obtained by employing a Wollensak FASTAX 16 mm Motion Analysis Projector, Model WF 329B. This projector has the capability of advancing the film a single frame at a time. A frame counter is attached to the drive mechanism of the projector. The time of various events can be determined since the speed of the camera shutter and film drive can be controlled. The camera was operated in accordance with the manufacturer's specifications. Thus a nearly constant rate of film exposure was obtained for each test. The nominal rate was pre-determined to be 1000 frames per second, so that each frame represents 1/1000 second of time.

The centi-revolution clock provided an additional time record on the film. The clock was operated by a synchronous motor turning at 1800 revolutions per minute. The clock was calibrated by stroboscopic light technique. Therefore, one revolution of the clock hand represented 1/30 second of time.

Two means of recording time were thus available. Time computed by

frame count and by the centi-revolution clock were correlated and found to be in good agreement for each test. Examples of correlation are contained in Appendix C. Correlation of the clock and the frame count was improved in the later tests. The improvement can be observed by comparing the plot for Test 35 with that of Test 41. Instrumentation errors are inherent in each timing system, but the clock has been considered to be more reliable in the earlier tests, because the camera motor had not been started soon enough in these tests. Correlation was made for each test in order to verify the time record provided by the centi-revolution clock, and the clock record was employed for all data reduction procedures.

Reference markers at predetermined length intervals were established on the side of the crash vehicle in each test. Strips of tape were applied at one-foot intervals to the side of the vehicle in Tests 32, 33, and 35. An improvement in reference markers was made in Tests 39, 40, and 41 by employing stadia markers having a triangular configuration painted on a six-inch wide strip of sheet metal. This strip of sheet metal was attached to the side of the crash vehicle. The triangular configuration provided a three-inch increment of length on the film record. The one-foot increments established on earlier crash vehicles proved to be inadequate. In order to improve the precision of length data, it was necessary to subdivide the one-foot increments by marking lines

on the viewing screen. Precise establishment of subdivided lines proved to be a difficult task, and any slight movement of the projector or screen produced incorrect data.

Adoption of the triangular stadia markers alleviated the early difficulties encountered in determining crash vehicle displacements. An additional refinement was made in Tests 39, 40, and 41. This refinement was accomplished by placing vertical range poles adjacent to the impact area. These range poles provided a vertical reference line on the film. Some of the difficulties were thus eliminated, and the reproducibility of data was much improved.

Displacement and time data for each test were recorded and plotted. The procedure for analyzing data to determine changes in velocity and acceleration of the crash vehicle involves a process of graphical differentiation. Average velocity of the crash vehicle during an arbitrary increment of time may be defined as the slope of the Displacement-Time curve at the arbitrary instant of time. This may be stated

$$V = \frac{\Delta D}{\Delta T}$$

where $V$ is the average velocity during the arbitrary increment of time

$\Delta D$ is the displacement increment

$\Delta T$ is the time increment

Displacement-Time curves for fixed base support post (e.g., Tests 32 and 39) present a curvilinear configuration during the interval of time following impact. Such a curve is susceptible of a process of successive graphical differentiation. A first differentiation will produce a set of Velocity-Time values which may be plotted. The process of graphical differentiation may be applied to the resulting curve. Average acceleration of the crash vehicle during an arbitrary increment of time may be defined as the slope of the Velocity-Time curve at the arbitrary instant of time. This may be expressed as

$$A = \frac{\Delta V}{\Delta T}$$

where A is the average acceleration during the arbitrary increment of time

$\Delta V$ is the velocity increment

$\Delta T$ is the time increment

In a fixed base support post collision, the apparent displacement of a fixed reference point on the body of the vehicle occurs as the front end of the vehicle is crushed. This crushing continues for approximately one-tenth of a second following impact. Observation of the film record revealed that the support post is also crushed with an apparent displacement of the fixed reference point. The support post also deformed permanently, and this produced additional apparent displacement of the

fixed reference point. The exact duration of the collision incident is difficult to determine from the high-speed film because vertical as well as horizontal displacement of the vehicle occurs near the end of the incident. The vehicle also yaws near the end of the collision incident, and this yawing further complicates the Displacement-Time analysis. The process of successive graphical differentiation is illustrated in Figure 7, and a detailed discussion of Test 32 and 39 is contained in Chapter X.

The Velocity-Time curve provides a description of the velocity variation prior to impact and following impact. Notwithstanding the difficulties described previously, an estimate of the duration of the collision incident may be made by observing the time at which the computed velocity becomes zero. The Acceleration-Time curve also provides a description of the acceleration variation. An estimate of the peak negative acceleration may be obtained from the computed acceleration values. The two curves resulting from the graphical differentiation process are dependent upon the technique employed. Choce of plotting scale and number of increments employed as well as fitting a smooth curve to the plotted points affect the results of the process. Reproducibility of results by other analysts is thus speculative.

Displacement-Time curves for break-away base support post present a nearly linear configuration during the interval of time in which the vehicle is in contact with the support post. The apparent displace-

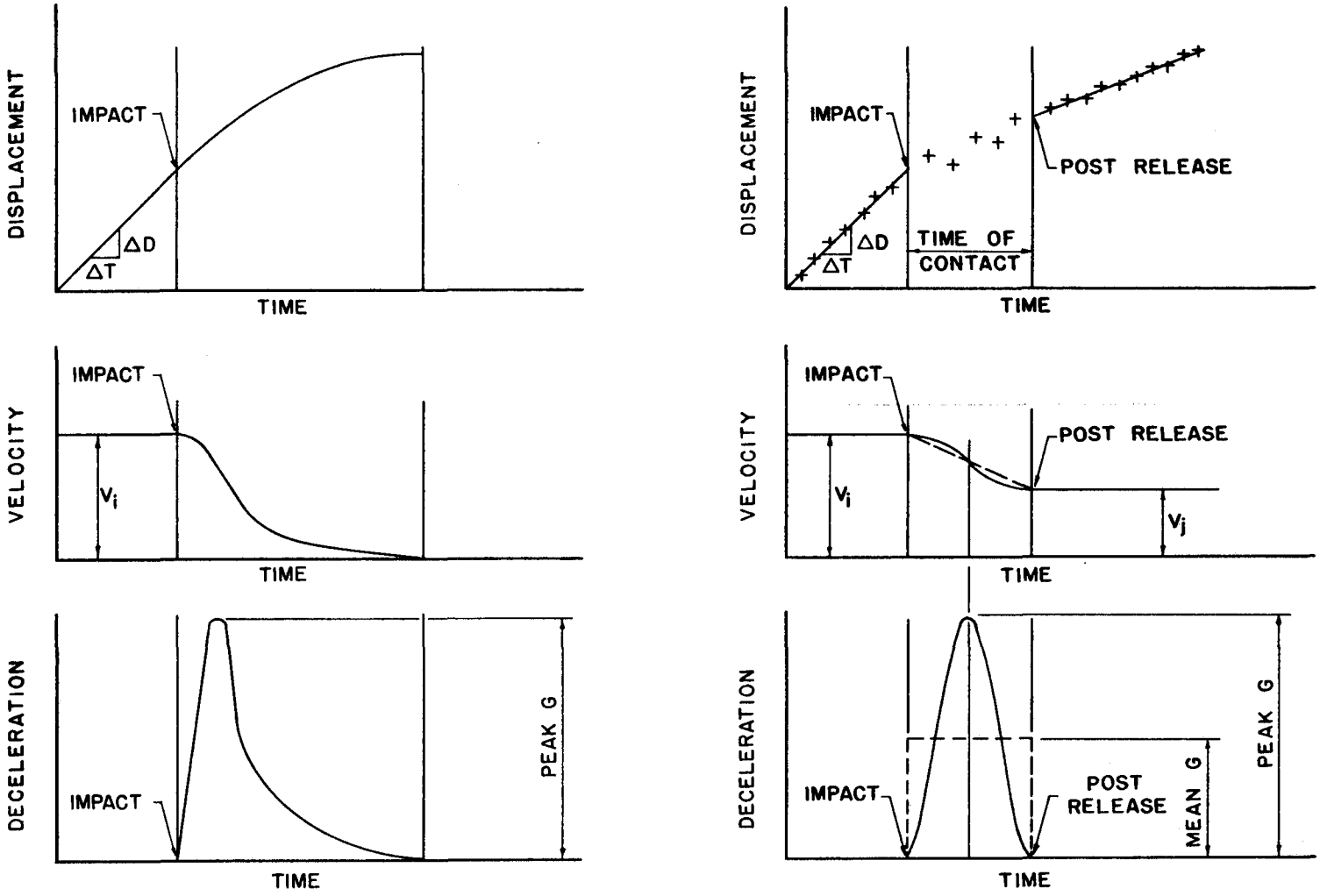


FIXED SUPPORT POST

BREAK-AWAY SUPPORT POST

FIGURE 7 – FILM ANALYSIS BY GRAPHICAL DIFFERENTIATION

ment of a fixed reference point on the body of the vehicle occurs as the front end of the vehicle is crushed, but this crushing continues for less than one-fortieth of a second. The support post moves with the vehicle and ultimately swings free of the vehicle. Once again, it is not possible to determine the exact duration of the collision event., The time at which the vehicle-post contact is terminated becomes a matter of judgment. The vehicle slows only slightly during the collision incident, and so an estimate of the duration of the collision incident by examination of the Velocity-Time curve is not possible. This is in marked contrast to the former analysis where the final velocity of the vehicle was zero. A glance at the process of graphical differentiation reproduced in Figure 7 for the break-away post illustrates the form of the curves which may be obtained. The short duration of the collision incident and the limitations of the stadia interval on the side of the crash vehicle combine to produce a small number of data points. These conditions could not be changed nor improved, and thus the description of velocity and acceleration variation following impact are of questionable value in the interval following impact of the crash vehicle.

The process of graphical differentiating Displacement-Time records and Velocity-Time curves produces magnification of minor irregularities in datum values. Considerable judgment is required in curve fitting. Therefore, the validity and reproducibility of data reduction is depend-

ent on the technique employed. Severy and Barbour[24] report that

> "Application of poor curve fitting techniques may introduce errors as high as 100%, even though correct differentiation is applied to correct basic data."

It should be stated emphatically that the methods of data reduction described depend upon the three-inch increments of length established on the side of the crash vehicle. A shorter length increment should improve the conditions which produce scattered datum points.

The Displacement-Time plot of high-speed film data was employed, however, to determine crash vehicle velocity prior to impact with the sign support post. A radar installation was employed in Tests 40 and 41. Comparable values of velocity of crash vehicles prior to impact are as follows:

CRASH VEHICLE VELOCITY PRIOR TO IMPACT

| Test No. | Film | | Radar | |
|---|---|---|---|---|
| | MPH | FPS | MPH | FPS |
| 40 | 44.6 | 65.4 | 42.0 | 61.6 |
| 41 | 42.5 | 61.3 | 41.0 | 60.1 |

The radar values were recorded as supplementary information, but have not been used in this work. Velocity prior to impact taken as the slope of the Displacement-Time curve has been used as initial data in the successive integration method. A plot of typical film data from

a break-away test is shown in Figure 8. Attempts were made to improve the technique by increasing the vertical scale of the Displacement-Time curve. The result was a magnification of the scattering of the data points in the interval following impact. The observation of Severy and Barbour quoted earlier was substantiated by the experience in this study.

A major objective of the present research was the development of information concerning the phenomenological behavior of the break-away support post. This objective implies the development of a reproducible description of Velocity-Time and Acceleration-Time variations of the vehicle during the interval following impact. This objective could not be realized by analysis of the high-speed film data because of the difficulties just recited. Another major objective of this study was the correlation of film and accelerometer data analyses. Reduction of vehicle accelerometer data was prosecuted concurrently with the attempt to reduce the high-speed film data. As the work progressed, it became apparent that a complete correlation of Displacement-Time, Velocity-Time, and Acceleration-Time descriptions was not possible by graphical techniques. However, correlation of observed Displacement-Time data from the high-speed film with computed Displacement-Time values from vehicle accelerometer data did prove to be possible. A description of this correlation follows.

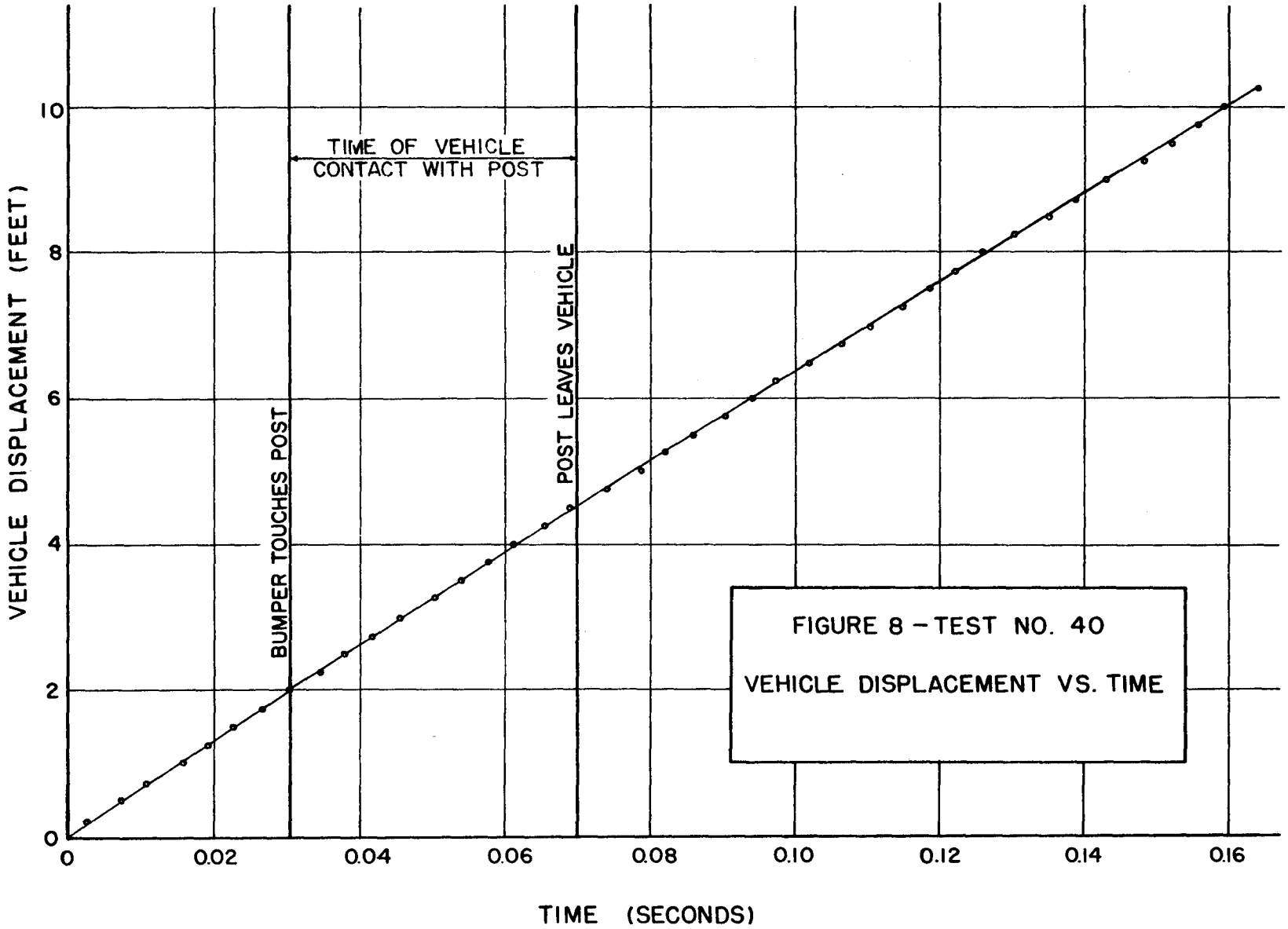


FIGURE 8 – TEST NO. 40

VEHICLE DISPLACEMENT VS. TIME

## Vehicle Accelerometer Analysis

Ar accelerometer was installed on the crash vehicle as described previously. Changes in acceleration with respect to time were recorded on photographic paper by means of a recording oscillograph. The signal transmitted from the accelerometer to a galvanometer produced a trace on light-sensitive paper. The oscillating trace thus produced is a record of the acceleration history of the accelerometer as a function of time. The configuration of this trace is idealized in Figure 9 (a). Changes in vehicle velocity and acceleration can be computed by employing a process of integration. Several methods of reducing data from the accelerometer trace were attempted. These methods included recording offsets from the null line at equal time intervals, measurement of the area bounded by the trace by means of a planimeter, and determination of this area by a graphical technique. The first method required excessive time and resulted in a large number of datum points, each of which was subject to human errors and mistakes. The planimeter method proved unsatisfactory because of the small areas involved. The third method consisted of using a piece of graph paper having squares each side of which had a dimension of one-twentieth of an inch. A light table was employed and the accelerometer trace was superposed on the graph paper. A satisfactory estimate of the areas was thus obtained.

The third method of estimating areas was selected. The decision

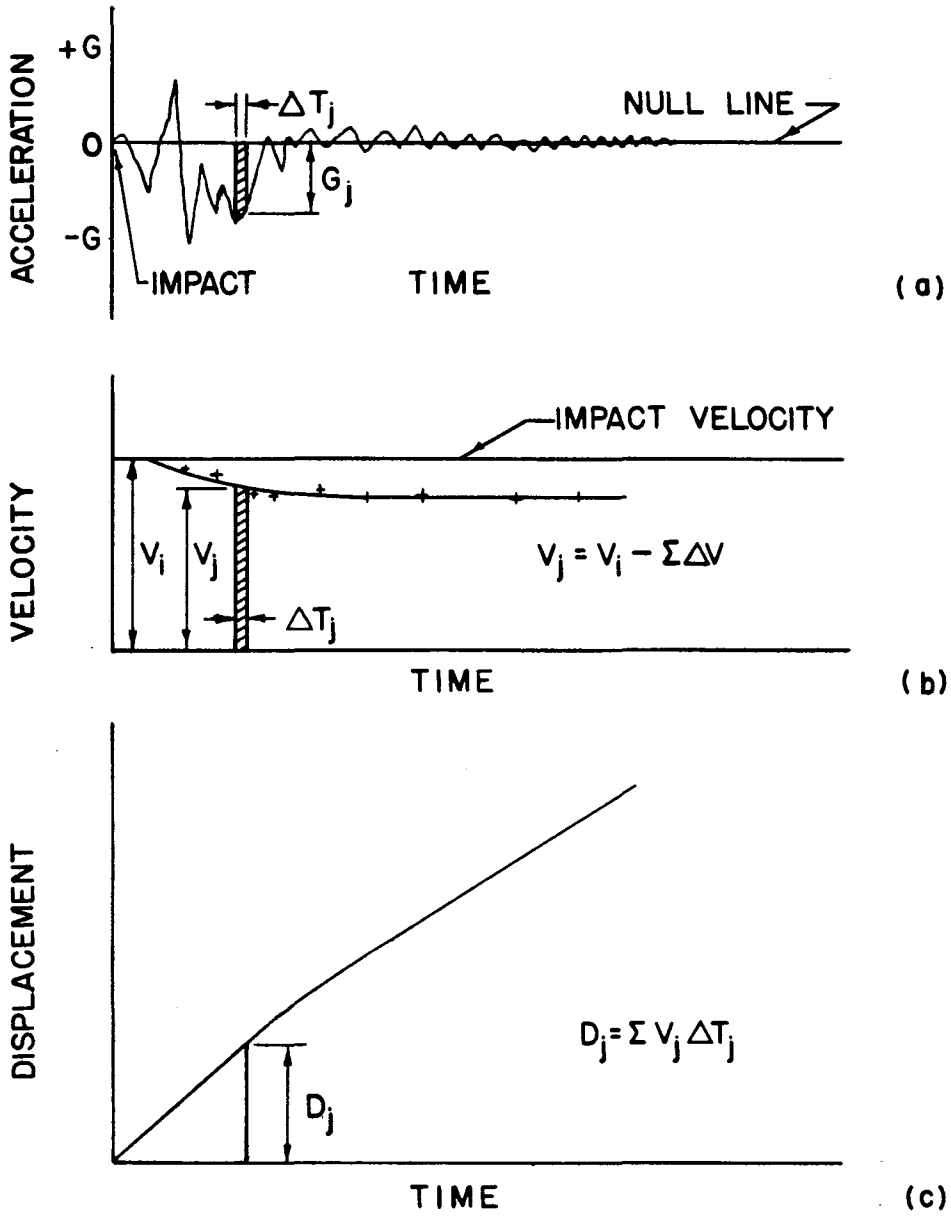


FIGURE 9

CRASH VEHICLE ACCELEROMETER

ANALYSIS BY GRAPHICAL INTEGRATION

was made to estimate areas in time increments corresponding to the peaks and null points of the galvanometer trace. This procedure was chosen because the trace was piecewise continuous in these intervals. Computations of areas yielded the change in velocity as a function of time.

This may be stated

$$\Delta V = \sum_{a}^{b} G_j \, \Delta T_j$$

where $\Delta V$ is the velocity increment

$G_j$ is the curve offset at time $j$

$\Delta T_j$ is the time increment

a, b are peak and null points

The Velocity-Time curve seen in Figure 9 (b) is obtained by plotting successive velocity increments at corresponding time intervals. The impact velocity, $V_i$ is obtained from the film data.

By a similar process of graphical integration incremental areas of velocity were summed to produce the Displacement-Time curve seen in Figure 9 (c). Actual plots of curves for Tests 33, 35, 40, and 41 are found in Appendix D. Computations were made by using the IBM 7094. A copy of the program and sample output is contained in Appendix E. The computational scheme is straightforward and self-explanatory.

Displacement-Time plots for each of the tests contain the results

of the data reduction and analysis from the accelerometer record. For comparison purposes, the Displacement-Time data from the film record have been superposed on the same sheet for each test. The correlation between the computed curve and the film data curve is remarkable. Confidence in the graphical integration technique for determining velocity changes as well as displacement changes is greatly enhanced.

Reduction of data from the trace of the accelerometer mounted on the frame of the vehicle has been discussed. The method developed in the present research ultimately resulted in a computer program entirely independent of curve fitting techniques. However, during the development of this data reduction procedure, an approximate velocity curve was fitted to the data as seen in Figure 10 for Test 41. The initial computations were made by using a desk calculator. In order to reduce the time required for the computations this approximate curve was used. Successive summing of areas contained by the Velocity-Time curve produced the Displacement-Time curve shown for Test 41 in Appendix D. The open circles represent values computed by desk calculator, and solid circles are the computer values. Both methods of calculation are in good agreement with the Displacement-Time values plotted from the high-speed film data. Impact velocity as shown on the Velocity-Time plot was taken from the plot of the high-speed film data.

Data reduction by digital computer is a process of successively

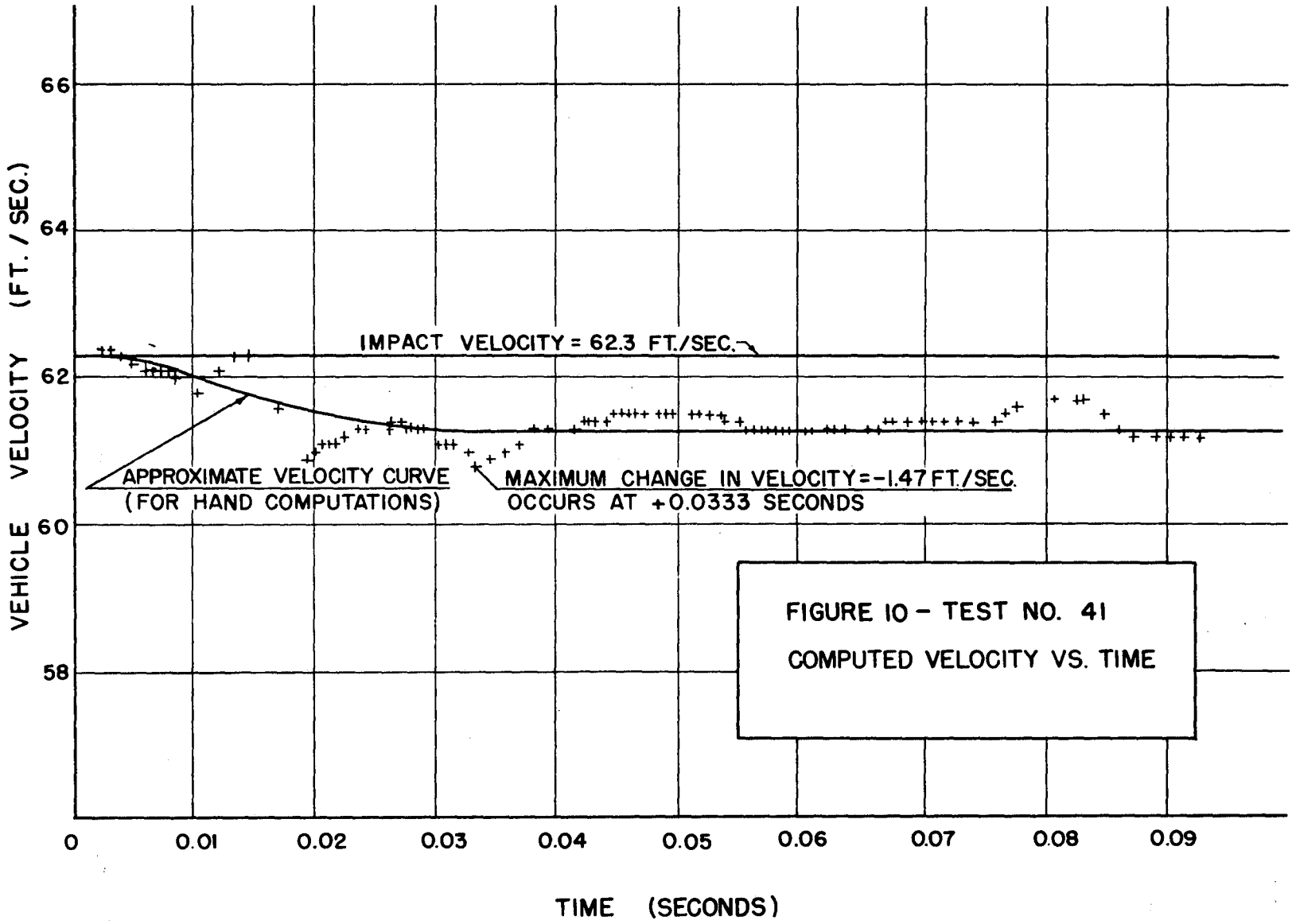


FIGURE 10 - TEST NO. 41

COMPUTED VELOCITY VS. TIME

TABLE VI

PEAK ACCELERATION AND MAXIMUM CHANGE IN VELOCITY
FROM VEHICLE FRAME ACCELEROMETER ANALYSIS

| Test No. | Impact Velocity (Ft./Sec.) | Primary Peak Negative Acceleration Acceleration (g's) | Primary Peak Negative Acceleration Time (Sec.) | Maximum Change in Velocity V (Ft./Sec.) | Maximum Change in Velocity Time (Sec.) |
|---|---|---|---|---|---|
| 32 | 57.50 | - 80 | 0.0220 | -57.50 | 0.1000 |
| 33 | 76.30 | - 5 | 0.0063 | - 2.54 | 0.0473 |
| 35 | 76.00 | - 9 | 0.0102 | - 2.68 | 0.0376 |
| 39 | 64.50 | -123 | 0.0380 | -64.50 | 0.0867 |
| 40 | 65.40 | - 30 | 0.0088 | - 3.41 | 0.0300 |
| 41 | 62.30 | - 21 | 0.0175 | - 1.47 | 0.0333 |

summing areas bounded by the accelerometer trace. This procedure can be employed for any accelerometer trace. Precision of results is dependent upon the method of determining input data for the computer. The analysis of data has been arbitrarily terminated at approximately one hundred milliseconds: actually, the duration of the accelerometer trace is several seconds.

Certain critical events which occur during the period of contact of the vehicle and the sign post are listed in Table VI. Impact velocity of the crash vehicle occurs at time zero: the time at which the strain gages on the support post become active. Primary peak negative acceleration is considered to be the first maximum deflection of the accelerometer trace which occurs after time zero.

Study of the Velocity-Time plots indicates that apparent increases in velocity occur at clearly defined points, and are related to the slipping of the break-away base under impact. The relationship of slipping of the break-away base to velocity change will be discussed in Chapter VII.

## Analysis of Linear Displacement Data

A reproduction of the linear displacement records of Tests 40 and 41 is found in Figure 11. These traces reflect the displacement of the break-away base. Examination of these records reveals a striking similarity in the plots. Each trace configuration consists of an initial

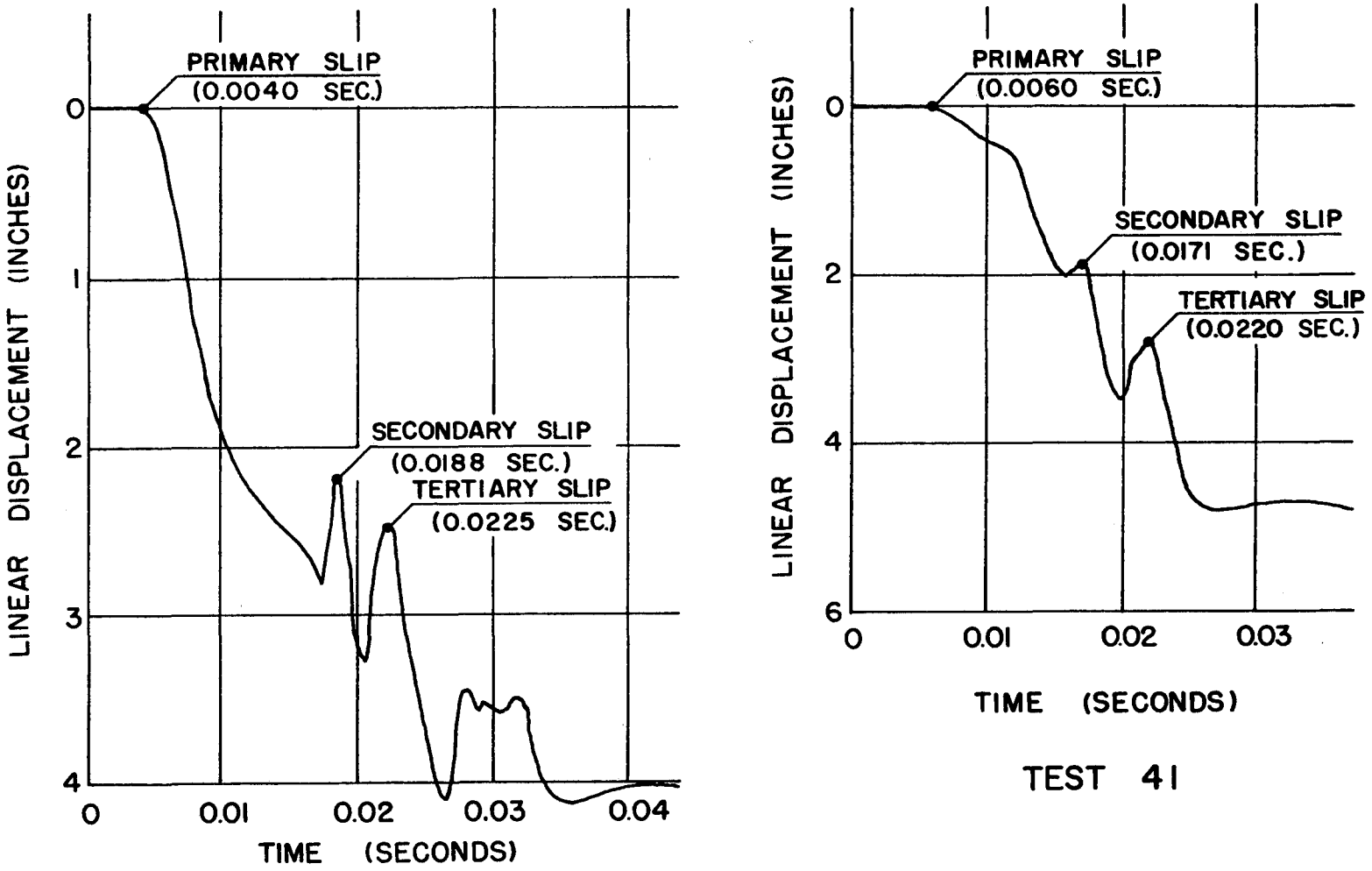


FIGURE 11 — BREAK-AWAY BASE LINEAR DISPLACEMENT

time interval during which no displacement occurs; this is followed by an interval of precipitous displacement terminated by a reversal in displacement, which in turn is followed by another precipitous displacement. This repetitive reversal in the traces is related to the slipping of the break-away base. A description of the history of this slipping is provided by these traces. The slipping is intermittent as reflected in the records.

Certain critical events in the slipping history are indicated on the plots of Figure 11. For purposes of identification these events have been termed primary slip, secondary slip, and tertiary slip. Primary slip occurred when the bolted base began to slip and was terminated by a resistance indicated by a decrease in displacement. Secondary slip then occurred as evidenced by an increase in displacement which continued until another abrupt decrease occurred. Finally tertiary slip occurred and continued for the duration of the record. The irregularities at the end of the record were induced by the impact of the sliding mechanism against the end of the measuring device. However, the significance of the reversals lies in their usefulness in defining the characteristic behavior of the break-away base.

## Discussion of Observed Critical Events

Behavior of the crash vehicle and sign support post was initially

dependent upon observation of high-speed films. Installation of an accelerometer on the frame of the vehicle provided additional quantitative information. Each of these methods of instrumentation provided an insight into the quantitative behavior of the event. A detailed description of the behavior of the break-away base was not clear from analysis of the films and oscillographic records. The linear displacement device was employed to provide a record of displacement of the break-away base during the short interval of time following impact.

Investigation of slip of bolted joints subjected to static load has been considered by others.[25] It is recognized that the experiments were conducted under conditions considerably removed from impact loads, and it is further recognized that notched plate break-away bases were not tested. However, in spite of these variations in testing conditions the following observation is considered to be pertinent to the present investigation:

> "When load was applied to specimens of this type, there was at first no large slip. A load was eventually reached at which the initial frictional resistance to slip was overcome, and the plates slipped with extreme rapidity".[26]

The traces of displacement from Tests 40 and 41 indicate that no initial slip occurred. This behavior is in accordance with the observation quoted. Plots of test data from the static load tests[27] reveal that slip of a bolted joint progresses intermittently. These plots show that under

continuous loading a bolted joint resists slip, then slipping occurs, then a resistance to slip is indicated by an increased load capacity of the bolted joint. Repetition of these events is found in the plot of the test data presented by the investigators. Consideration of these static tests led to the identification of the critical events in the slipping history of the break-away base. The magnitude of the reduction in slip indicated by the record is not a vital consideration in the definition. It is merely an indication that something occurred to reduce the rate of slip.

## Other Data Analyses

Data reduction and analyses of three types of information have been presented in this chapter. Usable information was provided by other instruments, and the analysis of this information is contained in subsequent chapters.

# CHAPTER VII

## DESCRIPTION OF SUPPORT POST BEHAVIOR

In Chapter V it was noted that a high-speed camera is the basic instrument for recording the history of a collision. A procedure for recording crash vehicle displacement as a function of time has been explained in Chapter VI. This procedure consists of frame-by-frame examination of the film record which provides a set of data points. These points, when plotted, result in a Displacement-Time curve which describes the vehicle displacement prior to impact with the support post, during contact with the post, and following contact with the post. The application of this information for analytical purposes has been described.

Re-examination of the film record also provides the investigator with provisional information concerning the support post. The time of occurrence of certain critical events can be visually observed. In this examination of the film record zero time is considered to be the time at which the vehicle bumper makes initial contact with the support post. The time at which the following critical events occur is recorded by an observer.

1. Break-away base is disengaged.
2. Mechanical fuse is activated.
3. Vehicle-post contact is terminated.

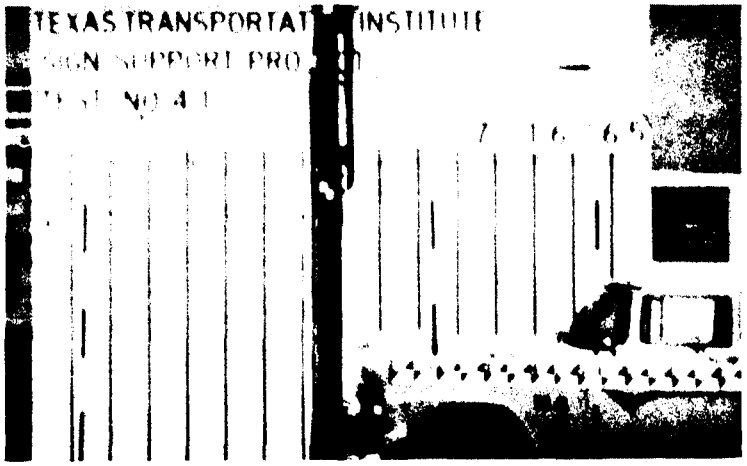


t = 0 BUMPER TOUCHES POST

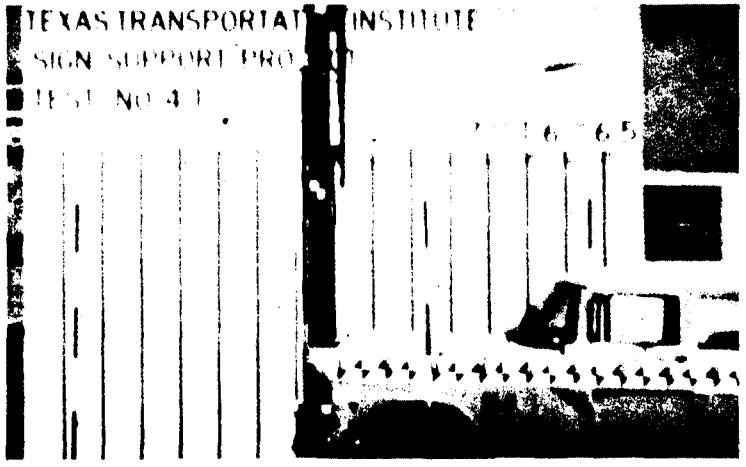


t = 0.015 BASE IS DISENGAGED

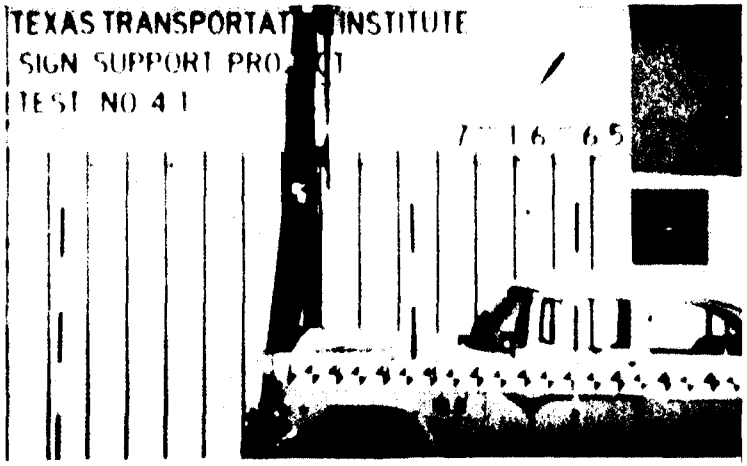


t = 0.027 FUSE IS ACTIVATED

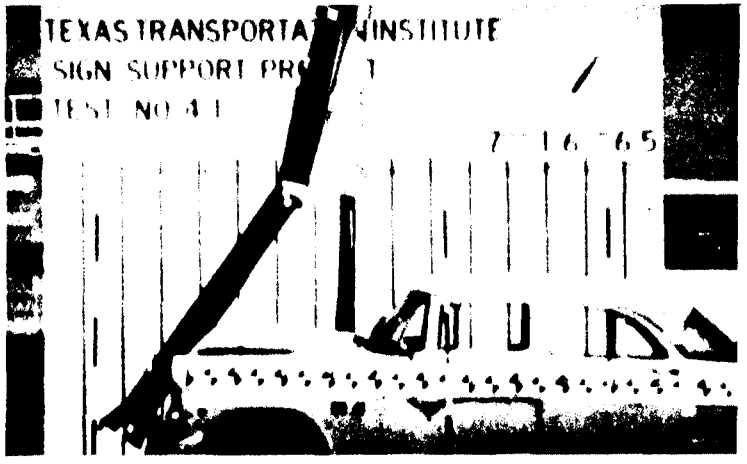


t = 0.069 CONTACT IS TERMINATED

FIGURE 12 - CRITICAL EVENTS

A record of the time of occurrence of these critical events provides a brief history of support post behavior. Such a record is contained in the sequence photographs seen in Figure 12.

A series of observations was made by individual observers in order to ascertain the approximate time at which each of the listed events occurs in each of the tests. Each of the observers was acquainted with the behavior of the break-away support post. Each observer was instructed to examine the film and to record the time of occurrence of each of the critical events. The time of occurrence of each of these events was recorded by ten observers; and each observer made his observations independently of the others. Film records for Tests 33, 35, 40, and 41 were examined. The results are recorded in Table VII. The arithmetic mean value and the range of recorded values are tabulated.

It is apparent that the observed values represent a considerable range of subjective determination. Difficulties in observation are aggravated by several factors. The film record is not consistently visible; some frames are not in focus, some are underexposed, and corresponding fixed points on adjacent frames frequently are displaced with respect to a reference point on the viewing screen. The moving vehicle creates a shadow over the break-away base. Termination of contact between the support post and the vehicle is difficult to

TABLE VII

OBSERVED TIME OF OCCURRENCE OF CRITICAL EVENTS
(FROM HIGH-SPEED FILM RECORDS)

| CRASH TEST NO. | BREAK-AWAY BASE DISENGAGED | | | MECHANICAL FUSE ACTIVATED | | | VEHICLE-POST CONTACT TERMINATED | | |
|---|---|---|---|---|---|---|---|---|---|
| | AVERAGE TIME VALUE (SEC.) | RANGE OF TIME VALUES | | AVERAGE TIME VALUE (SEC.) | RANGE OF TIME VALUES | | AVERAGE TIME VALUE (SEC.) | RANGE OF TIME VALUES | |
| | | MINIMUM (SEC.) | MAXIMUM (SEC.) | | MINIMUM (SEC.) | MAXIMUM (SEC.) | | MINIMUM (SEC.) | MAXIMUM (SEC.) |
| 33 | 0.014 | 0.006 | 0.019 | S E E N O T E | | | 0.079 | 0.056 | 0.106 |
| 35 | 0.013 | 0.009 | 0.017 | S E E N O T E | | | 0.093 | 0.070 | 0.151 |
| 40 | 0.015 | 0.011 | 0.018 | 0.021 | 0.018 | 0.029 | 0.065 | 0.037 | 0.086 |
| 41 | 0.015 | 0.012 | 0.020 | 0.022 | 0.014 | 0.028 | 0.069 | 0.037 | 0.088 |

NOTE: Cast-iron mechanical fuse did not fracture in this crash test.

observe owing to crumpling of the grill and hood of the vehicle. The event is thus obscured by the crumpled metal.

In the tests conducted in this investigation, electronic devices were employed as a supplement to the high-speed camera instrumentation. These devices have been described in Chapter V. An objective of this study has been to use electronic data analysis to enhance information obtained from the high-speed films. An ideal system of instrumentation would consist of a series of independent devices, each of which would produce data identical with data obtained from each of the other independent mensuration devices in the system. However, each measuring device contains aberrations within itself, and consequently the record provided by each instrument reflects instrument characteristics as well as the measurements sought. Another objective of this investigation was to provide a correlation of data from the several devices employed in this study.

An arbitrary set of critical events was identified by studying the linear displacement records reproduced in Figure 11. Re-examination of the Velocity-Time plots computed from frame accelerometer records discloses a set of corresponding critical events. These two curves for Test No. 40 have been plotted to a common time scale in Figure 13. Comparison of the curves reveals some remarkable similarities. The initial portion of each curve is nearly horizontal, each curve then

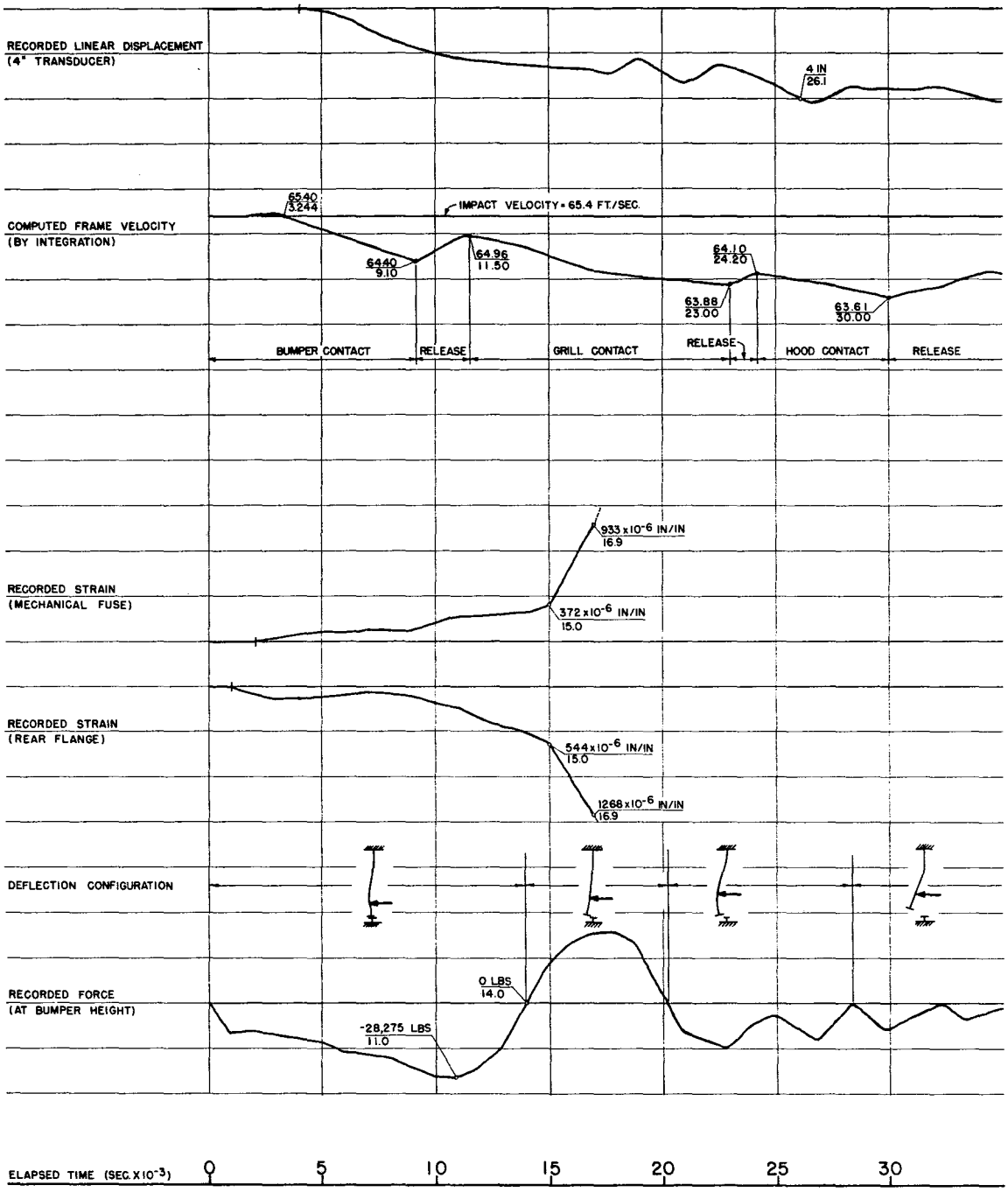


FIGURE 13 - CHRONOLOGY OF COLLISION - TEST 40

exhibits a sinuous configuration. Corresponding values for time of primary slip, secondary slip, and tertiary slip have been extracted from the Velocity-Time plot. A similar analysis of the curves for Test No. 41 has been made. The linear displacement curve and velocity curve are seen in Figure 14. A comparison of the results is contained in Table VIII.

The history of the break-away base may be described by the following set of arbitrarily defined critical events:

1. Impact of crash vehicle with the support post.
2. Primary slip of the base.
3. Secondary slip of the base.
4. Tertiary slip of the base.

A complete history of the collision incident must also include the time at which the vehicle and post are no longer in contact. This time has been taken to correspond to the time of maximum change in velocity.

This time is indicated on the Velocity-Time plots in Figures 13 and 14. A comparison of the time from high-speed film analysis and the time from the velocity plot indicates a considerable range in values. The discrepancy in the two values for this event is unresolved by this investigation. However, improvement in photographic technique or additional instrumentation in future tests may produce a closer correlation of time values.

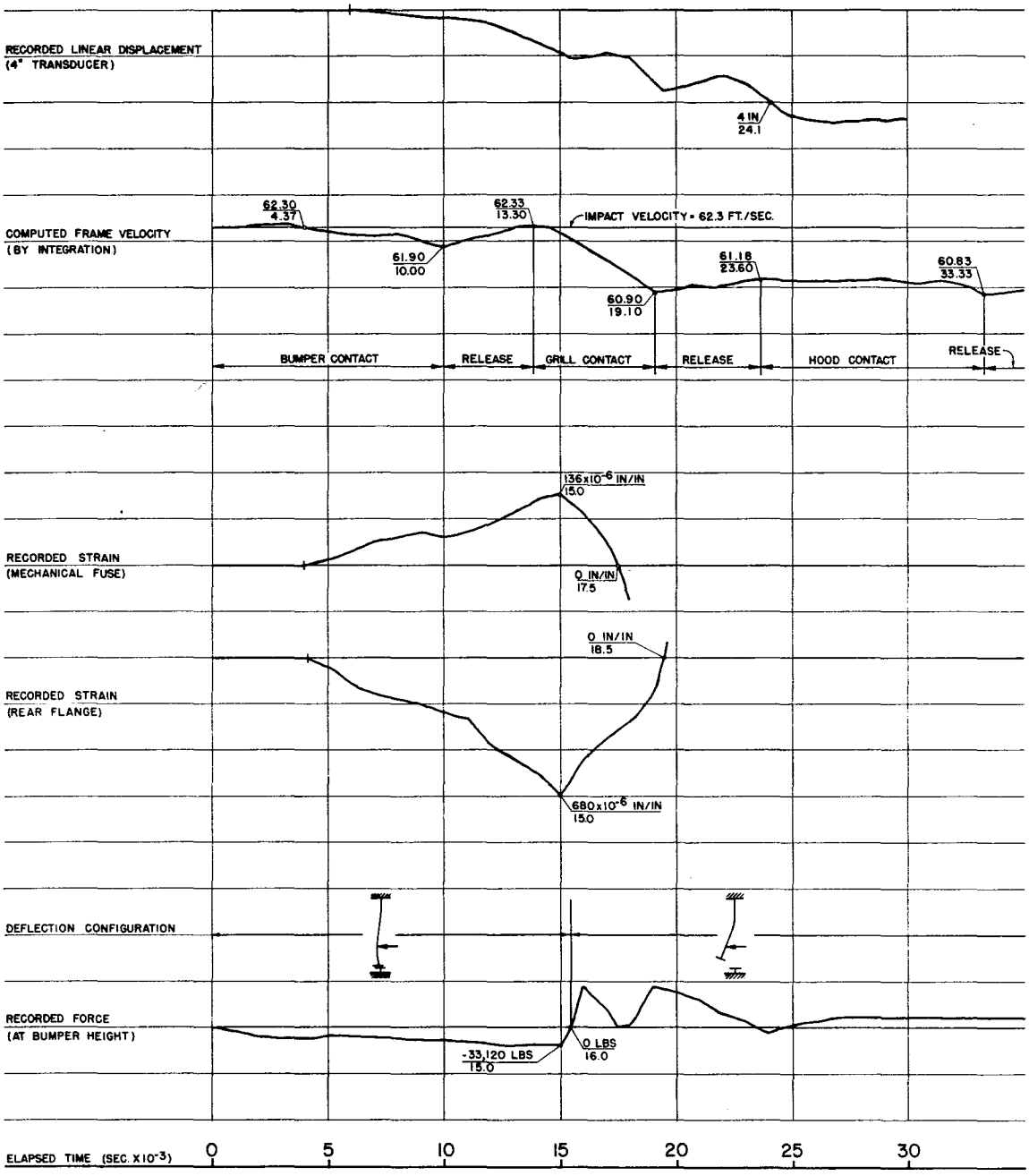


FIGURE 14 - CHRONOLOGY OF COLLISION - TEST 41

TABLE VIII

CRITICAL EVENTS DURING SLIP OF BREAK-AWAY BASE

| LINEAR DISPLACEMENT DEVICE | | | TEST NO. | VELOCITY PLOT | | |
|---|---|---|---|---|---|---|
| PRIMARY (SEC.) | SECONDARY (SEC.) | TERTIARY (SEC.) | | PRIMARY (SEC.) | SECONDARY (SEC.) | TERTIARY (SEC.) |
| -- | -- | -- | 33 | 0.0151 | 0.023 | 0.0315 |
| -- | -- | -- | 35 | 0.0109 | 0.0194 | 0.0376 |
| 0.004 | 0.0188 | 0.0225 | 40 | 0.0032 | 0.0115 | 0.0242 |
| 0.006 | 0.0175 | 0.0220 | 41 | 0.0044 | 0.0133 | 0.0236 |

A trace of strain as a function of time is provided by the electric resistance strain gage mounted on the mechanical fuse in Test 40. Examination of this trace, see Figure 13, provides a clue to the time at which the mechanical fuse became activated. The trace becomes uncertain at approximately seventeen milliseconds after impact (time zero). The mechanical fuse employed in this test was made of cast-iron. Fracture of the cast-iron plate would cause the strain gage to become inactive. Thus, one might surmise that the cast-iron fuse fractured at this time. However, the trace exhibits a precipitous descent, terminated by the limits of the recording paper. For this reason it is impossible to determine the exact time at which the gage became inactive.

The trace of strain as a function of time in Test 41 provides a more certain indication of the time at which the notched plate became disengaged. In this trace, see Figure 14, the strain increases to a maximum value and then decreases to zero. The trace crosses the zero strain value at 17.5 milliseconds after initial contact between the post and vehicle.

Corresponding traces provided by strain gages mounted on the rear flange in Test 40 and 41 produce comparable results. The strain gage on the rear flange in Test 41 provides a trace which has a peak at the same time as the peak indicated by the strain gage on the notched plate.

The time of zero strain is greater by approximately two milliseconds. This time lag might be anticipated, since the rear flange is intact at the time the notched plate becomes disengaged. The yield point in the flange is reached after the notched plate becomes disengaged.

A summary of results obtained from analysis of data from the several devices is contained in Table IX. The foregoing discussion relates the manner in which examination of the various records led to the summary. An arithmetic mean value for each of the critical events is contained in the table. It should be restated that the values tabulated for each device includes the characteristics of the device. The average values, however, provide a time for each critical event. These values can be useful in future investigations. The average value for termination of vehicle post contact is considered unreliable by the writer. This is an opinion based upon observation of high-speed film. The difficulties in making high-speed film observations of this event have been discussed previously in this chapter. Therefore, it is recommended that the time taken from the computed velocity plot be regarded as the most reliable value.

One additional trace is available for analysis, and this trace provides an indication of bending of the support post. This trace was provided by an electric resistance strain gage bridge mounted on the support post flanges at bumper height. The strain record for Test 40 is

TABLE IX

SUMMARY OF TIME OF OCCURRENCE OF CRITICAL EVENTS
IN HISTORY OF VEHICLE-POST COLLISION

| INSTRUMENT OR DEVICE | INITIAL SLIP (SEC.) | BREAK-AWAY BASE DISENGAGED (SEC.) | MECHANICAL FUSE ACTIVATED (SEC.) | VEHICLE-POST CONTACT TERMINATED (SEC.) |
|---|---|---|---|---|
| TEST NO. 40 | | | | |
| High-Speed Camera | Note 1 | 0.0150 | 0.0210 | 0.0650[3] |
| Linear Device | 0.0040 | 0.0188 | 0.0225 | Note 4 |
| Strain Gage (Fuse) | 0.0021 | 0.0150 | 0.0170[2] | Note 4 |
| Strain Gage (Flange) | 0.0011 | 0.0150 | 0.0170[2] | Note 4 |
| Velocity Plot | 0.0032 | 0.0115 | 0.0242 | 0.0300[5] |
| AVERAGE VALUE | 0.0026 | 0.0151 | 0.0203 | 0.0475 |
| TEST NO. 41 | | | | |
| High-Speed Camera | Note 1 | 0.0150 | 0.0220 | 0.0690[3] |
| Linear Device | 0.0060 | 0.0175 | 0.0220 | Note 4 |
| Strain Gage (Fuse) | 0.0040 | 0.0150 | 0.0175 | Note 4 |
| Strain Gage (Flange) | 0.0040 | 0.0150 | 0.0195 | Note 4 |
| Velocity Plot | 0.0044 | 0.0133 | 0.0236 | 0.0333[5] |
| AVERAGE VALUE | 0.0046 | 0.0152 | 0.0229 | 0.0512 |

NOTE 1 - Initial slip not observable on high-speed film.
NOTE 2 - Uncertain value for time of cast-iron fracture.
NOTE 3 - Vehicle-post contact termination time not observable on high-speed film.
NOTE 4 - Vehicle-post contact terminated after limit of device was exceeded.
NOTE 5 - This value considered to be most reliable.

plotted in Figure 13. An inspection of the trace reveals that the sense of the strain is negative between zero and fourteen milliseconds; a strain reversal is then apparent. During the ensuing six milliseconds, the sense of the strain is positive. Finally another strain reversal occurs and the sense of the strain is once again negative. Consideration of these strain reversals permits the sketching of the apparent deflection of the post during the brief history of the collision incident. The deflection configuration of the support post for each time interval just described is drawn adjacent to the Strain-Time trace.

A similar plot of the strain record for Test 41 is presented in Figure 14. Once again the pattern of strain reversal is apparent. The deflection characteristics of the support post are sketched for this test also. The trace recorded for this crash test is not completely similar to that recorded for Test 40. However, the initial fifteen milliseconds is comparable in sense, as is the ensuing nine milliseconds. It should be observed here that the attenuation chosen for the record of Test 40 was twice that selected for Test 41. This reduced scale factor employed in the latter test may have affected the oscillographic record. The variation in attenuation in the two tests was made in an attempt to determine scale factors for future testing programs. It has been stated earlier that one criterion of instrumentation was installation and variation for future testing experience. A similar observation concerning

choice of attenuation scales should be noted in the present discussion. The choice of the larger scale in Test 40 provided a better record for purpose of making an inductive description of support post deflection.

The electric resistance strain gage records have been analyzed to produce information concerning support post behavior. This information has been compared with high-speed film information and with computed velocity values obtained from vehicle frame accelerometer records. The resulting inductive description of support post behavior provides an indication of the time of occurrence of certain critical events in the chronology of the collision incident. This description is unique, and the validity and precision of the time of the critical events is left for others to ascertain.

Strain and stress in elements of the "plastic hinge" joint were discussed in this chapter and are treated more fully in Chapter VIII; and the measured force in the support post at bumper height is described more completely in Chapter IX.

# CHAPTER VIII

## STRAIN AND STRESS IN ELEMENTS OF THE "PLASTIC HINGE" JOINT

Electric resistance strain gages were mounted on the fuse plate and rear flange of the support post in Tests 40 and 41. These gages were located 6' 3" above the break-away base. The purpose of the gages was to obtain Strain-Time data. The gages were calibrated prior to the crash test, and the unit deflection of the galvanometer was determined. Strain readings were transcribed on the oscillographic record. Deflection of the galvanometer trace on this record was measured with an engineer's scale. Strain computations were made by multiplying the scaled deflection by the unit galvanometer deflection, and stress computations were accomplished by obtaining the product of computed strain and Young's Modulus for the material. Nominal values for Modulus of Elasticity were employed in the computations.

Strain and stress values were computed for each millisecond of time following impact, and are listed in Table X for Test 40. It must be recalled that the mechanical fuse was made of cast-iron in Test 40, whereas the fuse plate in Test 41 was fabricated from steel. Failure of the cast-iron fuse required fracture of the material, but failure of the notched plate fuse required slipping of the bolted joint. The difference in behavior of the two materials is apparent in the oscillographic records.

TABLE X - STRAINS AND STRESSES - TEST NO. 40

| | CAST-IRON FUSE (TENSION) | | | REAR FLANGE (COMPRESSION) | | |
|---|---|---|---|---|---|---|
| ELAPSED TIME (SEC.x$10^{-3}$) | GALVANOMETER DEFLECTION (INCHES) | FUSE STRAIN (IN/INx$10^{-6}$) | FUSE STRESS (PSI) | GALVANOMETER DEFLECTION (INCHES) | FLANGE STRAIN (IN/INx$10^{-6}$) | FLANGE STRESS (PSI) |
| 0 | ( T I M E Z E R O A T I M P A C T ) | | | | | |
| 1 | 0 | 0 | 0 | 0 | 0 | 0 |
| 2 | 0 | 0 | 0 | 0.08 | 72 | 2160 |
| 3 | 0.04 | 36 | 470 | 0.12 | 109 | 3270 |
| 4 | 0.08 | 72 | 940 | 0.10 | 91 | 2730 |
| 5 | 0.11 | 100 | 1300 | 0.11 | 100 | 3000 |
| 6 | 0.10 | 91 | 1180 | 0.08 | 72 | 2160 |
| 7 | 0.13 | 118 | 1530 | 0.05 | 45 | 1350 |
| 8 | 0.12 | 109 | 1420 | 0.06 | 54 | 1620 |
| 9 | 0.13 | 118 | 1530 | 0.08 | 72 | 2160 |
| 10 | 0.21 | 190 | 2470 | 0.18 | 163 | 4890 |
| 11 | 0.27 | 245 | 3180 | 0.22 | 199 | 5930 |
| 12 | 0.28 | 254 | 3300 | 0.35 | 317 | 9510 |
| 13 | 0.31 | 281 | 3650 | 0.42 | 381 | 11430 |
| 14 | 0.32 | 290 | 3770 | 0.50 | 453 | 13590 |
| 15 | 0.41 | 372 | 4840 | 0.60 | 544 | 16320 |
| 16 | 0.90 | 815 | 10600 | 1.00 | 906 | 27180 |
| 17 | 1.30 | 933 | 12130 | 1.40 | 1268 | 38040 |

Examination of the traces of Test 40, Figure 15, reveals that the strain in the cast-iron plate and the strain in the rear flange are substanitally the same in magnitude, but opposite in sense. Strain in the rear flange is initially greater in magnitude than strain in the cast-iron plate. Strain values are identical in magnitude at five milliseconds and at eleven and one-half milliseconds. During this middle time interval, strain in the fuse is greater than strain in the rear flange; finally, strain in the rear flange once again exceeds strain in the fuse. However, the trend of the strain curves indicates that strain is very nearly equal in the fuse and the rear flange.

On the other hand, as seen in Table X, the stress in the rear flange is greater than the stress in the cast-iron fuse except at seven milliseconds after impact. Rear flange stress values in excess of fuse stress values can be directly attributed to the fact that the modulus of elasticity is greater for steel than for cast-iron.

The history of strain and stress is terminated at approximately sixteen milliseconds. The value of computed stress at this time is substantially below the fracture stress of Class 30 cast-iron. Termination of the oscillograph record prior to the time failure stress in the fuse is achieved is a result of inadequate instrumentation. Examination of the oscillograph record reveals that the galvanometer deflected rapidly and the trace exceeded the limits of the paper.

Measured strain in the cast-iron fuse as a function of time is

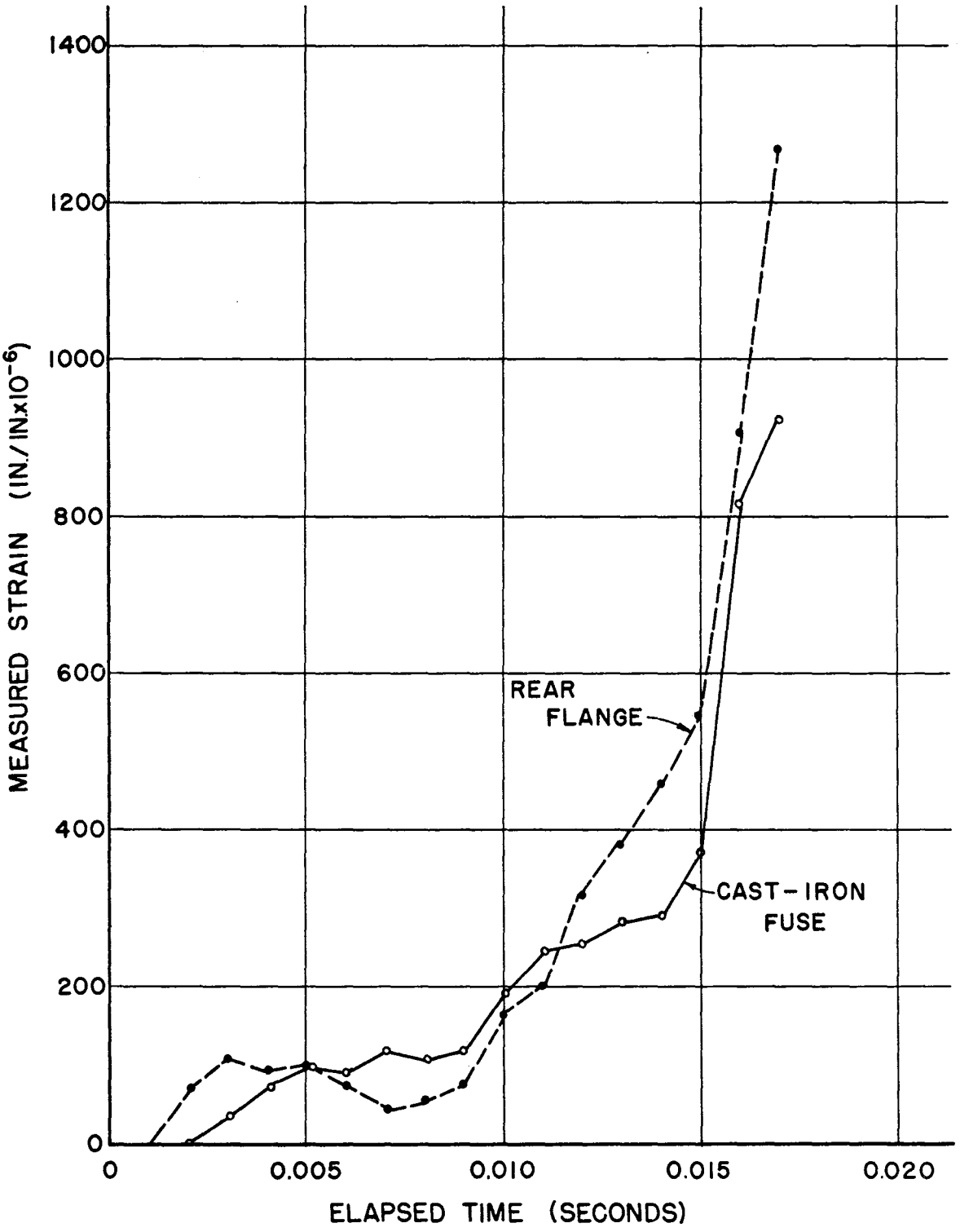


FIGURE 15 – MEASURED STRAIN, TEST NO. 40

plotted in Figure 15. Also plotted in the figure is measured strain in the rear flange. The horizontal co-ordinate represents elapsed time following impact of the crash vehicle.

Computed stress in the cast-iron fuse and computed stress in the rear flange are plotted in Figure 16. The sense of the stress values is shown for each element. The cast-iron fuse was subjected to tensile stress, while the rear flange of the support post was subjected to compressive stress.

Measured values of strain and computed values of stress are contained in Table XI for Test 41. The mechanical fuse employed in this test consisted of a notched plate bolted to the forward flange of the support post. This provides a friction connection between the abutting sawed portions of the support post. Careful examination of the recorded galvanometer trace of strain in the notched plate reveals that initially the notched plate is subjected to a compressive stress. This is apparent since a negative trace was produced on the oscillograph record during the initial four milliseconds following impact. The galvanometer trace of strain in the rear flange is zero valued during this initial interval. It is apparent for each subsequent value of time listed in the table that the recorded strain in the notched plate is less in magnitude than the recorded strain in the rear flange: the computed stress reflects a corresponding relationship. The smaller values of strain and stress in the notched plate are attributed to the ability of the bolted plate to slip.

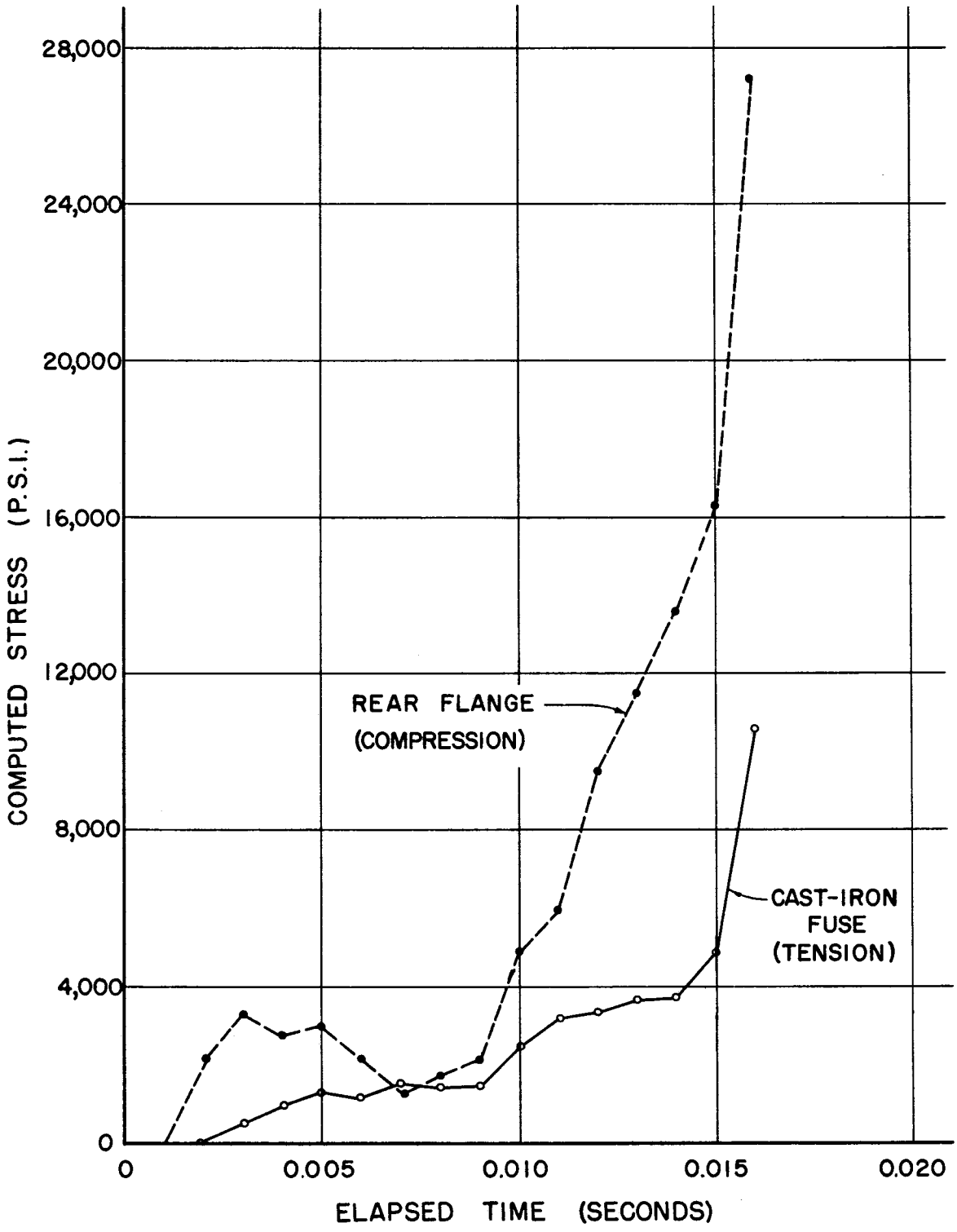


FIGURE 16-COMPUTED STRESS, TEST NO. 40

TABLE XI - STRAINS AND STRESSES - TEST NO. 41

| | NOTCHED PLATE FUSE | | | REAR FLANGE (COMPRESSION) | | |
|---|---|---|---|---|---|---|
| ELAPSED TIME (SEC.x$10^{-3}$) | GALVANOMETER DEFLECTION (INCHES) | FUSE STRAIN (IN/INx$10^{-6}$) | FUSE STRESS (PSI) | GALVANOMETER DEFLECTION (INCHES) | FLANGE STRAIN (IN/INx$10^{-6}$) | FLANGE STRESS (PSI) |
| 0 | ( T I M E Z E R O A T I M P A C T ) | | | | | |
| 1 | -0.05 | -45 | -1350 | 0 | 0 | 0 |
| 2 | -0.03 | -27 | - 810 | 0 | 0 | 0 |
| 3 | -0.01 | - 9 | - 270 | 0 | 0 | 0 |
| 4 | 0 | 0 | 0 | 0 | 0 | 0 |
| 5 | 0.01 | 9 | 270 | 0.02 | 45 | 1350 |
| 6 | 0.03 | 27 | 810 | 0.06 | 136 | 4080 |
| 7 | 0.05 | 45 | 1350 | 0.08 | 181 | 5430 |
| 8 | 0.06 | 54 | 1620 | 0.09 | 204 | 6120 |
| 9 | 0.07 | 63 | 1890 | 0.10 | 226 | 6780 |
| 10 | 0.06 | 54 | 1620 | 0.12 | 272 | 8160 |
| 11 | 0.07 | 63 | 1890 | 0.13 | 294 | 8820 |
| 12 | 0.09 | 82 | 2460 | 0.19 | 430 | 12900 |
| 13 | 0.11 | 100 | 3000 | 0.22 | 498 | 14940 |
| 14 | 0.14 | 127 | 3810 | 0.25 | 566 | 16980 |
| 15 | 0.15 | 136 | 4080 | 0.30 | 680 | 20400 |
| 16 | 0.11 | 100 | 3000 | 0.22 | 498 | 14940 |
| 17 | 0.05 | 45 | 1350 | 0.18 | 408 | 12240 |
| 17.5 | 0 | 0 | 0 | 0.14 | 317 | 9510 |
| 18 | - | - | - | 0.08 | 181 | 5430 |
| 18.5 | - | - | - | 0 | 0 | 0 |

The load is applied to a bolted mechanical fuse which is only partially restrained at the notches. The behavior of the completely restrained cast-iron plate of Test 40 contrasts sharply with the behavior of the notched plate.

Peak values of strain and stress occurred at fifteen milliseconds after impact in both the mechanical fuse and the rear flange. Strain and stress values drop precipitously to zero during the ensuing three and one-half milliseconds. The notched plate was disengaged at seventeen and one-half milliseconds, and the "plastic hinge" joint became active at one millisecond later. That is, the stresses in the rear flange exceeded the elastic limit of the material at this time.

Measured strain in the steel mechanical fuse is plotted in Figure 17, as is the measured strain in the rear flange. Computed stress in the fuse and computed stress in the rear flange are plotted in Figure 18. The sense of the computed stresses is shown for each element.

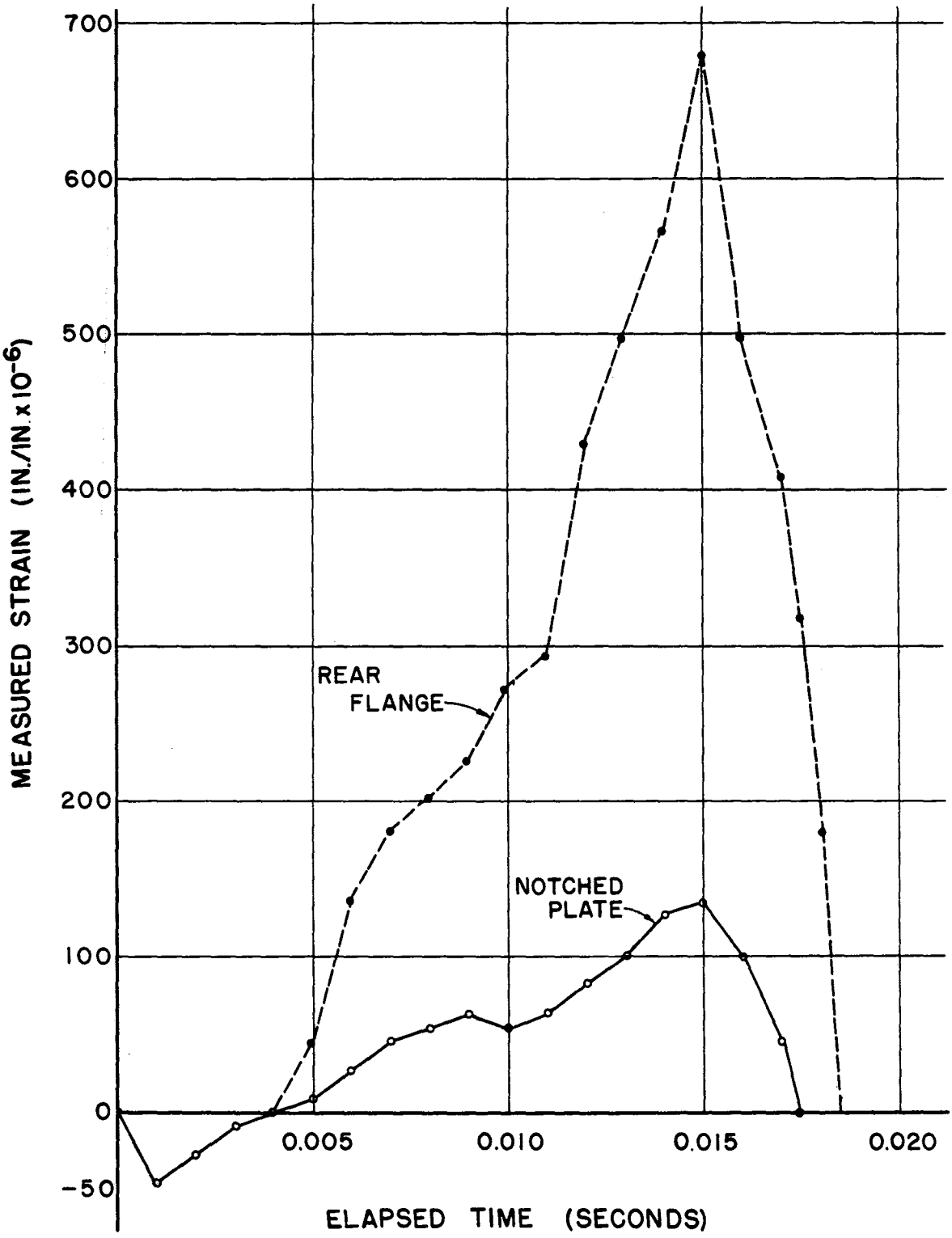


FIGURE 17 - MEASURED STRAIN, TEST NO. 41

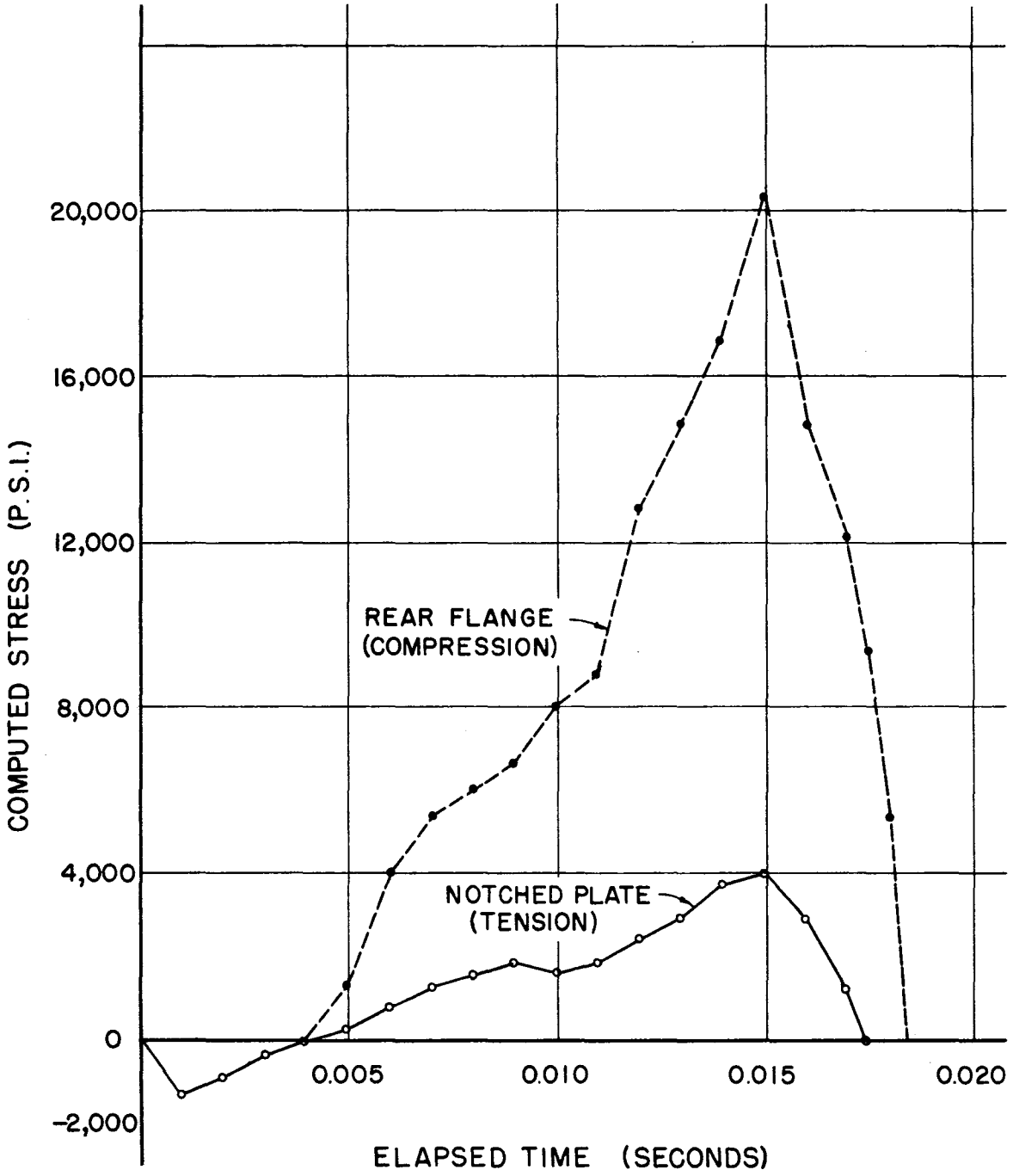


FIGURE 18-COMPUTED STRESS, TEST NO. 41

# CHAPTER IX

## FORCE IN THE SUPPORT POST AT BUMPER HEIGHT

An electric resistance strain gage bridge was installed on the support post at vehicle bumper height. The height was set at 14-1/4 inches above the break-away base. This installation was made on Tests 40 and 41 only. The strain gage bridge was located on the web of the support post and measured strain caused by bending stresses.

Calibration of the bridge to read directly in pounds was accomplished by supporting the post as a simple cantilever bolted to a fixed wall. Dead loads were placed on the beam in one hundred pound increments and corresponding strain readings were recorded. The linearity of the system was thus established. The strain gage bridge was connected to the recording oscillograph and the unit deflection of the recording galvanometer was recorded on light sensitive paper.

Examination of the traces recorded in Tests 40 and 41, and comparison with the unit deflection produced the data plotted in Figure 19. These curves indicate the magnitude of the bumper force as a function of time. The force increases with the passage of time to a peak value in each test. The peak value in Test 40 is 28,275 pounds and occur at eleven milliseconds after impact; and the peak value in Test 41 is 34,960 pounds occurring at thirteen milliseconds after impact. In each test the force becomes zero valued shortly after the peak value is

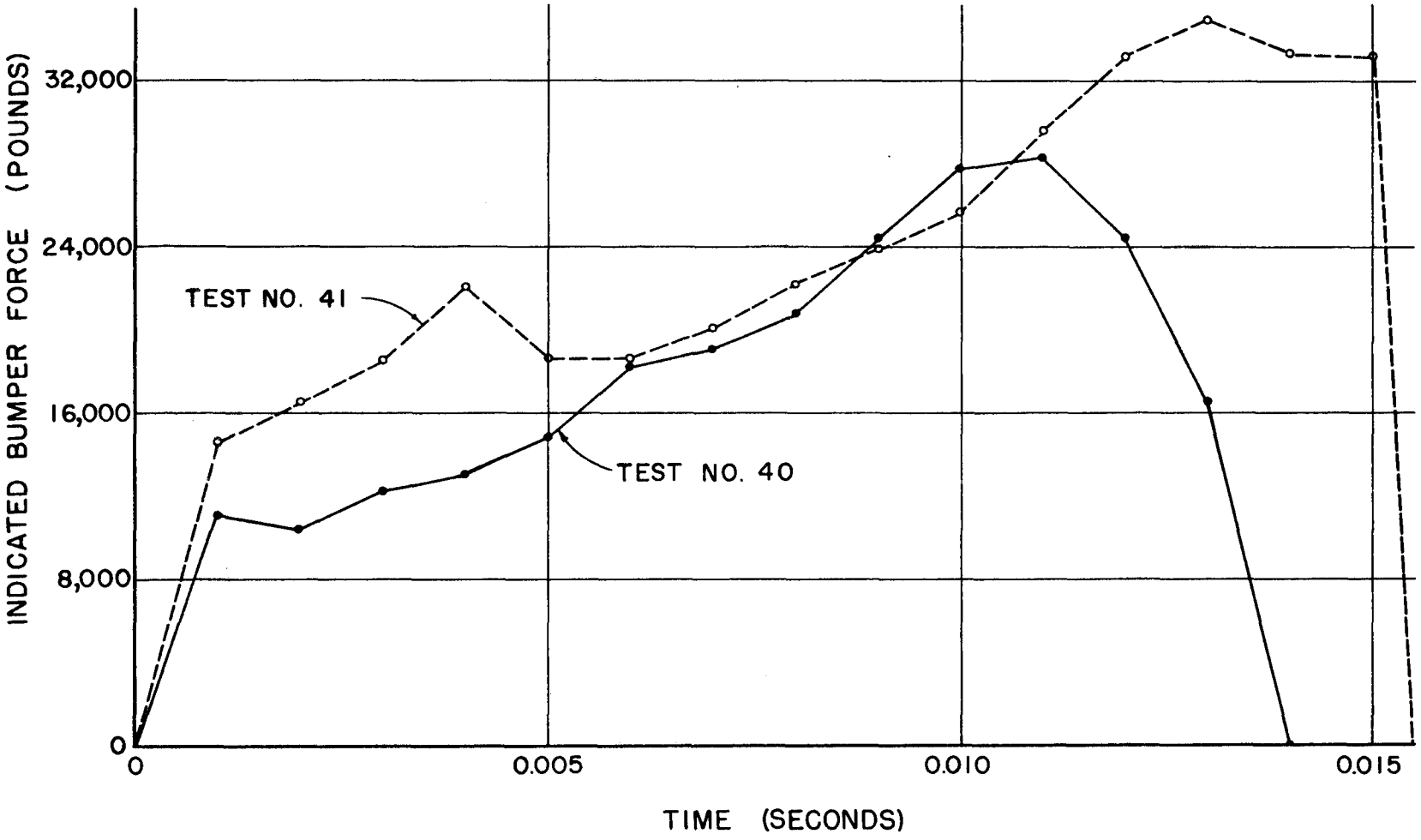


FIGURE 19-INDICATED BUMPER FORCE

reached. It is concluded that the bumper is no longer in influential contact with the post after the peak value of force is recorded.

Table XII contains values of trace deflection taken at one millisecond intervals from the oscillograph trace. The galvanometer unit deflections were:

Test 40 -- 1/2" = 43,500 lbs.

Test 41 -- 0.2" = 36,800 lbs.

Indicated force at bumper height, computed as the product of the trace deflection and unit deflection, is also found in Table XII.

TABLE XII STRAIN GAGE LOCATED AT BUMPER HEIGHT

| | TIME (SEC.x10$^{-3}$) | TRACE DEFLECTION (INCHES) | INDICATED FORCE (POUNDS) |
|---|---|---|---|
| TEST 40 | | | |
| | 1 | 0.13 | 11,310 |
| | 2 | 0.12 | 10,440 |
| | 3 | 0.14 | 12,180 |
| | 4 | 0.15 | 13,050 |
| | 5 | 0.17 | 14,790 |
| | 6 | 0.21 | 18,270 |
| | 7 | 0.22 | 19,140 |
| | 8 | 0.24 | 20,880 |
| | 9 | 0.28 | 24,360 |
| | 10 | 0.32 | 27,840 |
| | 11 | 0.325 | 28,275 |
| | 12 | 0.28 | 24,360 |
| | 13 | 0.19 | 16,530 |
| | 14 | 0 | 0 |
| TEST 41 | | | |
| | 1 | 0.08 | 14,720 |
| | 2 | 0.09 | 16,560 |
| | 3 | 0.10 | 18,400 |
| | 4 | 0.12 | 22,080 |
| | 5 | 0.10 | 18,400 |
| | 6 | 0.10 | 18,400 |
| | 7 | 0.11 | 20,240 |
| | 8 | 0.12 | 22,080 |
| | 9 | 0.13 | 23,920 |
| | 10 | 0.14 | 25,760 |
| | 11 | 0.16 | 29,440 |
| | 12 | 0.18 | 33,120 |
| | 13 | 0.19 | 34,960 |
| | 14 | 0.18 | 33,120 |
| | 15 | 0.18 | 33,120 |
| | 16 | 0 | 0 |

# CHAPTER X

## CONCLUSION

The time dependent description of vehicle and break-away support post behavior presented in this research provides a quantitative study based upon experimental observations: the critical events in the chronology of a collision incident have been defined. Corroborative evidence from independent data gathering systems has been presented. The correlation of results has been treated in Chapter VII, and is given in tabular form. Table IX contains a summary of the time of occurrence of critical events. This summary is based upon data taken directly from instrument records and upon data acquired from analytical procedures which were developed by this research.

In order to accomplish the general objective of producing a time dependent description of behavior during a collision incident, several specific objectives have been achieved. The development of a technique for obtaining and reducing high-speed film data, and the development of a technique for reducing and analyzing data from an accelerometer have resulted in a method of correlation of information from these two data acquisition systems. The details of development are presented in Chapter VI; and the results of employing the technique are contained in Appendix D.

Fixed base support post crash tests were performed to provide

values of peak negative acceleration and maximum change in velocity for comparison with break-away base support post values. The values are contained in Table VI of Chapter VI. It is apparent that the primary peak negative acceleration in the fixed base tests is substantially greater than that for the break-away base post: the maximum change in velocity is similarly comparable. The maximum change in velocity in the break-away post tests was found to be only a small fraction of the impact velocity. By contrast the maximum change in velocity in the fixed base test is the entire impact velocity; that is, the crash vehicle is at rest at the conclusion of the collision incident. Vehicle displacement in a break-away post test is a measure of the forward movement of a fixed point on the vehicle. Only a small amount of crumpling of the bumper and hood is experienced. The support post is accelerated forward by the vehicle impact and ultimately swings free of the vehicle. This behavior contrasts sharply with the fixed base post test, in which crumpling of the front end of the vehicle is considerable. Vehicle displacement in a fixed-base post is primarily a measure of this crumpling of the bumper, grill, and hood of the vehicle. In Tests 32 and 39 the support post leaned forward during the collision incident. This post action complicated comparison of film data and computed Displacement-Time data from frame accelerometer analysis. Displacement-Time curves for Tests 32 and 39 are contained in Appendix D. The

Displacement-Time curve for Test 32 as computed by analysis of the frame accelerometer record is in agreement with the high-speed film analysis during the first 40 to 50 milliseconds. Then the computed displacement values fall below the observed values. A re-examination of the film record revealed that the support post leaned forward at this time. A similar relationship of computed displacement values is seen for Test 39. Once again a re-examination of the film record revealed that the support post leaned forward. In this latter test the support post was broken from the base plate to which it had been welded.

The accelerometer record of Test 39 had to be adjusted in order to produce zero velocity at the end of the collision incident. The Velocity-Time plot of this test contains two sets of plotted values. The original values from summing areas contained by the accelerometer record did not produce zero velocity. For purposes of having a complete set of data for this series of tests, it was decided to adjust this record. The adjustment was made by forcing the velocity values to fit the known condition at the end of the collision incident. This was accomplished by applying a constant factor to each computed velocity. It is recommended that Test 39 be disregarded in future consideration of the method presented herein, because it is the only test which required adjustment.

Comparison of Displacement-Time data from high-speed film observation with computed Displacement-Time data from the accelerometer

record became particularly critical in the fixed base support post tests as described. It has been observed earlier that some investigators have analyzed high-speed film records, while others have analyzed accelerometer traces. One salient conviction which has emerged from the current study is that data from both photographic and electronic instrumentation must be examined thoroughly and carefully compared. The result of such a procedure is a correlated chronology of a collision incident as presented in Chapter VII.

Another conclusion of this investigation is that all recorded accelerometer data must be scanned in order to produce satisfactory results. Careful adherence to this principle will yield information concerning the time of critical events which occur in the collision incident. Arbitrary curve fitting techniques may obscure critical events. Future studies may lead to a clearer understanding of a collision incident, but until such a clearer understanding becomes available, consideration of all recorded accelerometer data is recommended.

Information concerning strain and stress in elements of the "plastic hinge" joint have been presented in Chapter VIII. The force in the support post at bumper height has been considered in Chapter IX. This information provides an indication of quantitative values secured directly from measuring systems installed on the support post. The magnitudes of the recorded values are subject to verification by future

investigators, and the values are presented to provide an initial statement of results.

# LIST OF REFERENCES


1. Samson, C. H., Rowan, N. J., Olson, R. M., and Tidwell, D. R., "Impact Behavior of Sign Supports," Research Report 68-1, Texas Transportation Institute, College Station, March, 1965.

2. See ibid., pages 1-3.

3. Stonex, K. A. and Skeels, P. C., "Development of Crash Research Techniques at the General Motors Proving Ground," Highway Research Record No. 4, January 1963, p. 32.

4. Beaton, J. L., "Full Scale Tests of Concrete Bridge Rails Subjected to Automobile Impacts," Highway Research Board Proceedings, Volume 35, 1956, pp. 251-267.

5. Henault, Gilles G., "Research on Different Types of Guide Rails, Metropolitan Boulevard, Montreal," paper given at the Annual General Meeting of the Engineering Institute of Canada, 1963.

6. Severy, D. M. and Mathewson, J. H., "Automobile - Barrier Impacts," Highway Research Board Bulletin 91, 1954, pp. 39-54.

7. Severy, D. M., and Mathewson, J. H., "Automobile Barrier and Rear End Collisions Performance," SAE Preprint 62C, 1958, p. 61.

8. Severy, D. M., Mathewson, J. H., and Siegel, A. W., "Automobile Head-On Collisions, Series II," SAE Preprint 31A, 1958.

9. Severy, D. M., Mathewson, J. H., and Siegel, A. W., "Automobile Side-Impact Collisions," SAE Special Publication 174, January 1960, p. 62.

10. Severy, D. M., "Correlates of 30-mph Intersection Collisions," Highway Research Record No. 4, January 1963, pp. 1-31.

11. Blamey, C., "Results from Impact Tests on Telegraph Poles," Department of Scientific and Industrial Research, Road Research Laboratory, Highways & Bridges, Volume 32, 1964, pp. 7-8.

12. Moore, R. L., and Christie, A. W., "The Design of Lamp Columns for Roads with Few Pedestrians," Light and Lighting, Volume 53, No. 11, 1960, pp. 330-334.

13. See ibid., p. 333.

14. Stapp, J. P., "Human Exposures to Linear Deceleration," Part I, U.S.A.F. Technical Report No. 5915, Aeromedical Laboratory, Wright-Patterson A.F.B., Dayton, Ohio, December, 1951, p.14.

15. See ibid., p. 14.

16. See ibid., p. 3.

17. See ibid., p. 16.

18. Beaton, J. L., and Field, R. N., "Dynamic Full Scale Tests of Median Barriers," Highway Research Board Proceedings, Volume 39, 1960, (Bulletin 266).

19. Christie, A. W., "Some Investigations Concerning the Lighting of Traffic Routes," Public Lighting, 1962, 27 (119), 189-99; Discussion, 199-204.

20. Lundstrom, L. C., and Skeels, P. C., "Full-Scale Appraisals of Guardrail Installations by Car Impact Tests," Highway Research Board Proceedings, Volume 38, 1959, pp. 353-355.

21. Cichowski, W. G., Skeels, P. C., and Hawkins, W. R., "Appraisal of Guardrail Installations by Car Impact and Laboratory Test," Highway Research Board Proceedings, Volume 40, 1961, pp. 137-149.

22. Jehu, V. J., "Vehicle Guard Rails for Roads and Bridges," Seventh Congress, International Association for Bridge and Structural Engineering, Rio de Janeiro, August 10-16, 1964, pp. 1097-1106.

23. Ball, E. F., and Higgins, J. J., "Installation and Tightening of Bolts," Transactions of the American Society of Civil Engineers, Volume 126, Part II, 1961, pp. 797-810.

24. Severy, D. M., and Barbour, P., "Acceleration Accuracy: Analyses of High-Speed Camera Film" Journal of the Society of Motion Picture and Television Engineers, Volume 65, No. 2, February, 1965, p. 99.

25. Hechtman, R. A., Young, D. R., Chin A. G., and Savikko, J. M., "Slip of Joints Under Static Loads," Transactions of the American Society of Civil Engineers, Volume 120, 1955, pp. 1335-1352.

26. See ibid., p. 1340.

27. See ibid., p. 1341.

# APPENDIX A

# OSCILLOGRAPHIC RECORDS

# TESTS 32, 33, AND 35

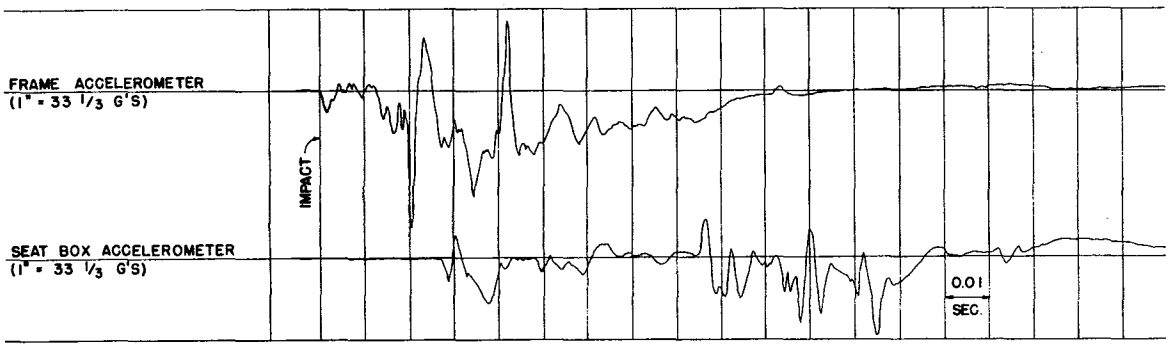


TEST NO. 32

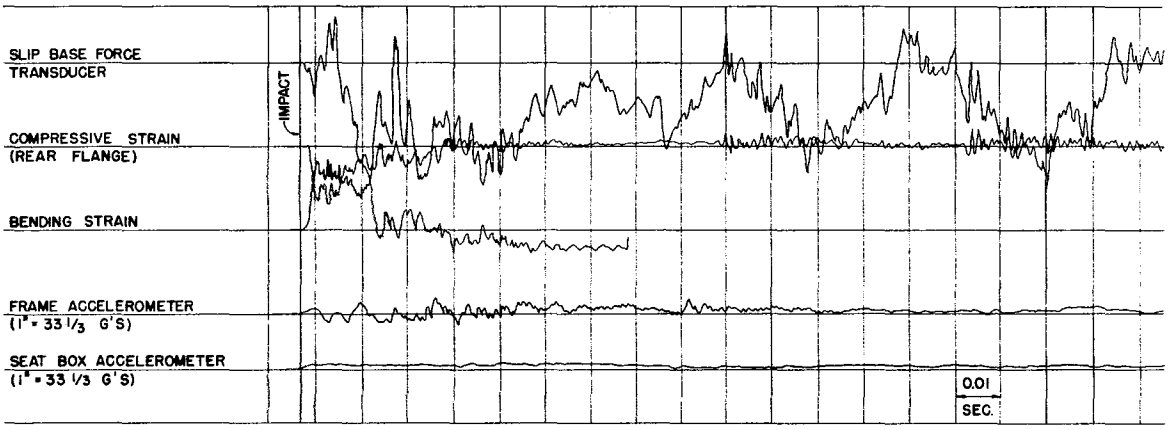


TEST NO. 33

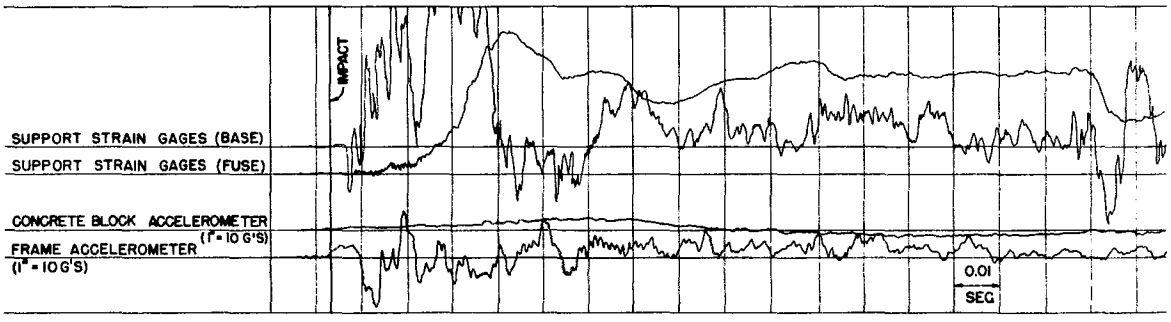


TEST NO. 35

# HONEYWELL MODEL 1508 VISICORDER RECORDS

# APPENDIX B

# OSCILLOGRAPHIC RECORDS

# TESTS 39, 40, AND 41

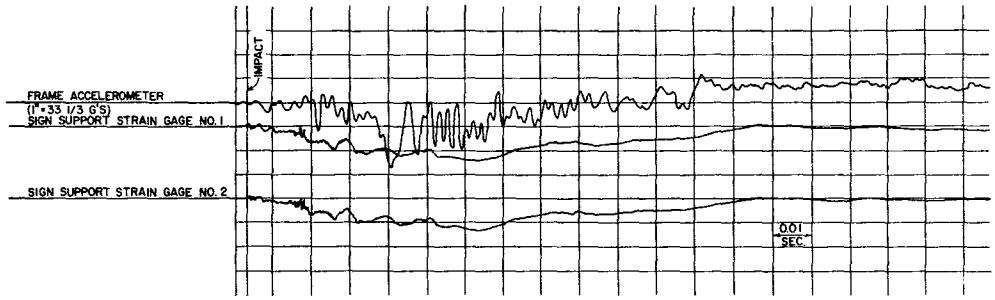


TEST NO. 39

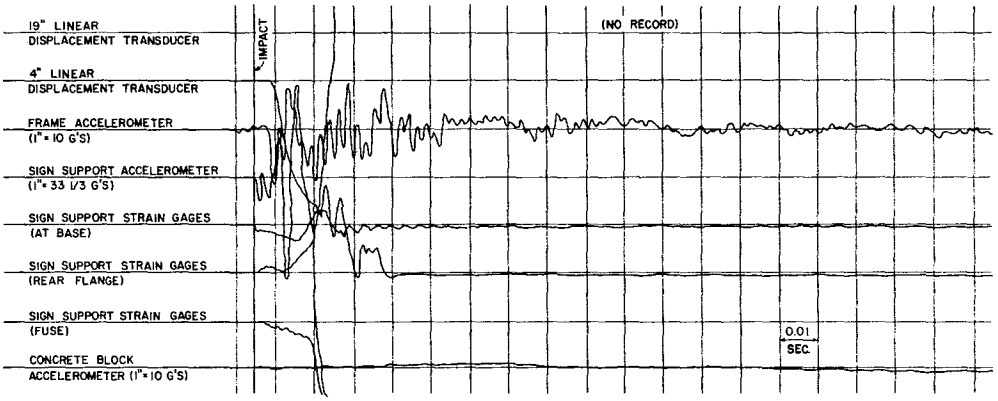


TEST NO. 40

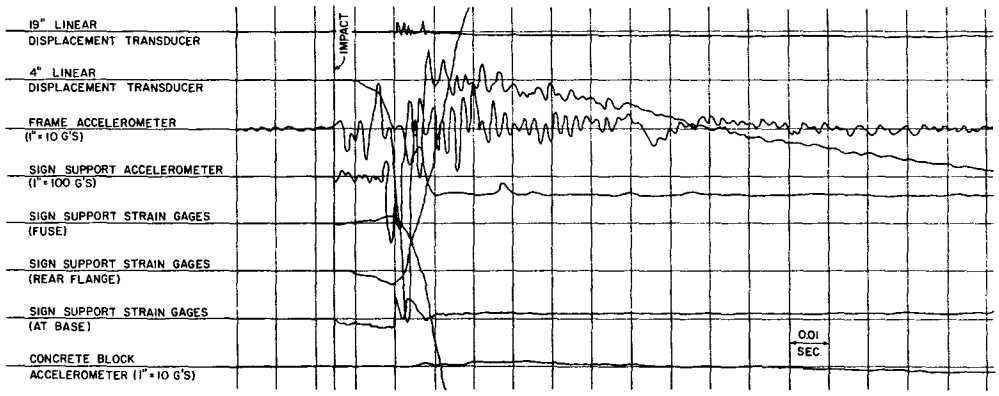


TEST NO. 41

# HONEYWELL MODEL 1508 VISICORDER RECORDS

# APPENDIX C

# CORRELATION OF CLOCK TIME AND FRAME COUNT

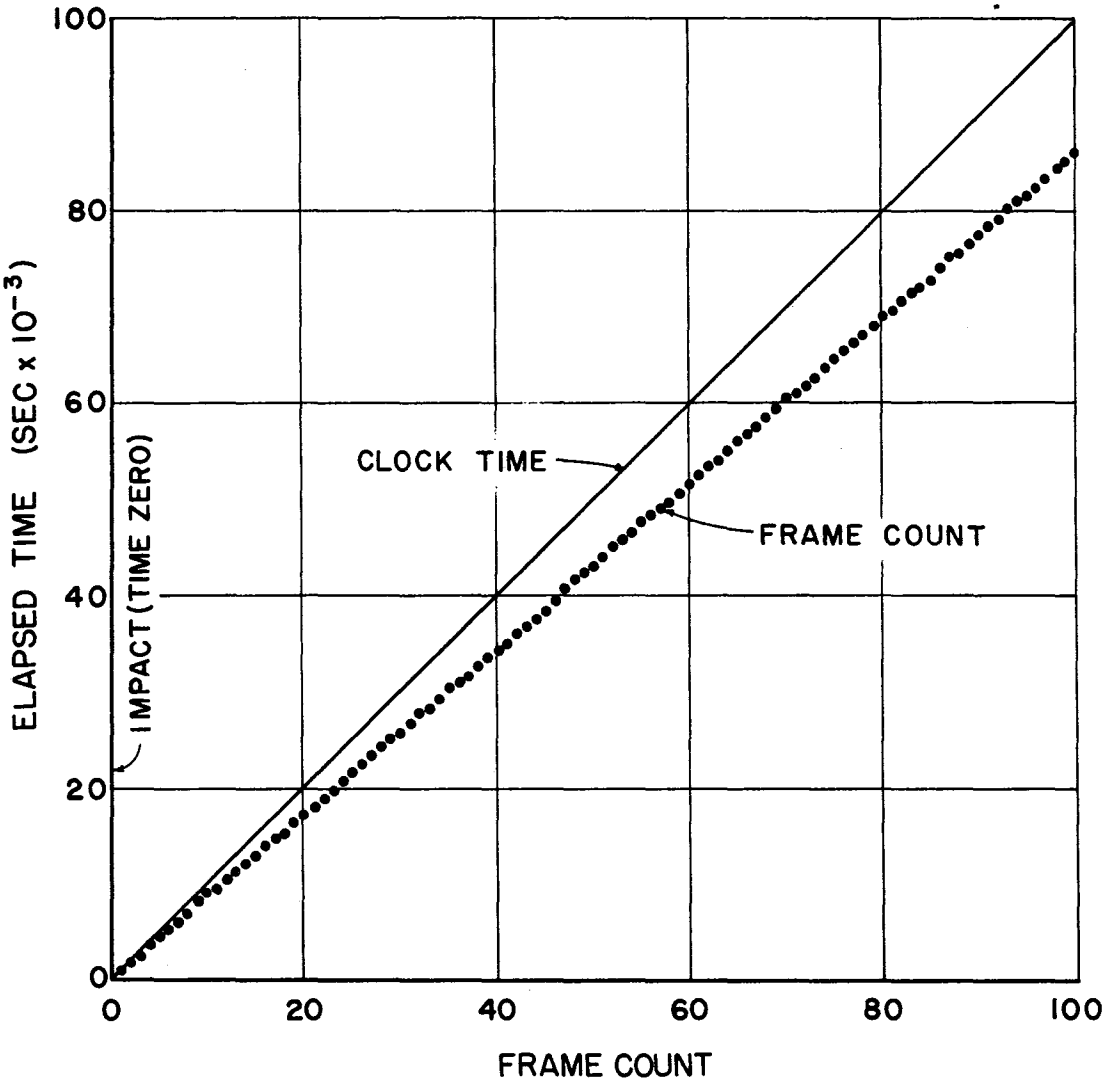


CLOCK TIME VS. FRAME COUNT, TEST 35

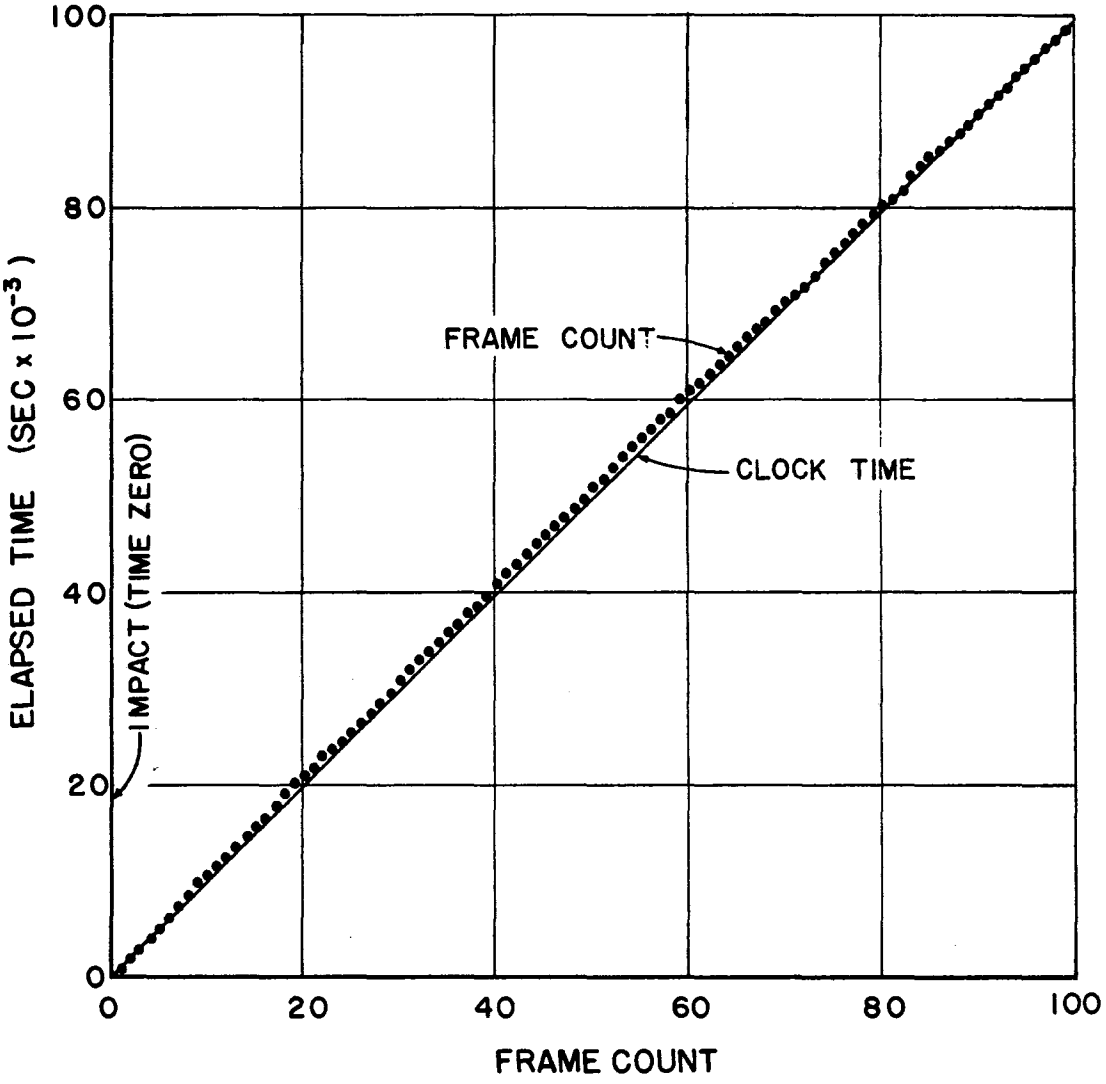


CLOCK TIME VS. FRAME COUNT, TEST 41

# APPENDIX D

# ACCELEROMETER ANALYSES

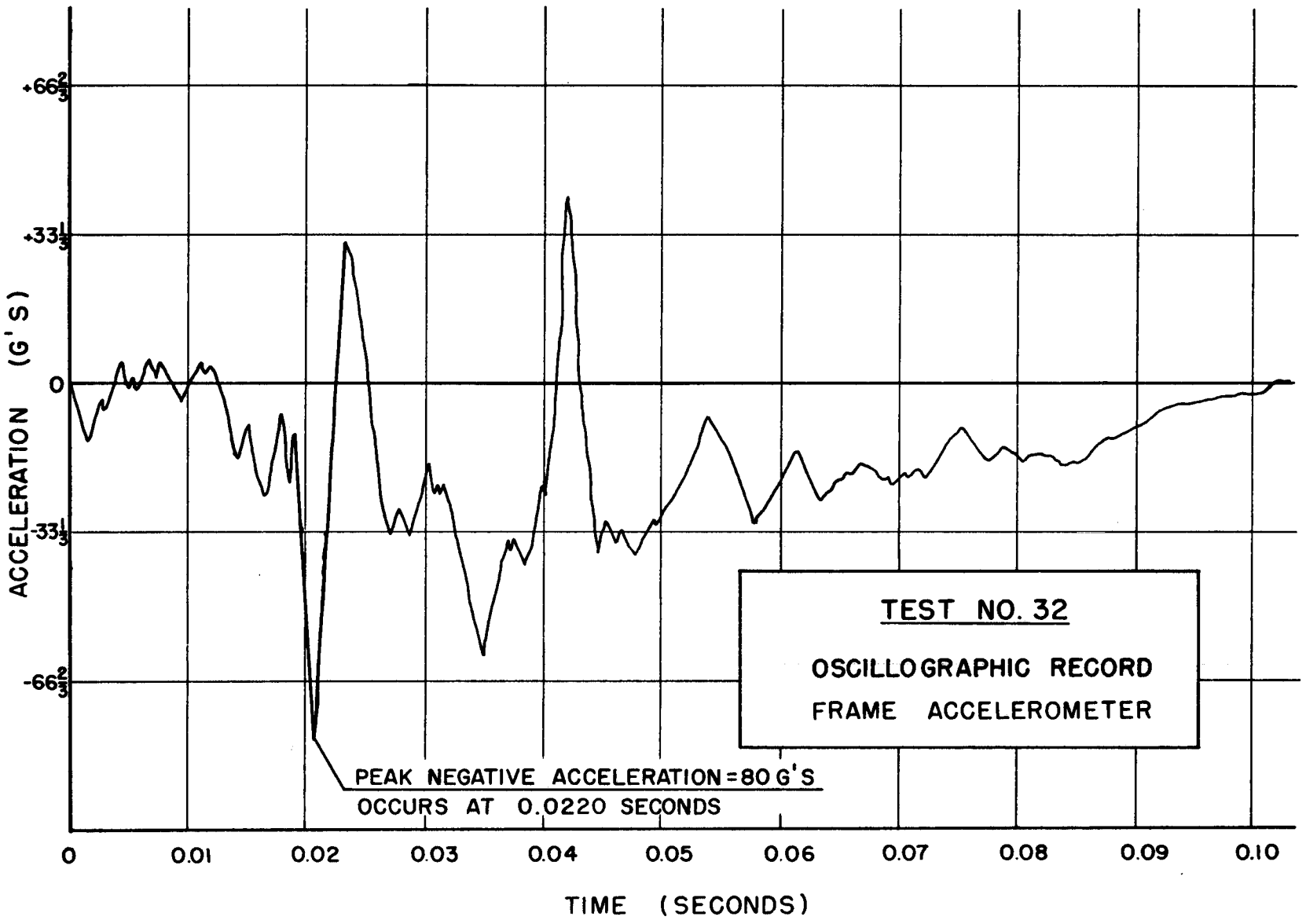
+66⅔
+33⅓
0
-33⅓
-66⅔
ACCELERATION (G'S)
0
0.01
0.02
0.03
0.04
0.05
0.06
0.07
0.08
0.09
0.10
TIME (SECONDS)
TEST NO. 32
OSCILLOGRAPHIC RECORD
FRAME ACCELEROMETER
PEAK NEGATIVE ACCELERATION = 80 G'S
OCCURS AT 0.0220 SECONDS

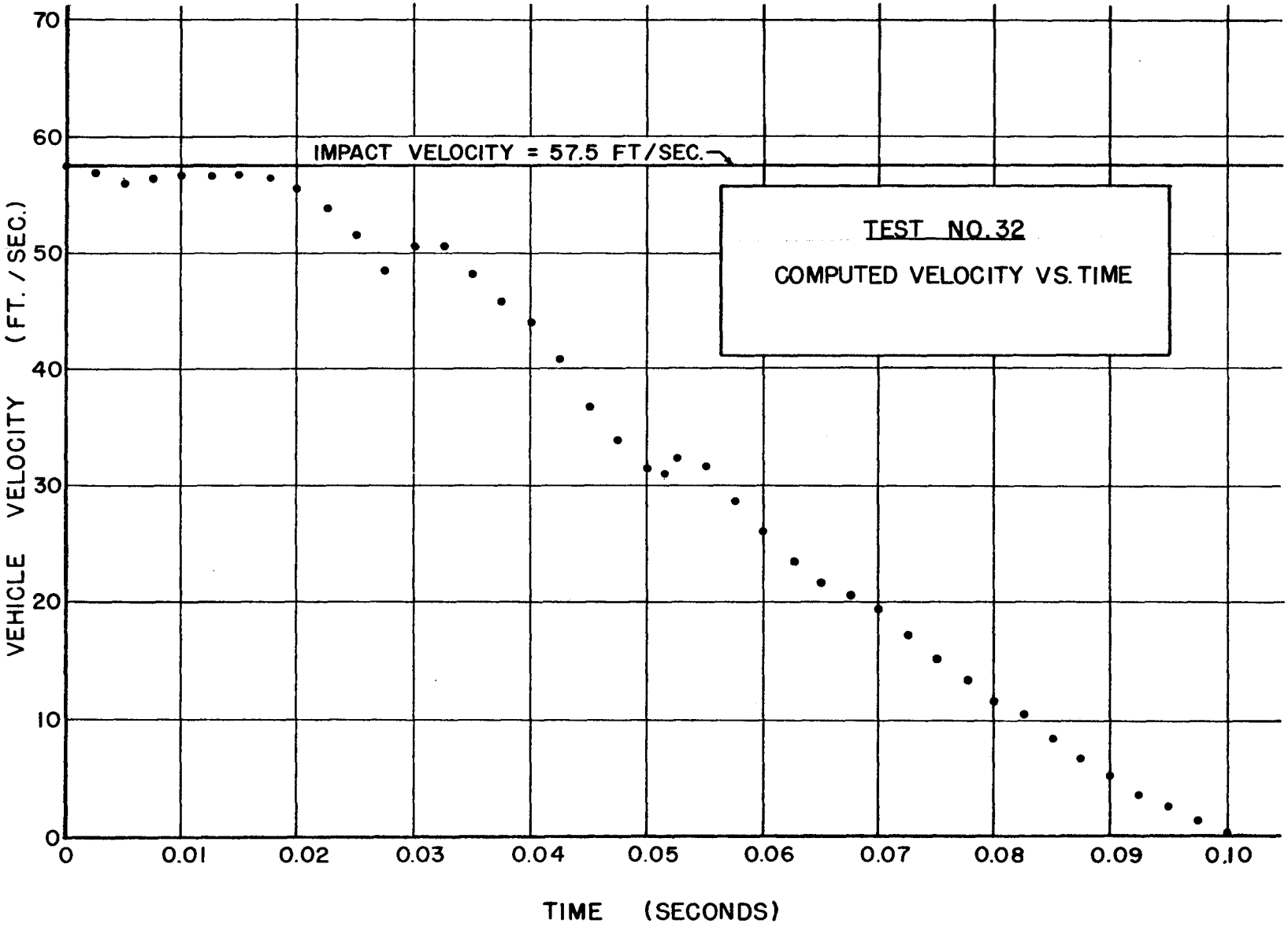
70
60
50
40
30
20
10
0
VEHICLE VELOCITY (FT. / SEC.)
IMPACT VELOCITY = 57.5 FT/SEC.
TEST NO. 32
COMPUTED VELOCITY VS. TIME
0
0.01
0.02
0.03
0.04
0.05
0.06
0.07
0.08
0.09
0.10
TIME (SECONDS)

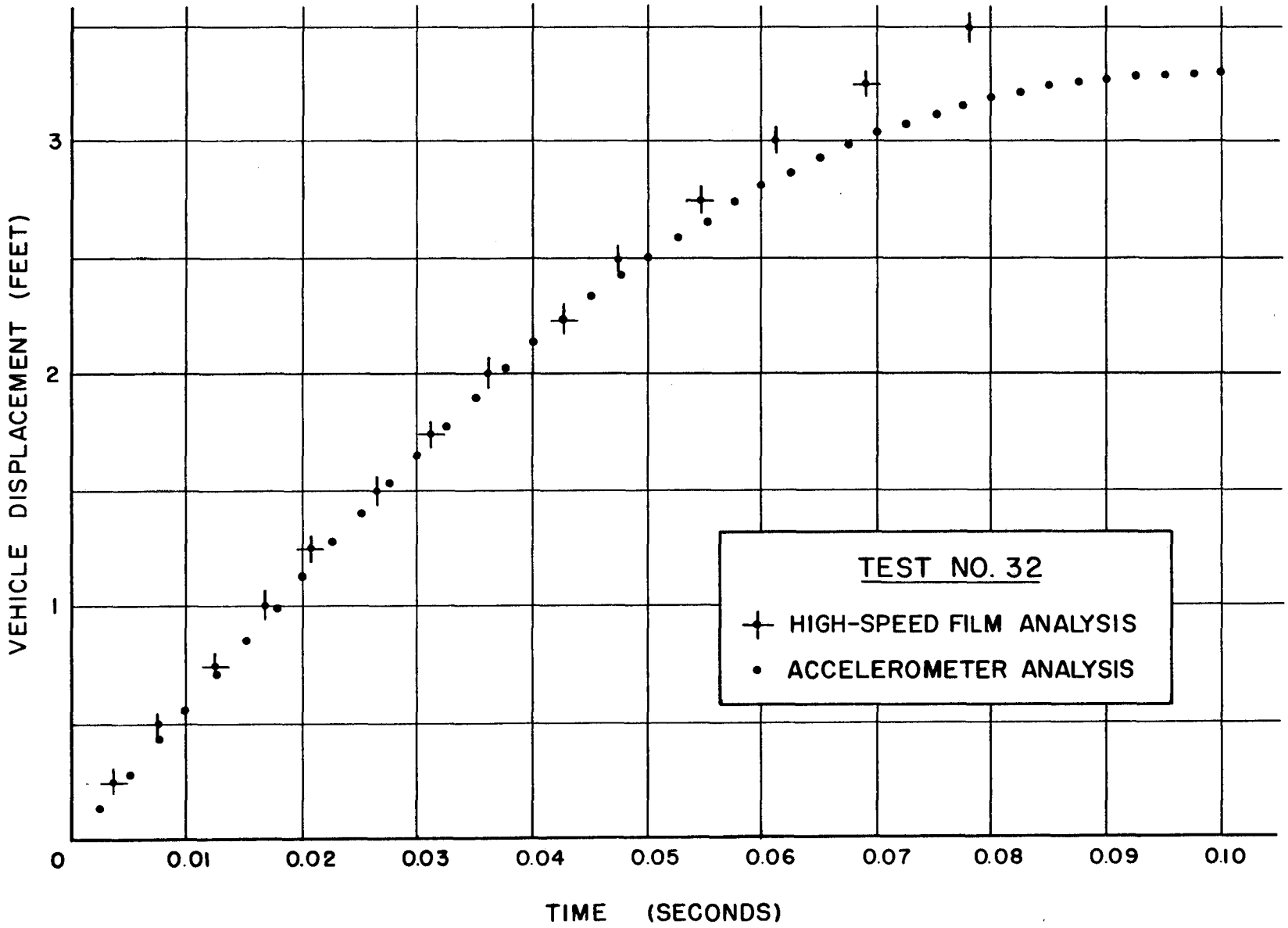
VEHICLE DISPLACEMENT (FEET)
0
1
2
3
0.01
0.02
0.03
0.04
0.05
0.06
0.07
0.08
0.09
0.10
TIME (SECONDS)
TEST NO. 32
HIGH-SPEED FILM ANALYSIS
ACCELEROMETER ANALYSIS

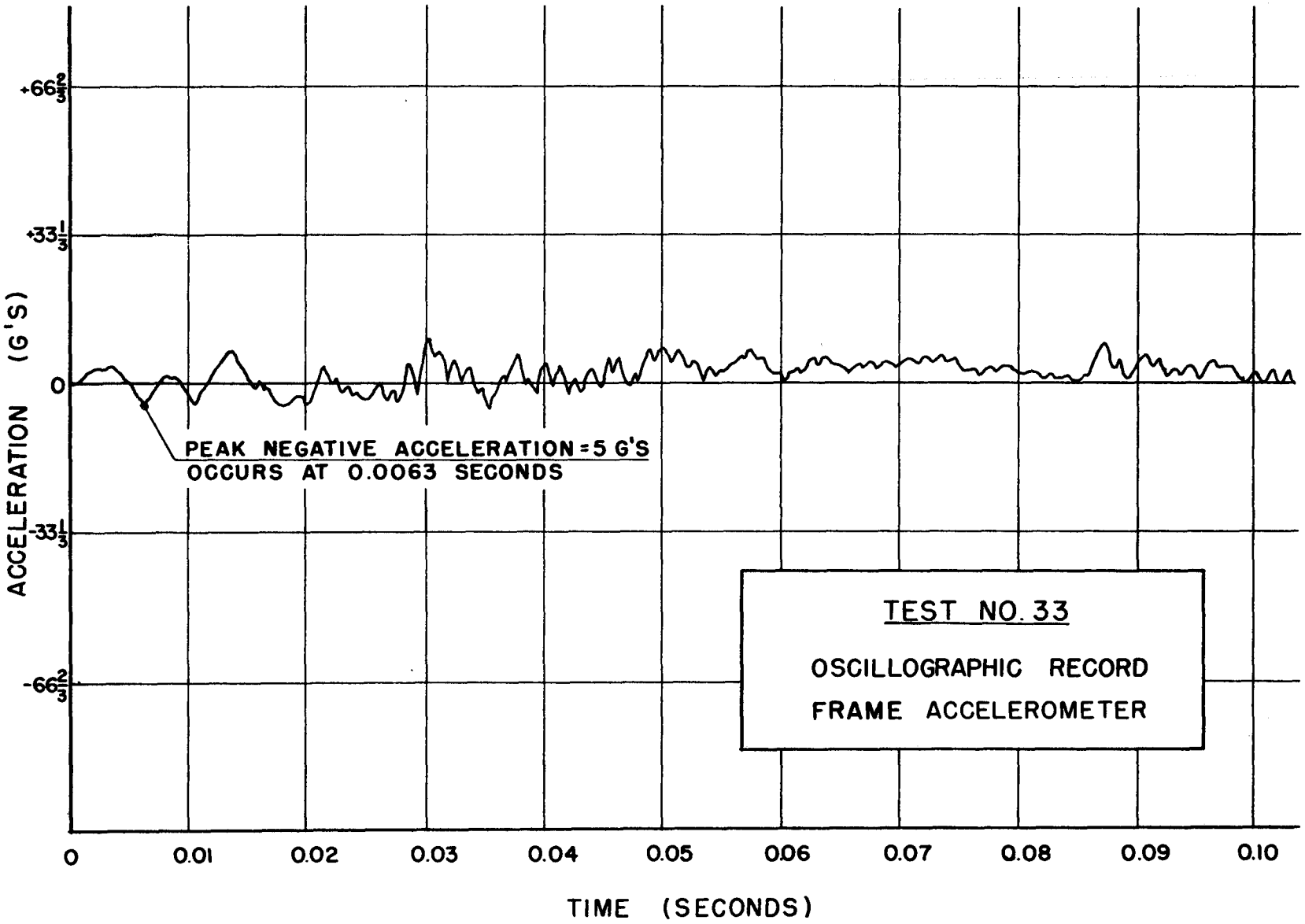
+66⅔
+33⅓
0
-33⅓
-66⅔
ACCELERATION (G'S)
PEAK NEGATIVE ACCELERATION = 5 G'S
OCCURS AT 0.0063 SECONDS
TEST NO. 33
OSCILLOGRAPHIC RECORD
FRAME ACCELEROMETER
0
0.01
0.02
0.03
0.04
0.05
0.06
0.07
0.08
0.09
0.10
TIME (SECONDS)

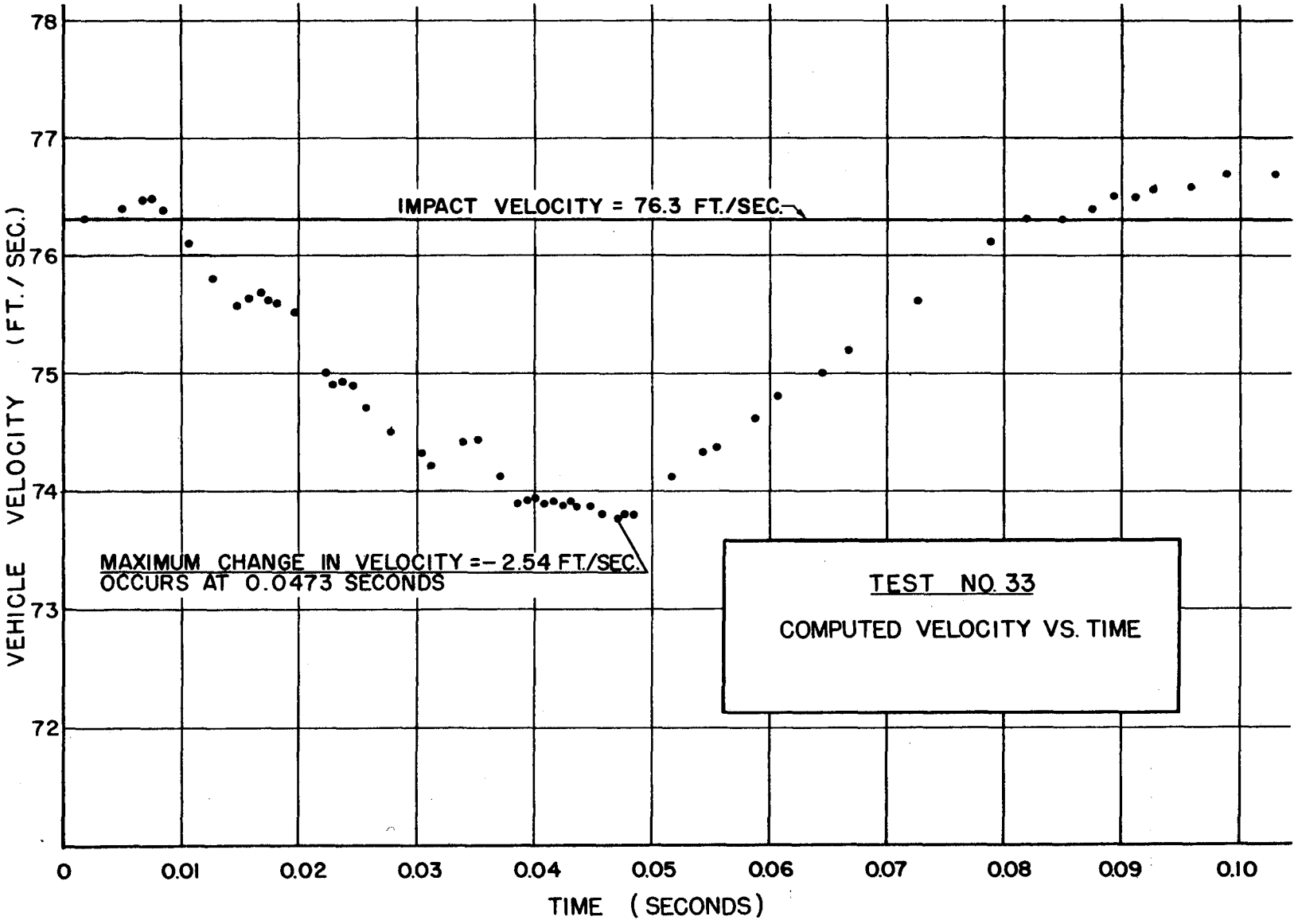
78
77
76
75
74
73
72
VEHICLE VELOCITY (FT./SEC.)
IMPACT VELOCITY = 76.3 FT./SEC.
MAXIMUM CHANGE IN VELOCITY = -2.54 FT/SEC.
OCCURS AT 0.0473 SECONDS
TEST NO. 33
COMPUTED VELOCITY VS. TIME
0
0.01
0.02
0.03
0.04
0.05
0.06
0.07
0.08
0.09
0.10
TIME (SECONDS)

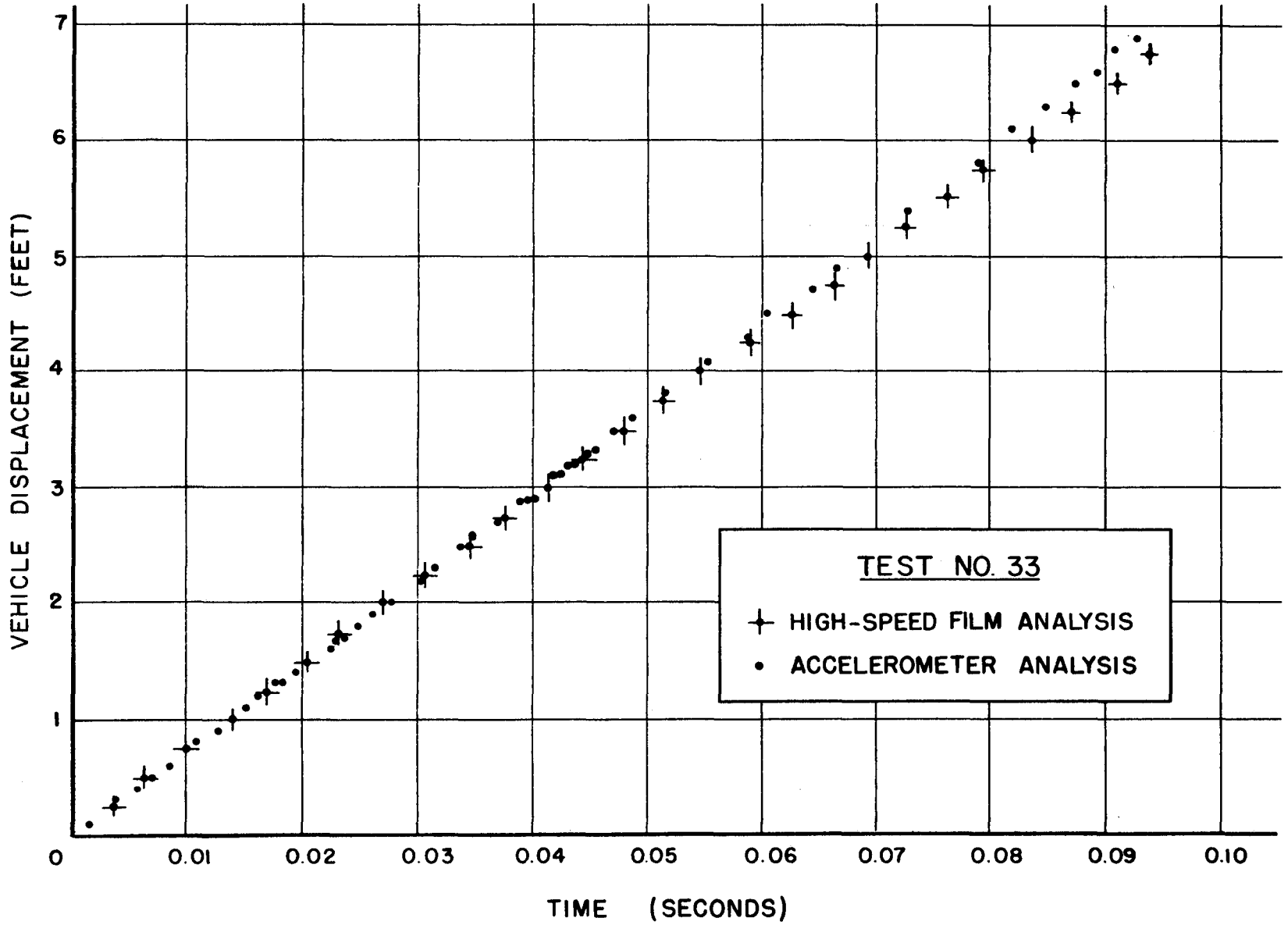
VEHICLE DISPLACEMENT (FEET)
7
6
5
4
3
2
1
0
0.01
0.02
0.03
0.04
0.05
0.06
0.07
0.08
0.09
0.10
TIME (SECONDS)
TEST NO. 33
HIGH-SPEED FILM ANALYSIS
ACCELEROMETER ANALYSIS

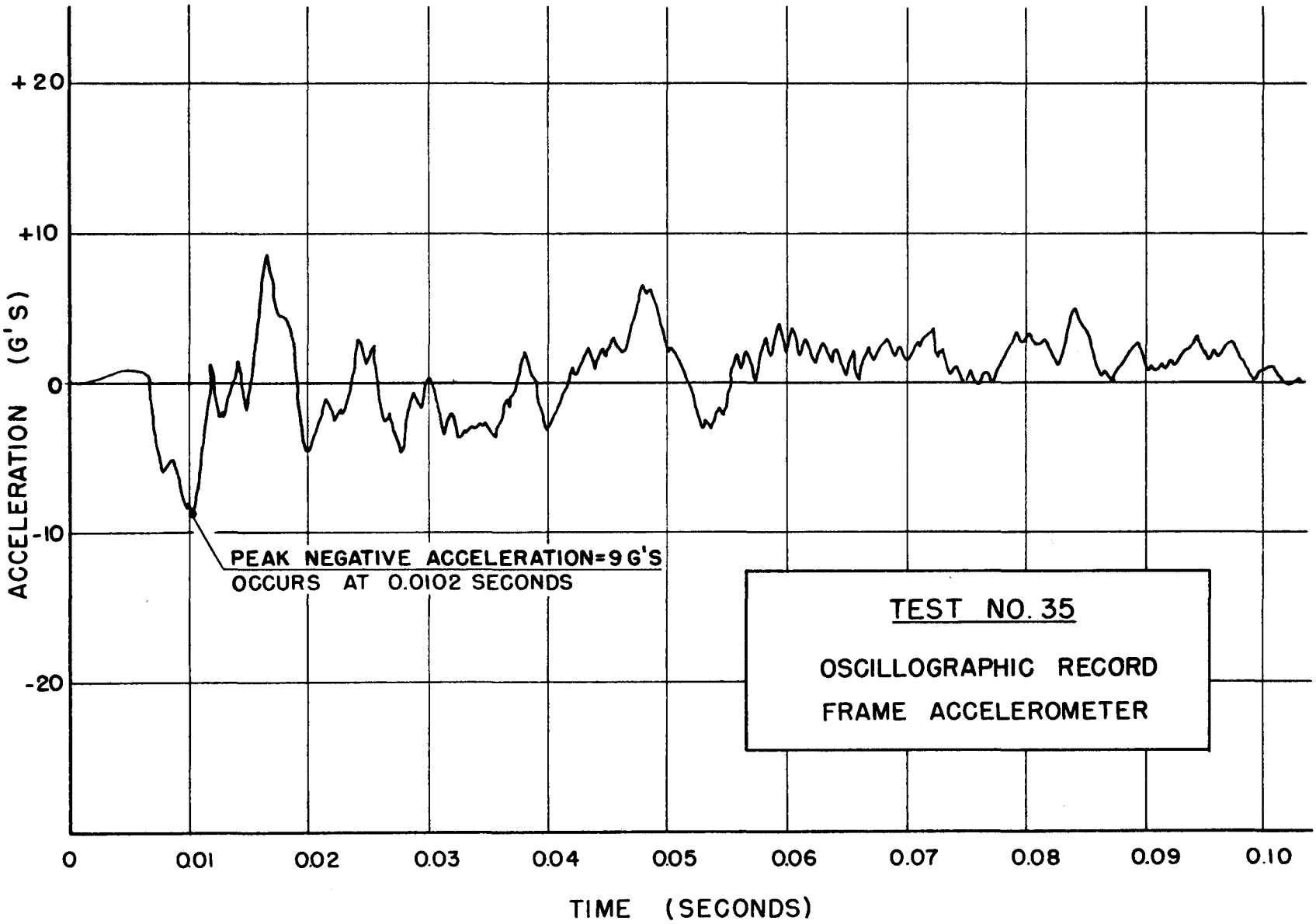
+20
+10
0
-10
-20
ACCELERATION (G'S)
PEAK NEGATIVE ACCELERATION=9 G'S
OCCURS AT 0.0102 SECONDS
TEST NO. 35
OSCILLOGRAPHIC RECORD
FRAME ACCELEROMETER
0
0.01
0.02
0.03
0.04
0.05
0.06
0.07
0.08
0.09
0.10
TIME (SECONDS)

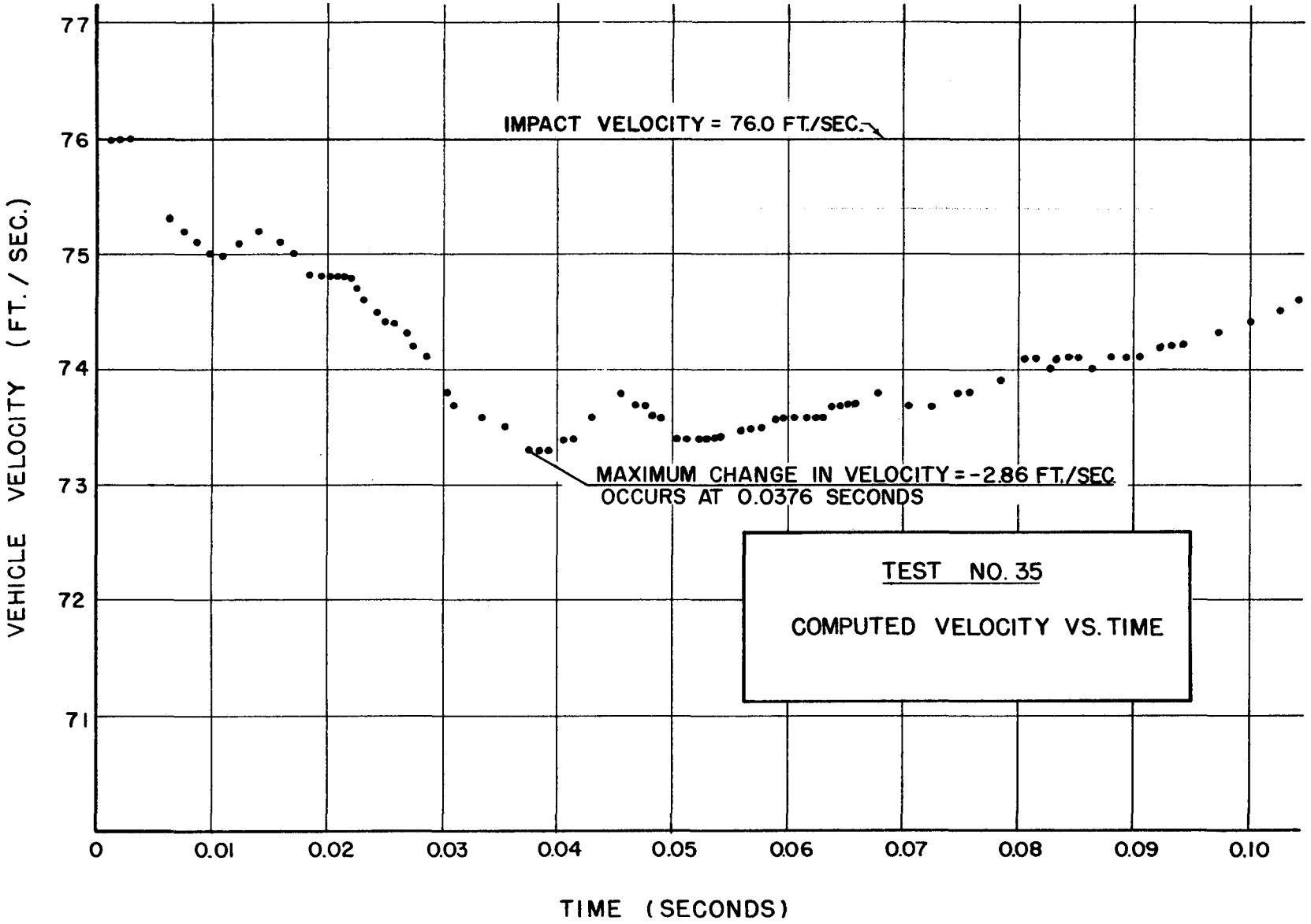
77
76
75
74
73
72
71
VEHICLE VELOCITY (FT./SEC.)
IMPACT VELOCITY = 76.0 FT./SEC.
MAXIMUM CHANGE IN VELOCITY = -2.86 FT./SEC
OCCURS AT 0.0376 SECONDS
TEST NO. 35
COMPUTED VELOCITY VS. TIME
0
0.01
0.02
0.03
0.04
0.05
0.06
0.07
0.08
0.09
0.10
TIME (SECONDS)

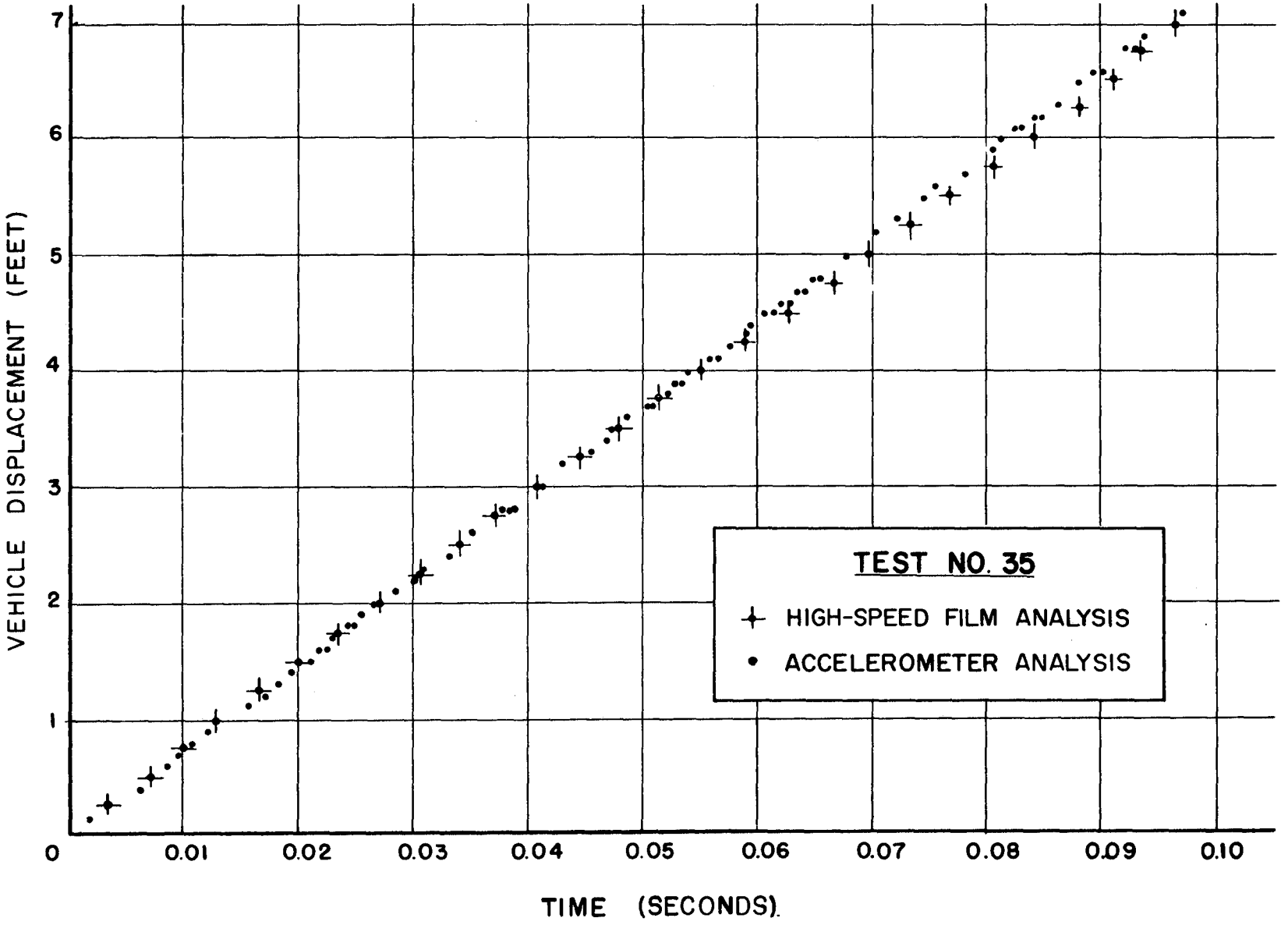
VEHICLE DISPLACEMENT (FEET)
7
6
5
4
3
2
1
0
0.01
0.02
0.03
0.04
0.05
0.06
0.07
0.08
0.09
0.10
TIME (SECONDS)
TEST NO. 35
HIGH-SPEED FILM ANALYSIS
ACCELEROMETER ANALYSIS

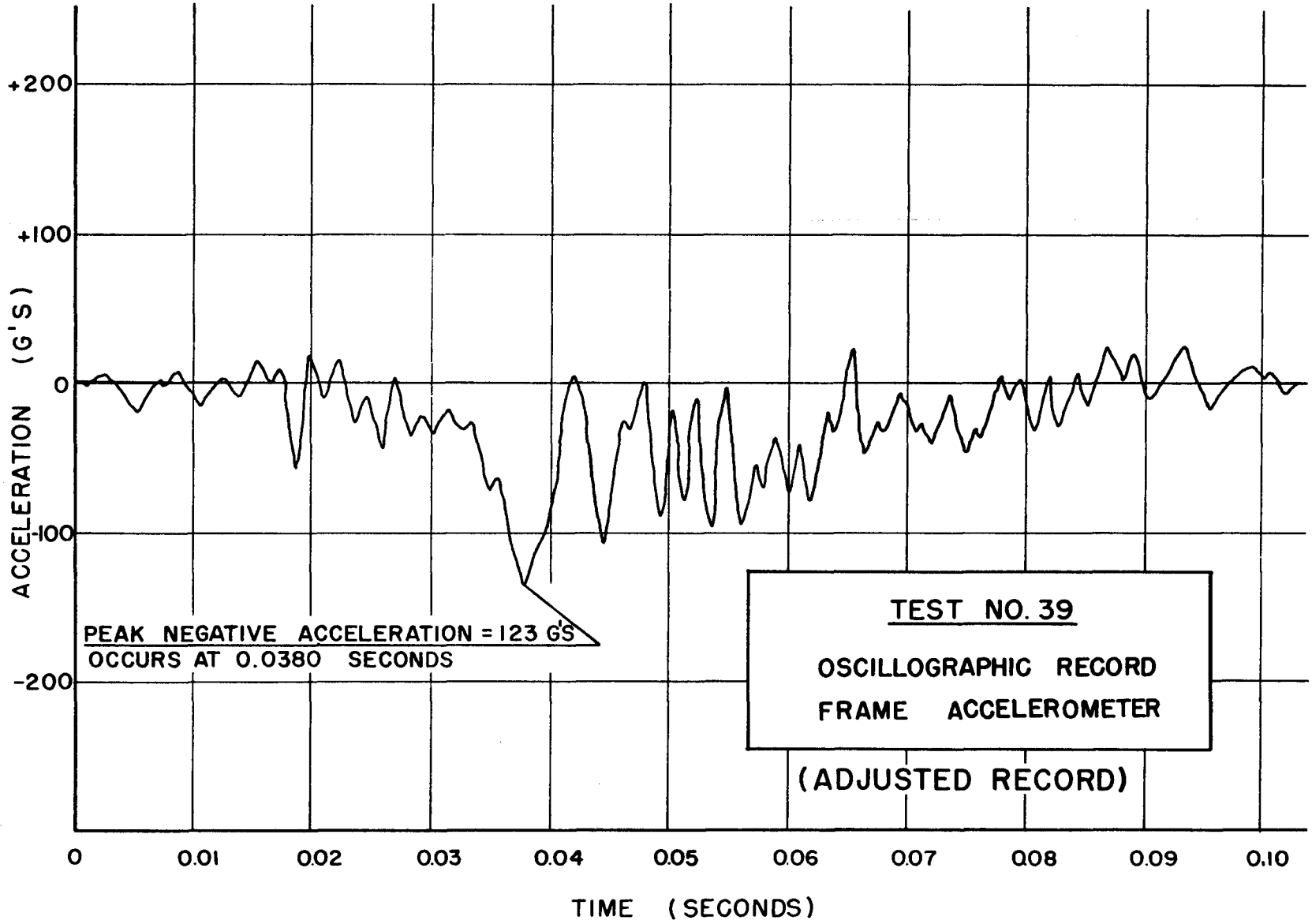
+200
+100
0
-100
-200
ACCELERATION (G'S)
PEAK NEGATIVE ACCELERATION = 123 G'S
OCCURS AT 0.0380 SECONDS
TEST NO. 39
OSCILLOGRAPHIC RECORD
FRAME ACCELEROMETER
(ADJUSTED RECORD)
0
0.01
0.02
0.03
0.04
0.05
0.06
0.07
0.08
0.09
0.10
TIME (SECONDS)

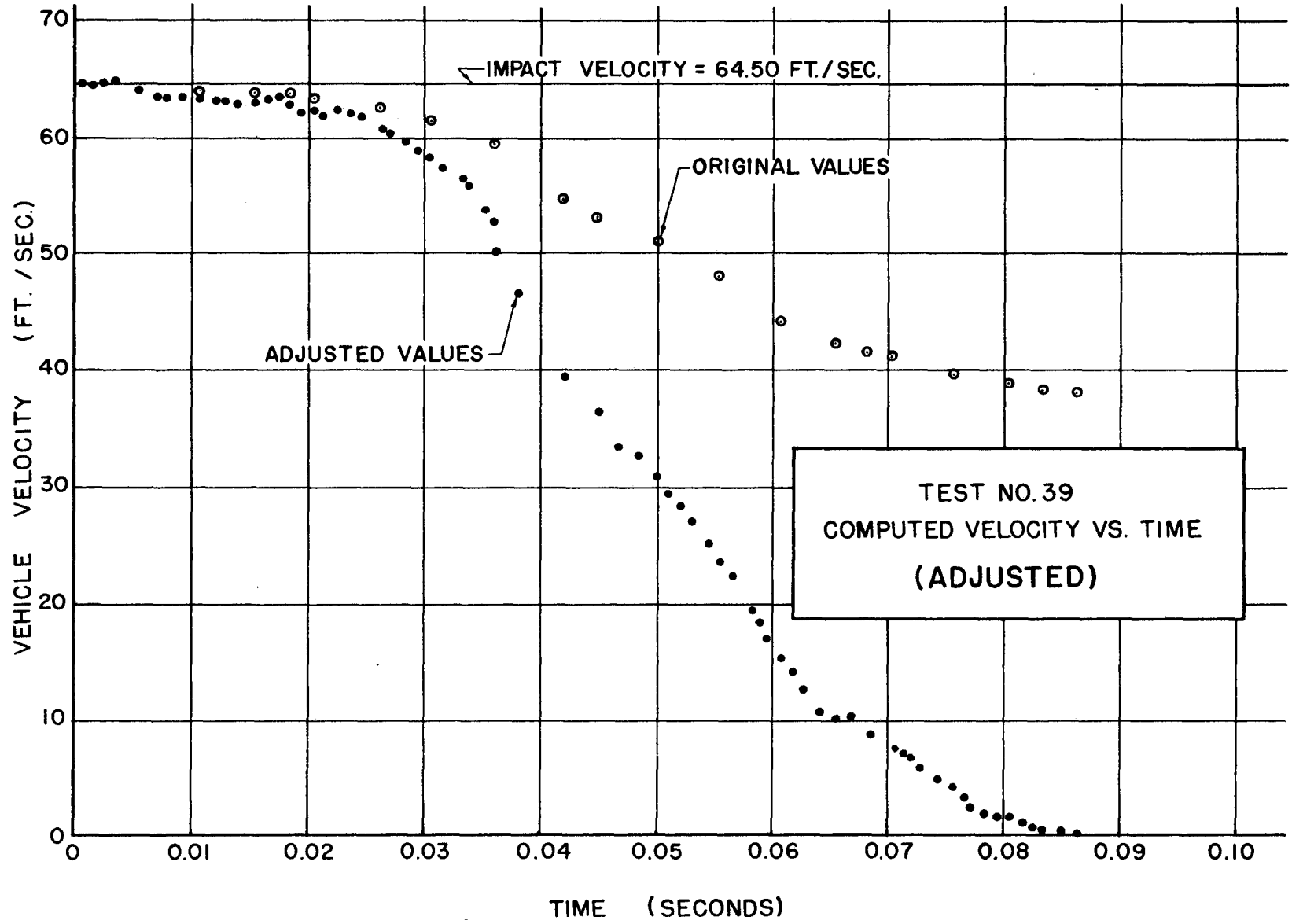
IMPACT VELOCITY = 64.50 FT./SEC.
ORIGINAL VALUES
ADJUSTED VALUES
TEST NO. 39
COMPUTED VELOCITY VS. TIME
(ADJUSTED)
VEHICLE VELOCITY (FT./SEC.)
TIME (SECONDS)
0
10
20
30
40
50
60
70
0
0.01
0.02
0.03
0.04
0.05
0.06
0.07
0.08
0.09
0.10

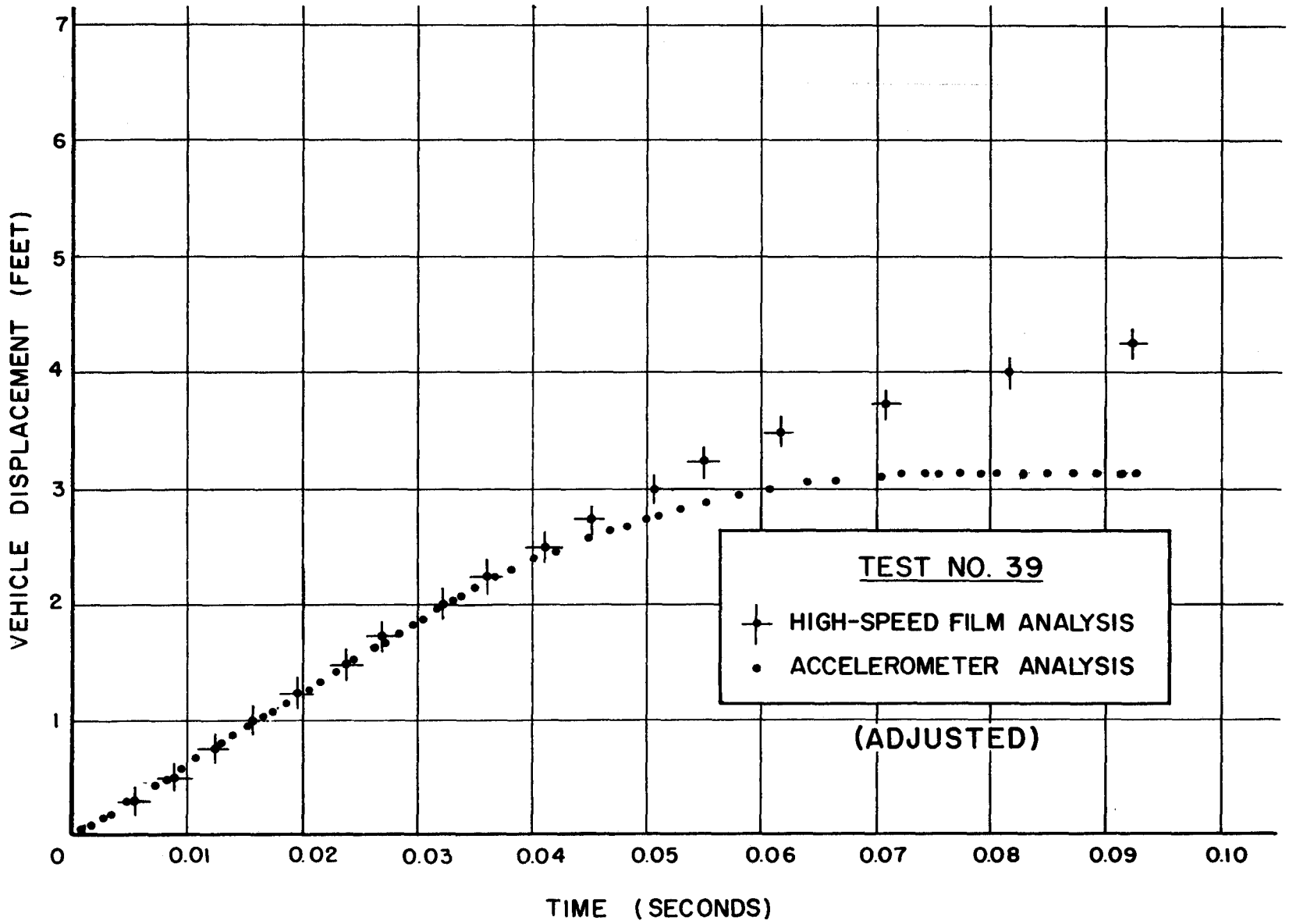
VEHICLE DISPLACEMENT (FEET)
7
6
5
4
3
2
1
0
0.01
0.02
0.03
0.04
0.05
0.06
0.07
0.08
0.09
0.10
TIME (SECONDS)
TEST NO. 39
HIGH-SPEED FILM ANALYSIS
ACCELEROMETER ANALYSIS
(ADJUSTED)

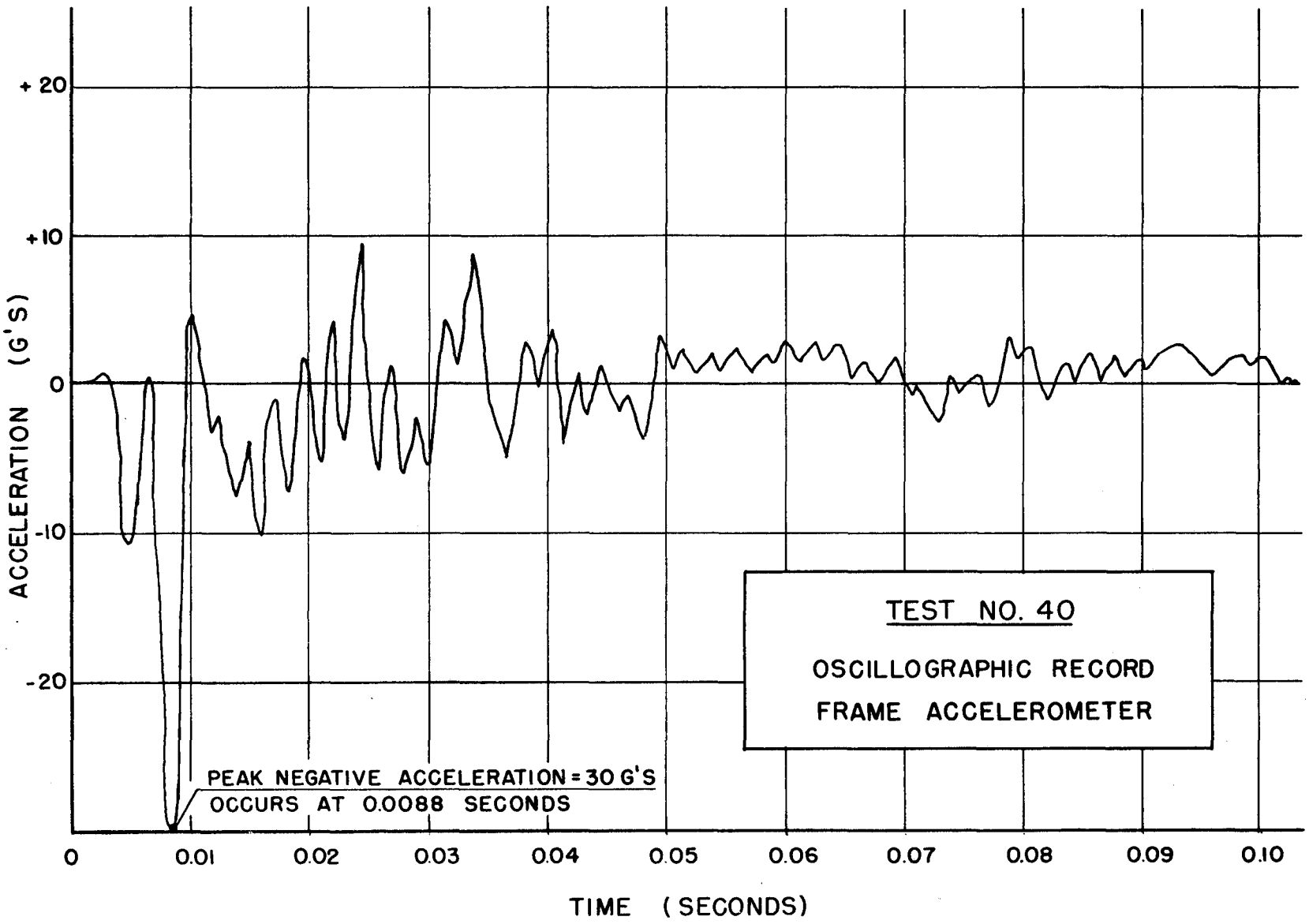
+ 20
+10
0
-10
-20
ACCELERATION (G'S)
PEAK NEGATIVE ACCELERATION = 30 G'S
OCCURS AT 0.0088 SECONDS
TEST NO. 40
OSCILLOGRAPHIC RECORD
FRAME ACCELEROMETER
0
0.01
0.02
0.03
0.04
0.05
0.06
0.07
0.08
0.09
0.10
TIME (SECONDS)

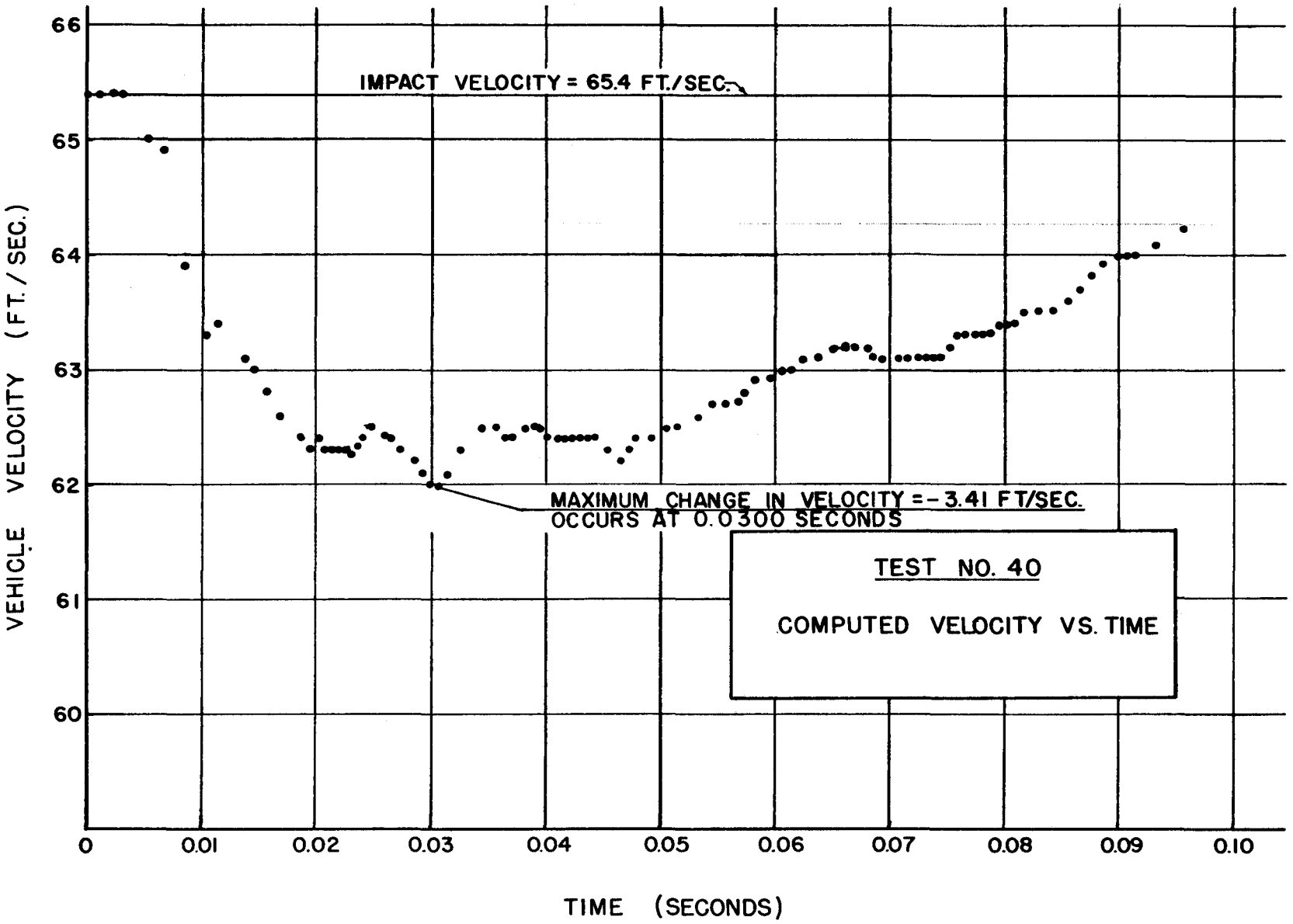
IMPACT VELOCITY = 65.4 FT./SEC.
MAXIMUM CHANGE IN VELOCITY = -3.41 FT/SEC.
OCCURS AT 0.0300 SECONDS
TEST NO. 40
COMPUTED VELOCITY VS. TIME
VEHICLE VELOCITY (FT./SEC.)
66
65
64
63
62
61
60
0
0.01
0.02
0.03
0.04
0.05
0.06
0.07
0.08
0.09
0.10
TIME (SECONDS)

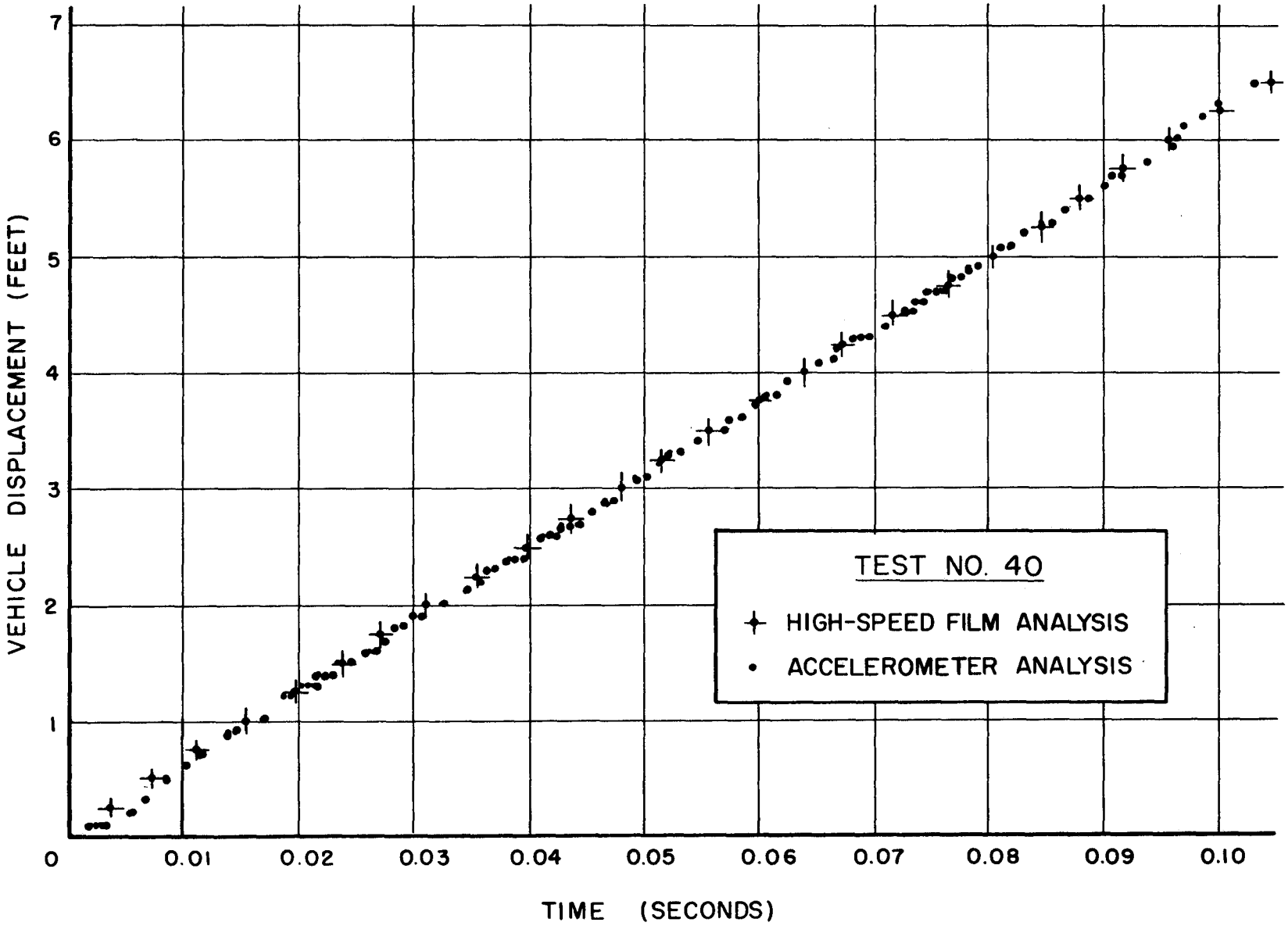
VEHICLE DISPLACEMENT (FEET)
7
6
5
4
3
2
1
0
0.01
0.02
0.03
0.04
0.05
0.06
0.07
0.08
0.09
0.10
TIME (SECONDS)
TEST NO. 40
HIGH-SPEED FILM ANALYSIS
ACCELEROMETER ANALYSIS

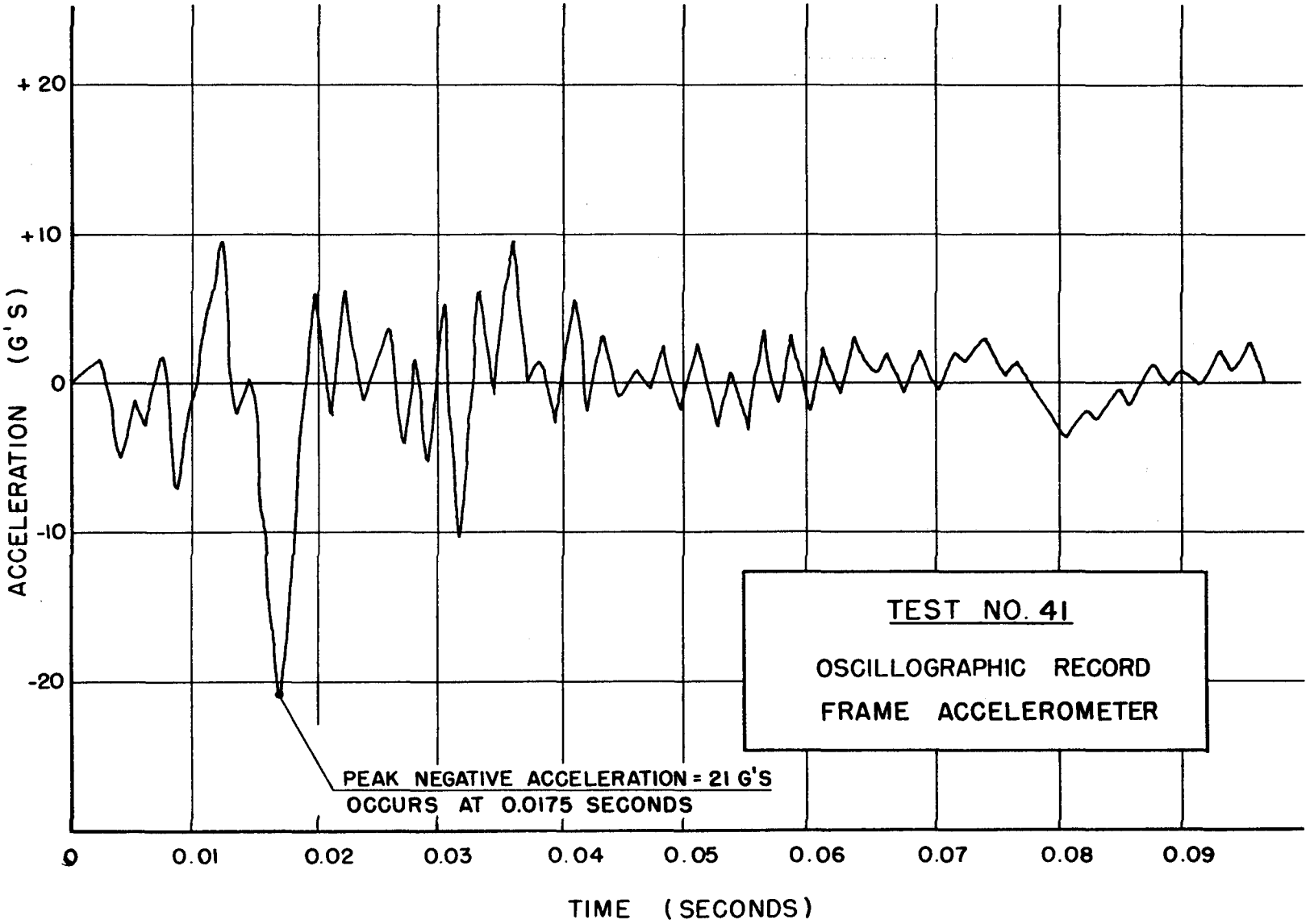
+ 20
+10
0
-10
-20
ACCELERATION (G'S)
0
0.01
0.02
0.03
0.04
0.05
0.06
0.07
0.08
0.09
TIME (SECONDS)
PEAK NEGATIVE ACCELERATION = 21 G'S
OCCURS AT 0.0175 SECONDS
TEST NO. 41
OSCILLOGRAPHIC RECORD
FRAME ACCELEROMETER

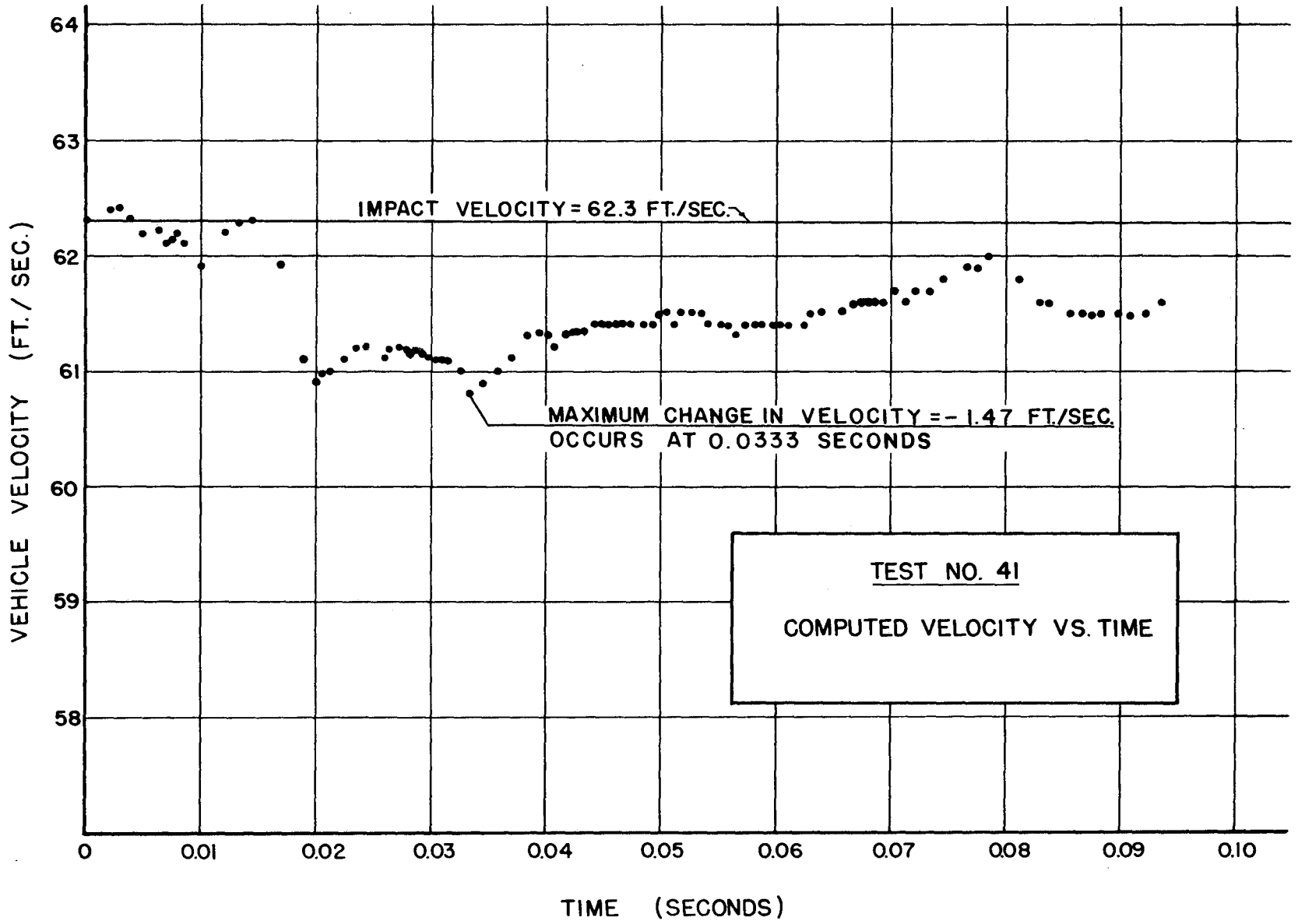
64
63
62
61
60
59
58
VEHICLE VELOCITY (FT./SEC.)
IMPACT VELOCITY = 62.3 FT./SEC.
MAXIMUM CHANGE IN VELOCITY = - 1.47 FT./SEC.
OCCURS AT 0.0333 SECONDS
TEST NO. 41
COMPUTED VELOCITY VS. TIME
0
0.01
0.02
0.03
0.04
0.05
0.06
0.07
0.08
0.09
0.10
TIME (SECONDS)

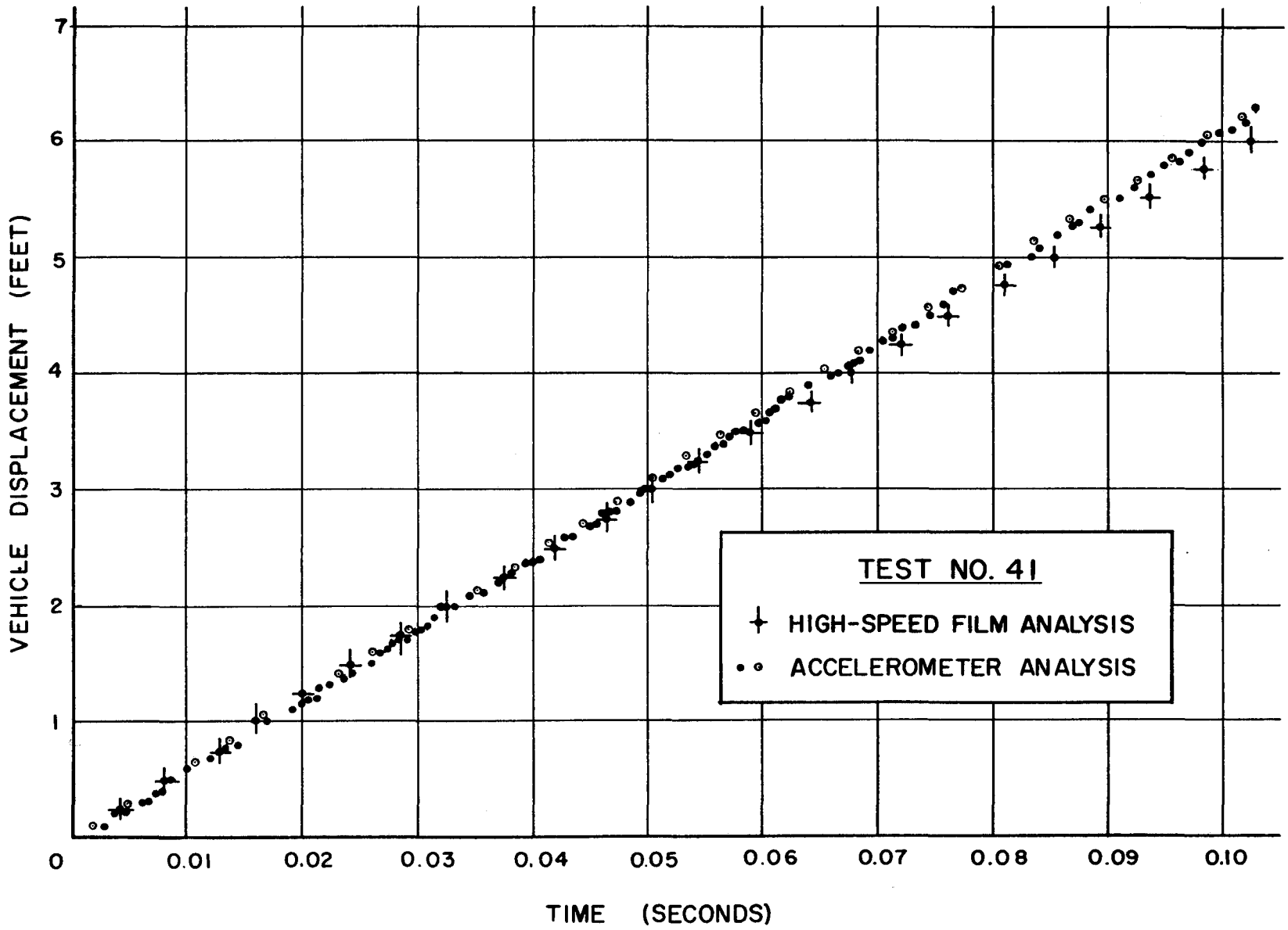
VEHICLE DISPLACEMENT (FEET)
7
6
5
4
3
2
1
0
0.01
0.02
0.03
0.04
0.05
0.06
0.07
0.08
0.09
0.10
TIME (SECONDS)
TEST NO. 41
HIGH-SPEED FILM ANALYSIS
ACCELEROMETER ANALYSIS

# APPENDIX E

## COMPUTER PROGRAM AND SAMPLE RESULTS

```
COMPUTER PROGRAM BY R. M. OLSON, OCTOBER 1965, TIMVELDISCOMP - TEST 41
      DIMENSION HORV(700),AREAV(700),TIMEV(700),DELV(700),VEL(700),VELAV
     1G(700),DELT(700),DELD(700),DISP(700)
  102 READ(5,2)N
    2 FORMAT(I3)
  103 READ(5,3)(HORV(I),AREAV(I),I=1,N)
    3 FORMAT(F6.1,F6.0)
  210 WRITE(6,10)
   10 FORMAT(9X,5HDATUM,2X,4HHORV,3X,5HTIMEV,6X,5HAREAV,3X,4HDELV,3X,8HV
     1ELOCITY,2X,6HVELAVG,3X,4HDELD,3X,12HDISPLACEMENT//)
      CO1=0.000606
      CO2=0.0097566
      VEL0=62.3
      TIMEV(1)=CO1*HORV(1)
      VEL(1)=VEL0+CO2*AREAV(1)
      VELAVG(1)=(VEL(1))*0.5
      DELT(1)=TIMEV(1)
      DELD(1)=VELAVG(1)*DELT(1)
      DISP(1)=DELD(1)
      DO 999 IDATA=2,N
      I=IDATA
      TIMEV(I)=CO1*HORV(I)
      DELV(I)=CO2*AREAV(I)
      VEL(I)=VEL(I-1)+DELV(I)
      VELAVG(I)=(VEL(I)+VEL(I-1))*0.5
      DELT(I)=TIMEV(I)-TIMEV(I-1)
      DELD(I)=VELAVG(I)*DELT(I)
      DISP(I)=DISP(I-1)+DELD(I)
  999 CONTINUE
  211 WRITE(6,11)(I,HORV(I),TIMEV(I),AREAV(I),DELV(I),VEL(I),VELAVG(I),D
     1ELD(I),DISP(I),I=1,N)
   11 FORMAT(1H ,9X,I3,3X,F5.1,3X,F6.4,5X,F4.0,3X,F6.3,4X,F5.1,4X,F5.1,3
     1X,F4.2,4X,F5.1)
      STOP
      END
```

SAMPLE RESULTS FROM THE COMPUTER PROGRAM

| DATUM | HOR | TIME | AREA | DELV | VELOCITY | DELD | DISPLACEMENT |
|---|---|---|---|---|---|---|---|
| 1 | 3.6 | 0.0022 | 6. | 0.00 | 62.36 | 0.07 | 0.07 |
| 2 | 5.0 | 0.0030 | 2. | 0.02 | 62.38 | 0.05 | 0.12 |
| 3 | 6.3 | 0.0048 | -7. | -0.07 | 62.31 | 0.05 | 0.17 |
| 4 | 8.0 | 0.0061 | -9. | -0.09 | 62.22 | 0.06 | 0.23 |
| *** | *** | **** | *** | ** | *** | ** | **** |
| 14 | 28.0 | 0.0171 | -74. | -0.72 | 61.58 | 0.15 | 0.99 |
| 15 | 31.5 | 0.0191 | -70. | -0.68 | 60.90 | 0.13 | 1.12 |
| *** | *** | **** | *** | ** | *** | ** | **** |
| 39 | 63.0 | 0.0382 | 19. | 0.19 | 61.29 | 0.07 | 2.28 |
| 40 | 65.0 | 0.0394 | 2. | 0.02 | 61.30 | 0.07 | 2.36 |
| *** | *** | **** | *** | ** | *** | ** | **** |
| 107 | 168.5 | 0.1021 | 2. | 0.02 | 61.83 | 0.07 | 6.22 |
| 108 | 170.5 | 0.1033 | 3. | 0.03 | 61.86 | 0.07 | 6.29 |

NOTE - THIS IS A PARTIAL LISTING OF RESULTS FROM THE COMPUTER PROGRAM.